A Model for Emergency Logistical Resource Requirements: Supporting Socially Vulnerable Populations Affected by the (M) 7.8 San Andreas Earthquake Scenario in Los Angeles County, California

by

Joseph Charles Toland

A Thesis Presented to the
Faculty of the USC Graduate School
University of Southern California
In Partial Fulfillment of the
Requirements for the Degree
Master of Science
(Geographic Information Science and Technology)

December 2018

To my brother, John. Ditto…

Table of Contents

List of Figures

List of Tables

Acknowledgments

I'd like to thank Dr. Karen Kemp for bringing this thesis to life, and for providing skillful editing and guidance in putting all of the material together. Also, thank you to the other members of my committee, Dr. Jennifer Swift and Dr. Katushiko Oda—and to COL Steven Fleming for his advice on disaster logistics. A special thanks to my friends and family for their support and assistance. Thank you Dad and Laura for your expert editing and writing advice. A special thanks to my brother, Dr. John R.E. Toland, for letting me discuss modeling issues at all hours of the night—even after you had been teaching and doing research all day. And thank you Mom for your support and curiosity—and the many meals made with love. Also, thank you to colleagues that have provided sponsorship for access to data and other information: Jami Childress-Byers, Dr. Chris Emrich, Dr. Ken Hudnut, Jesse Rozelle, Charlie Simpson and thank you to the USC Spatial Sciences Institute and staff for your support. But most importantly, this thesis must acknowledge the disaster survivors from Hurricane Katrina, the Haiti Earthquake, Hurricane Maria and many others—and for those in future events. Hopefully, we can learn from these events and build a more prepared and resilient future.

List of Abbreviations

AFO	Area Field Office
AOI	Area of Impact
AOR	Area of Responsibility
ATC	Applied Technology Council
CalOES	California Governor's Office of Emergency Services
CDF	Cumulative Distribution Function
CPG	Comprehensive Planning Guide
CUSEC	Central United States Earthquake Consortium
DHS	United States Department of Homeland Security
DLA	Defense Logistics Agency
E-R	Entity-Relationship
Esri	Environmental Systems Research Institute, Inc.
FEMA	Federal Emergency Management Agency
FGDB	Esri File Geodatabase
GIS	Geographic Information Systems
GIST	Geographic Information System Science and Technology
GLM	Generalized Linear Model
HAZUS-MH®	FEMA Hazards United States Multi-Hazard Software
HSPD-5	Homeland Security Presidential Directive 5
HVRI	Hazards and Vulnerability Research Institute, University of South Carolina
IAEM	International Association of Emergency Managers
ICS	Incident Command System

LOGRESC®	The Logistical Resource Model
M	Moment Magnitude
MAUP	Modifiable Areal Unit Problem
MAE	Mid-America Earthquake Center
MMI	Modified Mercalli Intensity
NRC	National Resource Council of the National Academies
NBI	National Bridge Inventory
NHPN	National Highway Planning Network
NIMS	National Incident Management System
NLCD	National Landcover Data
NYC	New York City
ODE	Ordinary Differential Equation
OEM	Office of Emergency Management
OPLAN	Southern California Catastrophic Earthquake Response Operational Plan
ORNL	Oakridge National Laboratories
PAGER	Prompt Assessment of Global Earthquakes for Response
PCA	Principal Component Analysis
PGA	Peak Ground Acceleration
PGD	Peak Ground Deformation
PGV	Peak Ground Velocity
PKEMRA	Post Katrina Emergency Management Reform Act of 2006
POD	Point of Distribution
SA10	(1.0 second) Peak Spectral Acceleration

SoVI®	University of South Carolina's Social Vulnerability Index
SPDE	Stochastic Partial Differential Equation
UAC	Unified Area Command
UASI	Urban Areas Security Initiative
UCERF3	Uniform California Earthquake Rupture Forecast
UCG	Unified Coordination Group
UNDRO	Office of the United Nations Disaster Relief
USACE	United States Army Corps of Engineers
USC	University of Southern California
USDA	United States Department of Agriculture
USGS	United States Geological Survey
UTM	Universal Transverse Mercator
VRP	Vehicle Routing Problems
WGS	World Geodetic System
WHO	World Health Organization

Abstract

Federal, state and local officials are planning for a (M) 7.8 San Andreas Earthquake Scenario in the Southern California Catastrophic Earthquake Response Plan that would require initial emergency food and water resources to support from 2.5 million to 3.5 million people over an eight-county region in Southern California. However, a model that identifies locations of affected populations—with consideration for social vulnerability, estimates of their emergency logistical resource requirements, and their resource requirements over time—has yet to be developed for the emergency response plan.

The aim of this study was to develop a modeling methodology for emergency logistical resource requirements of affected populations in the (M) 7.8 San Andreas Earthquake Scenario in Southern California. These initial resource requirements, defined at three-days post-event and predicted through a probabilistic risk model, were then used to develop a relative risk ratio and to estimate resources requirements over time. The model results predict an "at-risk" population of 3,352,995 in the eight-county study region. In Los Angeles County, the model predicts an "at-risk" population of 1,421,415 with initial requirements for 2,842,830 meals and 4,264,245 liters of water. The model also indicates that communities such as Baldwin Park, Lancaster-Palmdale and South Los Angeles will have long-term resource requirements.

Through the development of this modeling methodology and its applications, the planning capability of the Southern California Catastrophic Earthquake Response Plan is enhanced and provides a more effective baseline for emergency managers to target emergency logistical resources to communities with the greatest need. The model can be calibrated, validated, generalized, and applied in other earthquake or multi-hazard scenarios through subsequent research.

Chapter 1 Introduction

This study developed a modeling methodology for emergency logistical resource requirements of affected populations in the (M) 7.8 San Andreas Earthquake Scenario in Southern California. This earthquake scenario is expected to catastrophically impact populations, infrastructure and the economy throughout an eight-county region (Figure 1) in Southern California (Jones et al. 2008).

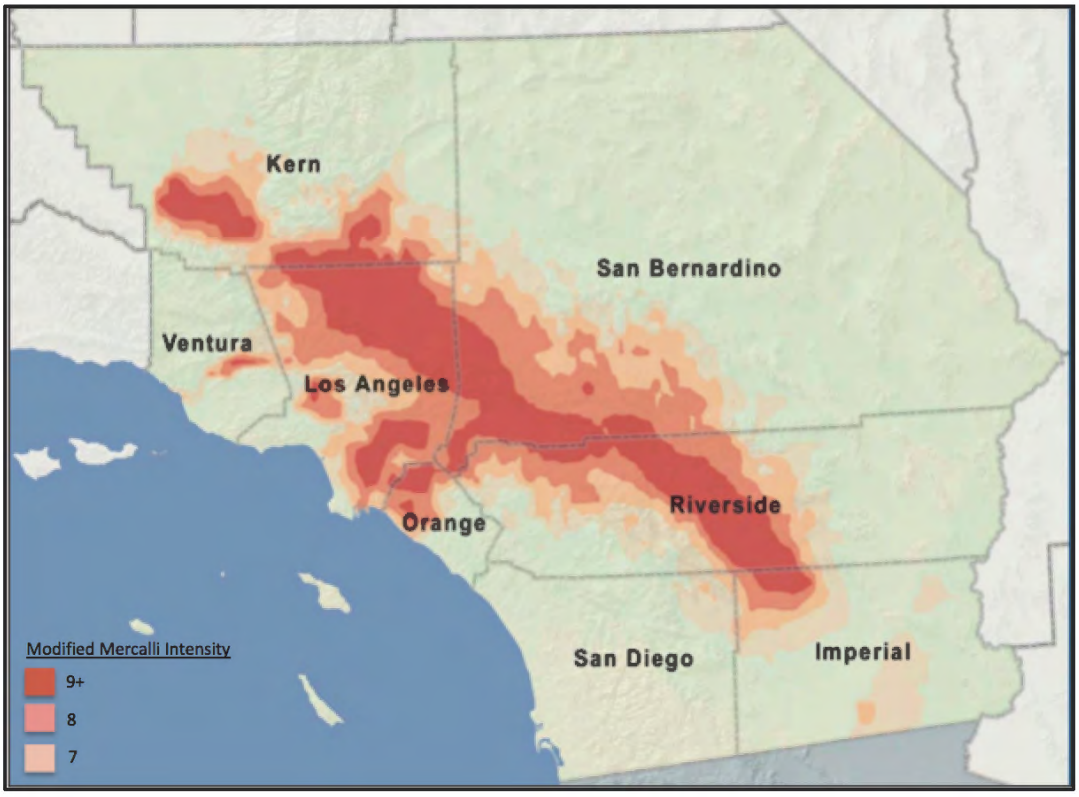

Figure 1. Eight-county Southern California study region from the ShakeOut scenario. Map from CalOES and FEMA (2011).

The (M) 7.8 San Andreas Earthquake Scenario, developed by the United States Geological Survey (USGS) for "The Great California ShakeOut" earthquake annual preparedness exercises, is the basis for the joint federal, state and local Southern California Catastrophic Earthquake Response Operational Plan (OPLAN) that will guide disaster response

efforts in the event of a catastrophic earthquake in the region (CalOES and FEMA 2011). The ShakeOut earthquake scenario and the OPLAN identify that a life-sustaining priority is to provide meals and water to support disaster-affected populations of between 2.5 million and 3.5 million (2 meals per person/day and 3 liters of water per person/day) in the eight-county study region, from three-days post-event. However, a model that identifies locations of affected populations—with consideration for social vulnerability, estimates of their emergency logistical resource requirements and their resource requirements over time—has yet to be developed for the emergency logistical response plan.

From Hurricane Katrina to recent events in Puerto Rico, identifying emergency resource requirements remains a perennial gap in emergency management capabilities and the lack of a standard modeling methodology directly affects the health, security and long-term sustainability of the most vulnerable communities. Planning for these resource requirements before an event occurs can mitigate against resource scarcity and food insecurity in the affected communities when disaster strikes. This study proposes to begin to fill this gap in the literature and in emergency management capabilities with a novel methodology for modeling emergency logistical resource requirements in the (M) 7.8 San Andreas Earthquake Scenario.

1.1. Motivation

The United States Geological Survey (USGS) predicts in the Uniform California Earthquake Rupture Forecast (UCERF3) that there is a 31 percent chance of a (M) +7.5 earthquake occurring in Los Angeles County, California, in the next 30 years (Field et al. 2013). The (M) 7.8 San Andreas Earthquake ShakeOut Scenario and the OPLAN identify that an emergency logistical commodity mission will be required to provide life-sustaining support to nearly 10 percent of the regional population (CalOES and FEMA 2011). However, the ShakeOut

scenario and the OPLAN do not include tools such as high-resolution models of affected populations and their requirements over time, nor plan for the amplifying effects of social vulnerability. As the literature suggests (e.g. Juntunen 2006; Philips et al. 2010; Gillespie and Zakour 2013; Lindell 2013) socially vulnerable populations have proportionally higher emergency resource requirements than the general population and will take longer to recover.

Several recent incidents have highlighted the need for the identification of vulnerable populations and the locations of high-risk areas that may be used as priority food and water distribution points in coordination with community groups. In review of the Hurricane Sandy response, the Hurricane Sandy After Action Report recommended development of a Food and Water Distribution Task Force. This task force could then be activated before a coastal storm occurs to target resources to vulnerable communities (NYC 2013).

Most recently in Puerto Rico, resource shortages severely impacted the local populations and mass migration out of the region was widespread. The 2017 FEMA Hurricane Maria After Action Report acknowledged that federal agencies faced difficulties knowing what was needed and where in the aftermath of the storm (FEMA 2018a). An investigative report by *The Guardian* noted that:

> Federal officials privately admit there [was] a massive shortage of meals in Puerto Rico three weeks after Hurricane Maria devastated the island. Officials at the Federal Emergency Management Agency (FEMA) say that the government and its partners are only providing 200,000 meals a day to meet the needs of more than 2 million people. That is a daily shortfall of between 1.8 million and 5.8 million meals (Wolffe 2017, 1).

Without estimation of initial affected populations, their location and a model of their long-term resource requirements, the failure of the emergency logistical resource mission is much more likely and can result in humanitarian catastrophe (Paci-Green and Berardi 2015). While the current study and study area are scenario specific and do not relate to hurricane events

per se, such as with Hurricane Maria in Puerto Rico, nor the unique socioeconomic, demographic and physical environment found there, these events support the objectives of the current study and the conclusion that further research is warranted in order to generalize and calibrate the modeling methodology for additional types of catastrophic disaster response events.

This study also provides an innovative interdisciplinary application in the development of Geographic Information System Science and Technology (GIST) through an integration of the emergency management/logistical planning, spatial analysis/Geographic Information Systems (GIS) and mathematical modeling problem spaces. In this integrated problem space, a perennial issue in emergency management planning capabilities is addressed in a scenario that requires contributions from all three disciplines to be successfully managed. In so doing, this study provides a public service and social benefit to disaster response planning by providing tools to mitigate impacts to those populations most vulnerable to disruptions in life-sustaining food and water supplies in the event of a catastrophic incident.

1.2. Thesis Organization and Research Objectives

As this is an interdisciplinary approach to a complex problem, this thesis research is directed at several audiences with the ultimate goal of developing a *probabilistic risk model* (or probabilistic risk assessment) for emergency logistical resource requirements of affected populations (at three-days post-event) in the (M) 7.8 San Andreas Earthquake Scenario. A probabilistic risk model is a systematic and comprehensive methodology to evaluate risks associated with natural hazards and can provide a standard modeling methodology for estimation of "at-risk" populations for emergency logistical resource requirements—and so can begin to address these gaps in emergency management capabilities (Dwyer et al. 2004).

In Chapter 2, an overview of emergency management, the ShakeOut earthquake scenario and the OPLAN are provided. This chapter provides the context for the commodity mission in the eight-county study region along with an overview of food insecurity and its impacts in the ShakeOut scenario. Chapter 2 is intended for emergency managers, community planners, humanitarian relief and disaster logistics specialists and other non-technical audiences. These audiences can then directly apply the results provided in Chapter 5 and the Appendix D, “Logistical Resource Summary Report", into their mission without further background.

Chapter 3 is intended for the science and engineering community that require a deeper background in the model design and methodology. In this chapter, the design of a probabilistic risk model for populations “at-risk” for emergency logistical resource requirements is investigated in detail for application in the commodity mission. This chapter introduces each component of the model, provides a technical background with support from the literature and the theoretical framework used to produce the model results. After reading Chapter 3, technical audiences can proceed to Chapter 4, to computationally replicate the results, or go directly to Chapter 5 and the appendices.

In Chapter 4, the methodology for computational implementation of the probabilistic risk model is presented, along with applications of the model to calculate relative risk in the eight-county study area and to calculate resource requirements over time. This chapter is intended for a technical GIS audience, with all of the information required for successful replication of the results of the model in ArcGIS 10.6 and other software. The results and discussion are then presented in Chapter 5 and Chapter 6 respectively, for all audiences.

In Appendix D, resource requirements over time in Los Angeles County as predicted by the model are summarized by the community Points of Distribution (PODs) for the commodity

mission in the OPLAN. This report is designed for non-technical audiences in supporting operational planning by emergency managers and community planners in the commodity mission.

Organization of the current study is shown in Figure 2, along with the key components in the model design to develop a probabilistic risk model for emergency logistical resource requirements, which are introduced in the next section.

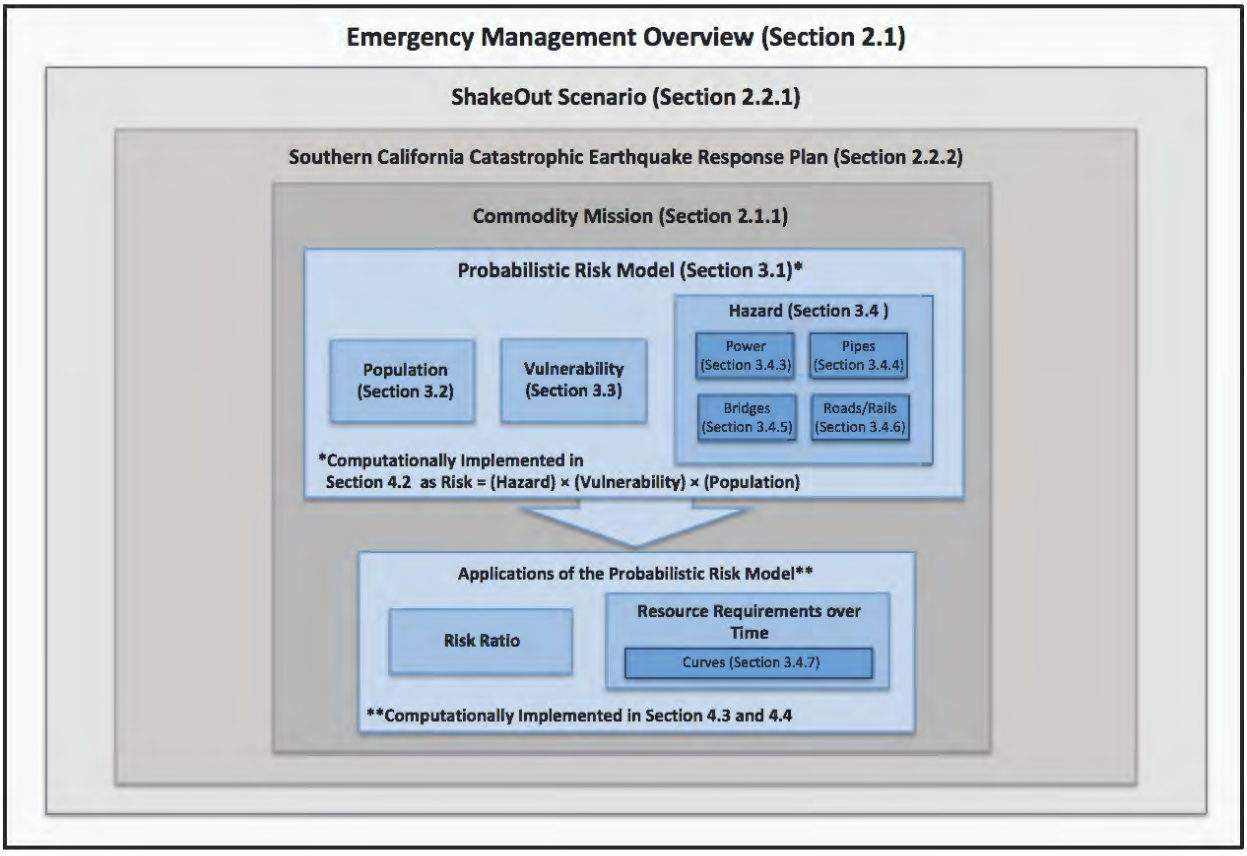

Figure 2. Organization of the current study within an emergency management context

1.2.1. *Development of a Probabilistic Risk Model for Emergency Resource Requirements*

The main research objective in this study is to develop a probabilistic risk model for emergency logistical resource requirements of affected populations in the (M) 7.8 San Andreas Earthquake Scenario. The proposed methodology to implement this goal includes several key

components, which are introduced below with reference to their corresponding section in the thesis document.

The probabilistic risk model is based on computational implementation of the *risk* equation as identified by Dwyer et al. (2004), and originally defined by the Office of the United Nations Disaster Relief (UNDRO), to determine the expected population "at-risk" with respect to the general population. In this equation, *risk* is defined as the product of *vulnerability*, *population* and *hazard*—and is used to directly calculate the "at-risk" population for emergency logistical resource requirements. This risk equation guides the entire framework of the current study and is further investigated in Section 3.1, along with the *vulnerability*, *population* and *hazard* components.

Modeled ground-motion data from the ShakeOut scenario is used to represent the geophysical properties of the earthquake in the current study, and is presented in Section 2.2.2 from Jones et al. (2008). *Ground-motion* data represent the characteristic geophysical properties of an earthquake in measurements such as magnitude, intensity, velocity and acceleration over a geographic region.

The OPLAN is used to establish the assumptions for population impact, food insecurity and resource requirements and support, which is discussed in Section 2.2.3. LandScan 2015 "global" and LandScan USA 2012 "conus_night" population databases are used to represent the affected *population* and are described in Section 3.2. The University of South Carolina's Social Vulnerability Index (SoVI®) model from Cutter et al. (2003) is investigated in Section 3.3 and is used to characterize *vulnerability* in impacted populations.

From the literature, impacts to six infrastructure *indicators* are shown to be key factors affecting food insecurity in disasters. These are investigated in Section 3.4 and are identified as

electric power system damage (Section 3.4.3), natural gas and water pipeline damage (Section 3.4.4), bridge damage (Section 3.4.5), road and rail damage (Section 3.4.6). *Indicators* are a means of converting data into usable information, where the data are chosen to be relevant to the problem of concern, consistent over both time and space and measurable (Dwyer et al. 2004).

Damage functions (or fragility curves) and *restoration functions* of these six infrastructure indicators from the *Hazards United States Multi-Hazard* (HAZUS-MH® 4.0) Technical Manual and Applied Technology Council report (ATC-13) are then used to characterize the *hazard* component of the model, in Chapter 4. *Damage functions* are mathematical models used in structural engineering to calculate the probability of direct physical damages to infrastructure induced by geophysical ground-motion (FEMA 2003). These damage functions are incorporated into *restoration functions* (also called restoration curves or restoration timelines), which determine the general timeframe (in days) for repair or replacement back to full capacity.

Social vulnerability (investigated in Section 3.3) is also a key factor in food insecurity, as it is a measure of the socioeconomic and demographic factors that affect a community's ability to respond to and recover from environmental hazards (Cutter et al. 2003). In the methodology of Section 4.2, the new *hazard* curve is then amplified by the social vulnerability from the SoVI model. In the current study, *amplification* (or attenuation) is defined through local social vulnerability conditions that proportionally increase (or decrease) the population's *vulnerability* to the *hazard*. In general, *amplification* increases a hazard and traditionally represents the magnifying local site conditions of surficial soils, topography or other environmental factors (FEMA 2003).

Finally, in the methodology for development of the probabilistic risk model, the resulting probabilities of emergency logistical resource requirements are applied to the LandScan 2015 "global" population data (from Section 3.2) developed by Bhaduri et al. (2007). The expected population impacted in the model then determines the final "at-risk" populations for emergency logistical resource requirements in the eight-county study area. These final model results are aligned with the OPLAN assumption of supporting resource requirements for between 2.5 million and 3.5 million people (2 meals per person/day and 3 liters of water per person/day) in the eight-county study region, at three-days post-event (CalOES and FEMA 2011).

The model is validated (Section 4.2.2) to quantify the distributions and relationships of the underlying indicator variables in the model results. Logistic regression and associated statistical tests are performed for analysis of variable contributions in the results and to determine a confidence interval for these estimates. The final result is a probabilistic risk model for emergency logistical resource requirements of affected populations in the eight-county study region, at three-days post-event.

1.2.2. *Applications of the Probabilistic Risk Model*

In Section 4.3, the results from the probabilistic risk model are applied to develop a *relative risk ratio* for emergency resource requirements in the eight-county study region. In general, a *relative risk ratio* is the ratio of the probability of an event occurring in an exposed population to its occurrence in the general population. In the current study, this is defined as the calculation of the ratio of populations "at-risk" for emergency resource requirements versus the general population (Bithell 1990). Community trends in relative risk can then be identified for community vulnerability planning in the preparedness and mitigation phases of the disaster lifecycle (Dwyer et al. 2004).

In Section 4.4, the results from the probabilistic risk model are applied in Los Angeles County through LandScan USA 2012 "conus_night" population data to determine logistical *resource requirements over time* for the commodity mission in the OPLAN (CalOES and FEMA 2011). The "at-risk" populations and their resource requirements at three-days post-event are used as the initial conditions for a set of restoration curves for resource requirements (from Section 3.4.7) for Los Angeles County. From these curves, at-risk populations and their emergency logistical resource requirements at future time intervals within the disaster lifecycle (e.g. at t = 7, 14, 30, 45, 60 and 90-days) are simulated. From these results, estimates of total resources are calculated for response operations and logistical commodity mission planning support. Emergency managers can then identify and prioritize communities with ongoing resource requirement issues.

The final results of the modeled resource requirements in Los Angeles County are provided in Appendix D as a summary report designed for emergency managers and community planners. Results are aggregated for all of the 143 Point of Distribution (POD) sites in Los Angeles County identified in the OPLAN (CalOES and FEMA 2011), which are discussed in Section 2.1.1. Areas of Responsibility (AORs) for each POD are modeled in Appendix A to allow aggregation of the results to PODs. In this report, "at-risk" populations and their resource requirements (as truckloads and pallets of food and water) for seven operational periods in the recovery timeline are calculated, based on standard shipping formulas and logistical metrics (Johnson and Coryell 2016).

Through the development of this modeling methodology, and its results, the planning capability of the Southern California Catastrophic Earthquake Response Operational Plan (OPLAN) is enhanced. This provides a more effective baseline for emergency responders to

target resources to communities with the greatest need. The model can be calibrated, validated, generalized and applied in other earthquake and multi-hazard scenarios through subsequent research.

Chapter 2 Emergency Management, Response Operations and Emergency Relief Logistics

This chapter situates the development of a modeling methodology for emergency logistical resource requirements of affected populations in the (M) 7.8 San Andreas Earthquake Scenario within the discipline of emergency management and establishes the general framework for disaster response and emergency logistical relief missions. The later sections explore the (M) 7.8 San Andreas Earthquake Scenario and its implementation in the Southern California Catastrophic Earthquake Response Operational Plan (OPLAN), which serves as the specific context for this study. Food insecurity and its impacts in the (M) 7.8 San Andreas Earthquake Scenario are then addressed in the final section, which serves as the primary motivation for this study.

2.1. Emergency Management Overview

A *disaster* can be defined as a sudden event, such as an accident or a natural catastrophe that causes great damage or loss of life (Cutter et al. 2006). A disaster (alternatively an *incident* or *event* in some jurisdictions) is the result of risk, hazard and vulnerability where a singular large-scale, high-impact event can affect populations, infrastructure, property, the environment and the economic stability of a region. *Emergency management* is the discipline that manages disasters through international, federal, state, local, tribal, voluntary and private sector organizations and their respective authorities (FEMA 2006).

Emergency management is defined by the Federal Emergency Management Agency (FEMA) and the International Association of Emergency Managers (IAEM) as "the managerial function charged to create the framework within which communities reduce vulnerability to hazards and cope with disasters" (FEMA 2006, 2). Emergency management and disaster

response operations (at all levels) prioritize the following: (1) Reduce the loss of life; (2) Minimize property loss and damage to the environment; and (3) Plan and prepare for all threats and hazards (FEMA 2006). This is accomplished through the disaster life-cycle model shown in Figure 3, which was developed by FEMA for comprehensive emergency management. The disaster lifecycle model is composed of four phases of emergency management: Preparedness, Mitigation, Response and Recovery (FEMA 2006).

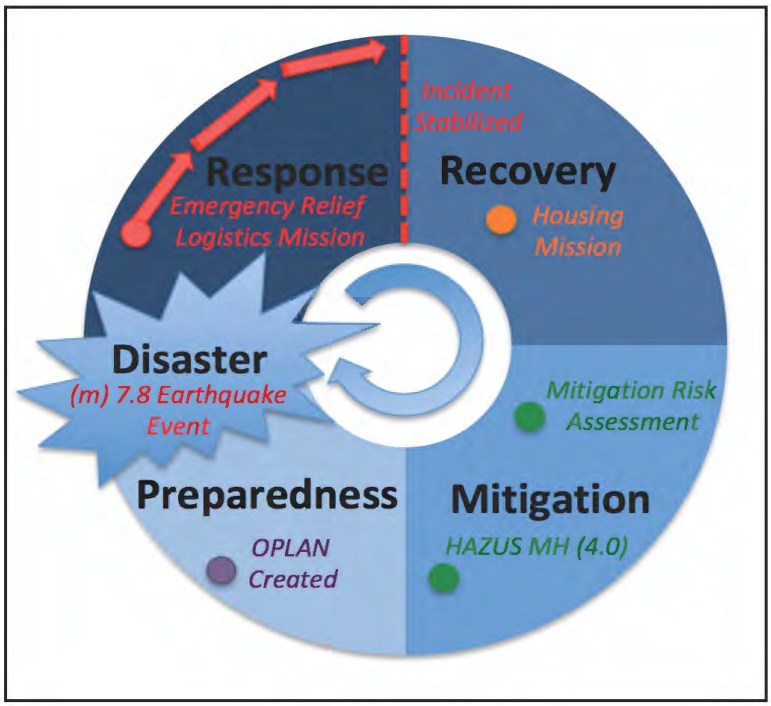

Figure 3. The disaster life-cycle model (FEMA 2006)

Response operations coordinate life-saving and life-sustaining missions by emergency management authorities to save lives, protect property and the environment and to meet basic humanitarian needs after an event has occurred. *Recovery* operations include missions such as housing and infrastructure restoration and repair that can support the rebuilding of an impacted community. *Mitigation* lessens the impacts of disasters through building increased disaster

resilience in communities. *Preparedness* provides the capabilities to identify and plan for risks before an incident occurs (FEMA 2006).

When a disaster such as the (M) 7.8 San Andreas Earthquake Scenario occurs, the response phase of the disaster lifecycle begins. One of the highest priorities in response operations is the mission for the distribution of life-sustaining emergency logistical resources (i.e. commodities), such as food and water, to affected populations (CalOES and FEMA 2011; Lu et al. 2016). Within the incident, joint federal, state and local priorities are managed by senior leadership in the Unified Coordination Group (UCG), through the Incident Command System (ICS) and the Incident Action Planning process (FEMA 2006). The Incident Action Planning process is the standardized, on-scene, all-hazards approach to incident management established by the National Incident Management System (NIMS) under Homeland Security Presidential Directive 5 (HSPD-5).

In the Incident Action Planning process, the Area of Impact (AOI) is identified and operational periods are established. The AOI represents the area directly affected by the disaster and may be further divided into geographic Areas of Responsibility (AORs) and Operational Branches and Divisions, under a Unified Area Command (UAC) managed at an Area Field Office (AFO). Operational periods generally range from 12 to 24 hours in the response phase, and are important in the current study as they are key points in time at which to model future resource requirements. One of the benefits of the UAC is that it can manage large-scale integrated resource ordering and distribution during each operational period, supporting complex emergency relief logistics missions in response operations (FEMA 2006).

While the emergency logistical resource mission begins in the response phase, its end can generally be considered the point at which the incident is stabilized and priorities can be shifted

to recovery. The literature notes that the long-term success of the logistical resource mission can stabilize impacted communities and decrease the likelihood of displacement of populations through mass migration out of the region, as well as prevent the public health issues that will arise in communities unable to meet basic humanitarian needs (Paci-Green and Berardi 2015).

These emergency relief missions are supported by impact models and through population and demographic data analysis in the impacted area (NRC 2007). The results of these analyses are used for decision support and situation awareness in the emergency logistical resource mission. Population data can support the determination of priorities for how much and what types of aid (e.g. food, water and medical supplies) are needed and provide a community-level determination of where the aid should be delivered (UASI 2014). Geographic Information Systems (GIS) has provided an important intersection for emergency relief logistics and response operations and has made it possible for emergency managers to target resources to areas with the greatest risk, or after an event, to those with the greatest impact (Cova 1999).

2.1.1. *Emergency Relief Logistics and the Commodity Mission*

Emergency relief logistics (also known as emergency logistics, disaster logistics, or humanitarian logistics) refers to the process of planning, executing and efficiently controlling the request, procurement, movement, staging, storage and dissemination of life-sustaining commodities throughout the entire supply chain management process until reception at the demand locations (CalOES and UASI 2015). Logistics is a key capability for disaster response and is a key component for emergency response planning at the local, regional, state, tribal and national level. Logistics planning for a disaster involves understanding of the environmental, sociopolitical, demographic and physical characteristics of the region. In general, logistical planning addresses the following issues:

- What resources are required, how many, where and for how long?
- How can they be obtained or procured?
- How can they be transported to the demand locations?
- How can they be received, staged, stored, distributed and tracked?
- Which entities and actors have roles in management of the logistics supply chain?

A priority for emergency relief logistics is to establish primary staging areas at pre-designated locations for logistical resource receiving, storage and distribution. Secondary staging areas may also be established at transportation hubs, military bases, shelters or other facilities that can support the response. A major function of the staging areas is to support the distribution of commodities to the Point of Distribution (POD) sites in the impacted community (UASI 2014).

A POD site is a central location in the community where affected populations receive life-sustaining commodities, such as pre-packaged, shelf-stable meals and bottled water following a disaster (UASI 2014; CalOES and UASI 2015). Resource ordering and fulfillment for each POD site is managed through the Operational Divisions and Branches by the UAC with the Unified Coordination Group (UCG). Each community POD site should be publicly accessible and situated within an Area of Responsibility (AOR) that represents the affected community in the immediate vicinity. POD sites can also be co-located with emergency shelter sites or other facilities involved in the disaster response effort.

In the current study, AORs are calculated using the Huff Model, a probability of travel model, to estimate the populations closest to the POD site that will be served. This supplemental analysis is documented in Appendix A. The POD sites from the OPLAN with the AORs from Appendix A are shown below in Figure 4 (CalOES and FEMA 2011).

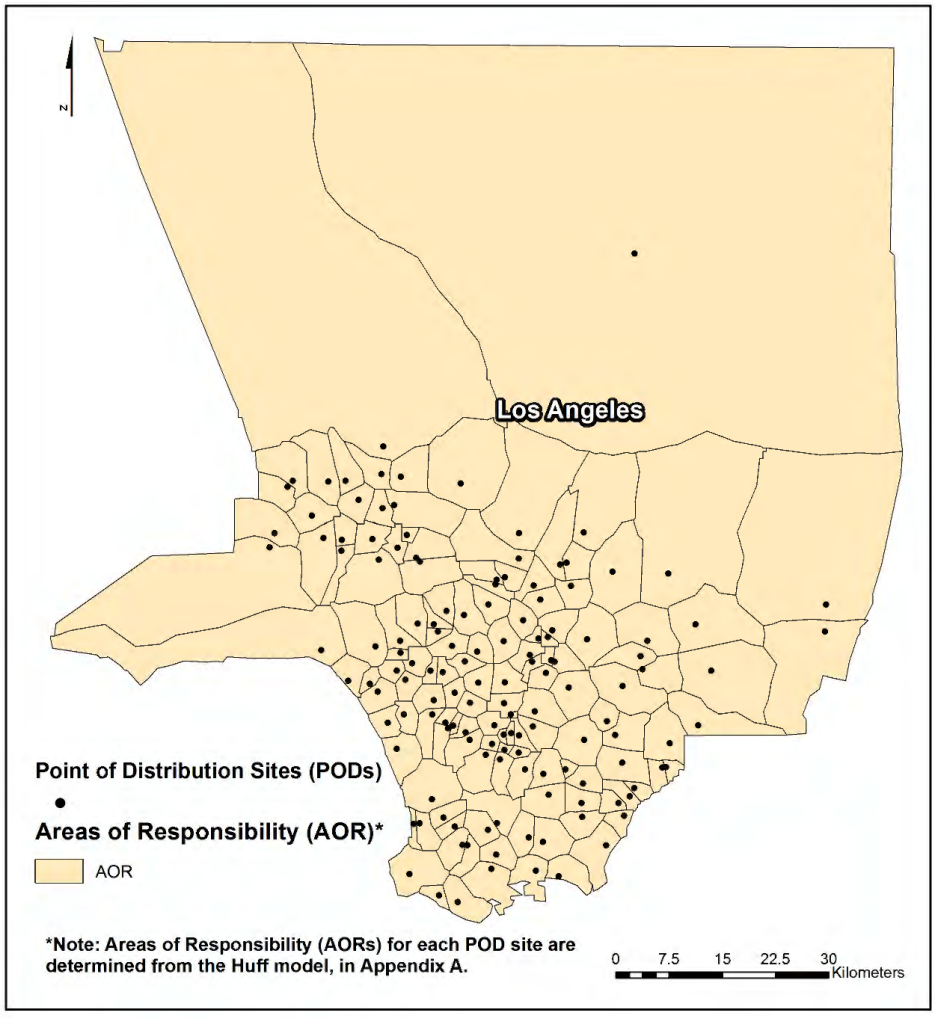

Figure 4. Point of Distribution (POD) sites from the OPLAN and AORs in Los Angeles County

POD operations are encouraged to integrate with the general humanitarian mass feeding and food supply-chain restoration strategy in coordination with the voluntary agencies and private sector to best serve the emergency resource requirements of the impacted community. These resource requirements may be met through pre-packaged, shelf-stable meals and bottled water, but also by voluntary agency hot-meal kitchen services or private sector relief (CalOES and UASI 2015).

Shipments of food commodities are delivered to the staging areas and are distributed to each POD in a "hub-and-spoke" model during the operational period (Figure 5). Resource

ordering is based reactively on the "burn rate" of the previous operational period and projected population served (CalOES and UASI 2015). This model naturally divides the logistical planning process into a "supply-side", composed of the distribution components such as the POD sites and staging areas and a "demand-side", which includes the population resource requirements.

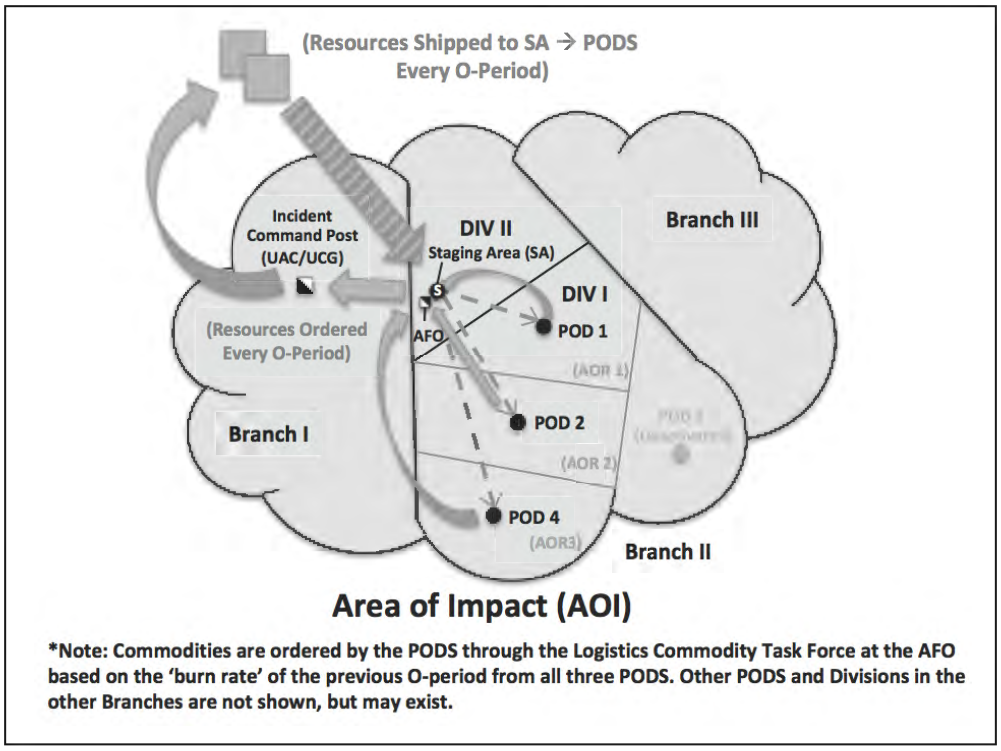

Figure 5. The "hub-and-spoke" model in emergency relief logistics (UASI 2015)

Many studies focus on "supply-side" resource supply allocation models and investigate construction and optimization of a linear resource distribution network "hub-and-spoke" structure (e.g. from the staging areas to the PODs, in the OPLAN). These "supply-side" research questions have been addressed in various linear programming and mathematical models for multi-modal emergency distribution transportation problems proposed for emergency logistics planning. These are often related to vehicle routing problems (VRP), emergency logistics distribution models, cost-optimization and location-allocation models for emergency logistical resource distribution in disasters (e.g. Fiedrich et al. 2000; Sheu 2007; Lu et al. 2016).

There are surprisingly few studies that focus on the "demand-side" through modeling resource requirements of the affected populations in the AORs up to the spoke nodes. A few examples can be found in Yi et al. (2007) and Huang (2016). In the (M) 7.8 San Andreas Earthquake Scenario, the POD site locations are fixed and determining optimal distribution locations and routing of resources to these facilities is outside of the scope of the current study. Therefore, a probabilistic "demand-side" resource requirements model is an appropriate research objective in consideration of the OPLAN and ShakeOut scenario.

2.2. The (M) 7.8 San Andreas Earthquake Scenario and OPLAN

The catastrophic (M) 7.8 San Andreas Earthquake Scenario, developed by the United States Geological Survey (USGS) for "The Great California ShakeOut" earthquake annual preparedness exercises, is the basis for the joint federal, state and local Southern California Catastrophic Earthquake Response Operational Plan (OPLAN) that guides disaster response efforts in the event of a catastrophic earthquake in the region (CalOES and FEMA 2011). The emergency relief logistics mission and identification of the emergency logistical resource requirements for affected populations can be implemented in the framework of the (M) 7.8 San Andreas Earthquake Scenario, and operationalized through the Southern California Catastrophic Response Operational Plan.

2.2.1. *The Great California ShakeOut Scenario*

The USGS predicts in the Uniform California Earthquake Rupture Forecast (UCERF3) that there is a 31 percent chance of a (M) +7.5 earthquake occurring in Los Angeles in the next 30 years (Field et al. 2013). The catastrophic (M) 7.8 San Andreas Earthquake Scenario, developed by the USGS for "The Great California ShakeOut" earthquake annual preparedness exercises and updated for the "Ardent Sentry" exercises is a (M) 7.8 earthquake on the

southernmost 300 km (200 mi) of the San Andreas Fault between the Salton Sea and Lake Hughes (Jones et al. 2008) as shown in Figure 6.

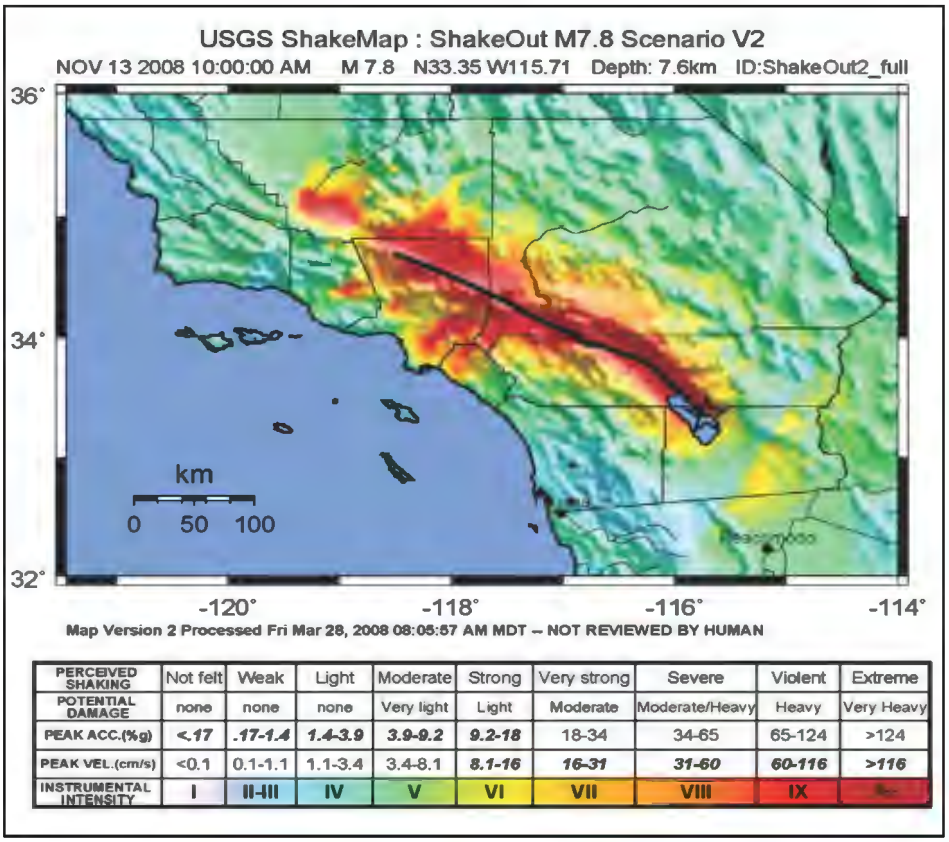

Figure 6. USGS ShakeMap for The (M) 7.8 San Andreas Earthquake Scenario. Figure from Jones et al. (2008).

The southern San Andreas Fault has produced earthquakes of magnitude 7.8 roughly every 150 years and was identified in UCERF3 as the most likely source of a large earthquake in California (Field et al. 2013). The segment of the fault modeled in the ShakeOut earthquake scenario most recently ruptured over 300 years ago—so a large earthquake is overdue (Jones et al. 2008). For the ShakeOut earthquake scenario, the USGS developed modeled ground-motion ShakeMap data on this portion of the San Andreas fault (Figure 7). *ShakeMap* is developed by the USGS Earthquake Hazards Program and is the tool that produces maps and modeled ground-motion data in standard GIS compatible formats (Earle et al. 2009).

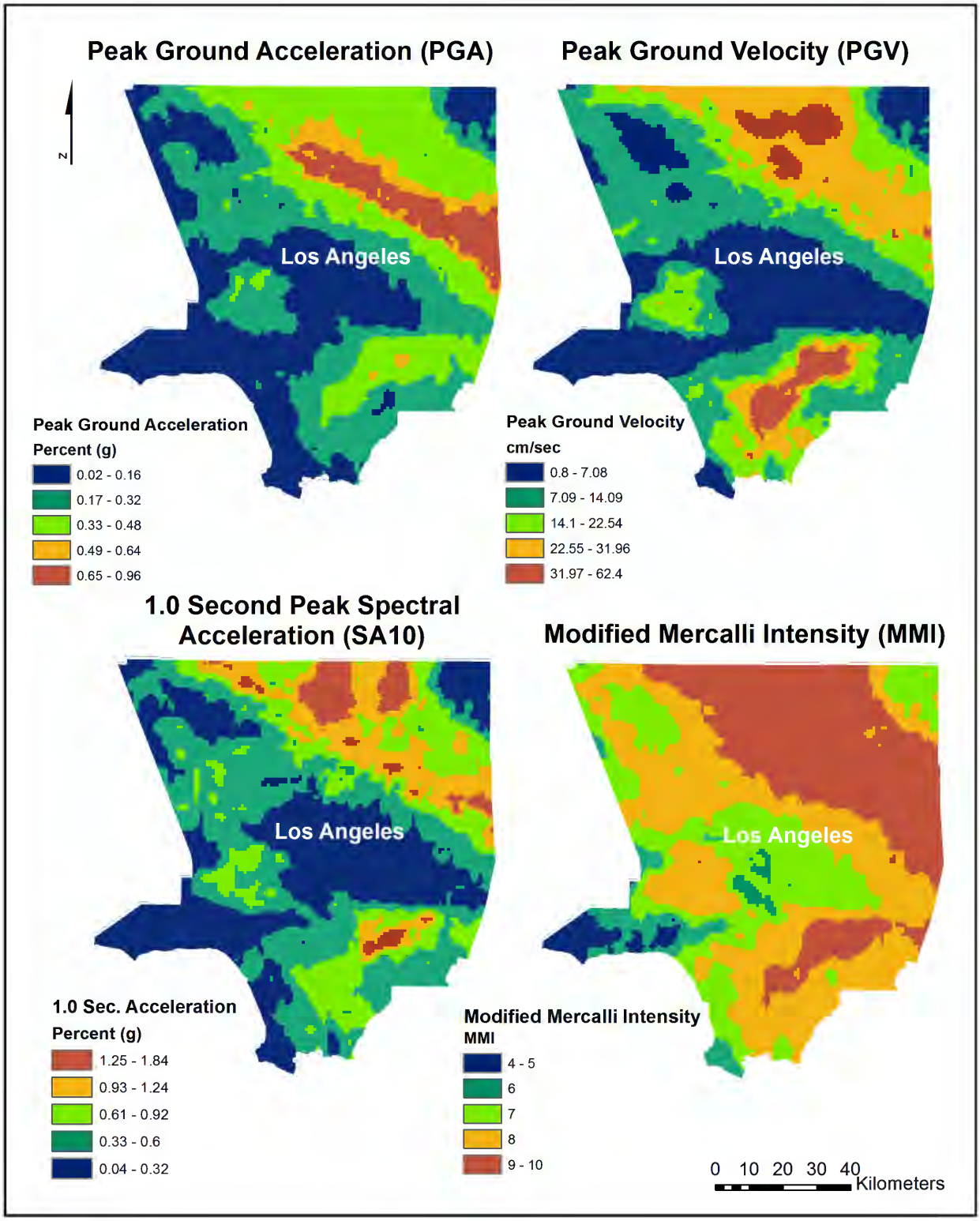

Figure 7. Modeled ground-motion data for the ShakeOut scenario. *Above left*, PGA; *right*, PGV; *below left*, SA10; *right*, MMI. Coverage in the eight-county study region is similar. Data from Jones et al. (2008).

In the ShakeOut scenario, the FEMA Hazards United States (HAZUS-MH) multi-hazard loss estimation software, along with recommendations from expert panels, was used to estimate damage to building stock and lifeline infrastructure. Physics-based modeled ground-motion ShakeMaps, as shown in Figure 7 for Peak Ground Acceleration (PGA), Peak Ground Velocity (PGV), 1.0 Second Spectral Acceleration (SA10) and Modified Mercalli Intensity (MMI), replaced the default HAZUS-MH data for the (M) 7.8 San Andreas Earthquake Scenario (Jones et al. 2008). The FEMA HAZUS-MH loss estimation results were then supplemented with the outcomes of 18 focus-studies and panel discussions by experts in sectors with catastrophic impacts in the ShakeOut scenario.

Several observations from the ShakeOut scenario are relevant to the current study. Many of the HAZUS-MH loss estimation approaches were found insufficient and so were abandoned in favor of expert opinion or supplemental studies (Jones et al. 2008). These included 10 lifeline studies for highways, oil and gas pipelines, rail, water supply and electric power. As the ShakeOut scenario was not successfully able to produce a network system analysis to model electric power system damage and outages, estimates are based only on the expert opinion from the ShakeOut panel discussions (Jones et al. 2008).

One successful result in the ShakeOut scenario was the development of a transportation network analysis and damage assessment. This was completed through a supplemental study and indicated that bridge damage was one of the most significant factors in the initial transportation impacts and restoration timeline (Werner et al. 2008). These observations are important in investigation of infrastructure indicator damage and the infrastructure restoration timelines used in the modeling methodology of Chapter 3.

The intention behind the development of the ShakeOut scenario was for it to be integrated with emergency response and recovery exercises, seminars and plans (Jones et al. 2008). These response operations missions are addressed in the Southern California Catastrophic Response Plan described in the next section.

2.2.2. *The Southern California Catastrophic Response Operational Plan (OPLAN)*

The Southern California Catastrophic Response Operational Plan (OPLAN) is developed based on the six-step planning process established in the FEMA Comprehensive Planning Guide 101 (CPG) for catastrophic planning, under authority of the Post Katrina Emergency Management Reform Act of 2006 (PKEMRA). The OPLAN is currently in the second-step of the six-step planning process, "Understanding the Situation", which is focused on assessing risk (FEMA 2010). While the OPLAN is a living document and several small revisions of the (M) 7.8 San Andreas Earthquake ShakeOut Scenario have been made, both remain essentially unchanged since 2011. The OPLAN is jointly developed by the California Governor's Office of Emergency Services (CalOES) and the Federal Emergency Management Agency (FEMA). Access to the OPLAN was granted for the purpose of this study.

The OPLAN incorporates the ShakeOut scenario from the (M) 7.8 San Andreas Earthquake event and then investigates impacts with a focus on emergency management and response operations in the eight-county Southern California region as shown in Figure 1 above. These counties and their 2015 population estimates are: Los Angeles (10.17 million), Kern (882,176), Ventura (850,536), Orange (3.17 million), San Bernardino (2.13 million), Riverside (2.36 million), San Diego (3.3 million) and Imperial (180,191). Population estimates provided by the United States Census Bureau.

Planning assumptions in the OPLAN are based on the expert opinion of over 1,500 emergency management professionals in the federal, state, local, voluntary organization and private sector (CalOES and FEMA 2011). Estimates provide information such as the number of displaced and affected population as well as casualties, with a focus on response operations mission priorities. The OPLAN projects that there will be:

- 1,800 deaths
- 53,000 injuries
- 300,000 buildings with "extensive" or "complete" damage
- Immediate displacement of 255,000 households with 542,000 individuals requiring immediate mass care and shelter
- 2.5 million individuals needing basic logistical resources (e.g. food and water) after three days
- $213 billion in damages

The OPLAN identifies the immediate displaced population (from $t = 0$ to $t < 3$ days) based on the ShakeOut scenario with expected emergency logistical resource requirements planned for 542,000 displaced persons over three-days (at 2 meals per person/day and 3 liters water per person/day). The planning assumptions for ($t = 3$ days) and beyond from the OPLAN that 2.5 million individuals that shelter in place will require basic resource support. This is extended up to 3.5 million people in the "Commodity Estimate" planning section and is the basis for the current study (CalOES and FEMA 2011).

2.2.3. *Food Insecurity and the ShakeOut Scenario*

The Greater Los Angeles Basin Region is not self-sufficient in food, as much of the perishable food for the region is regularly transported by rail or truck from San Joaquin Valley and Imperial County sources (Jones et al. 2008). The OPLAN concludes that there will be a food

distribution crisis in the first two weeks after the earthquake and that an emergency logistical commodity mission will be required to sustain a feeding program for an estimated 45 to 90 days (CalOES and FEMA 2011). Resources to support these disaster-affected populations will be required in the eight-county Southern California Region, after three-day local and emergency supplies of food are depleted and until utility service, food distribution and food industry services are restored. Therefore, the ShakeOut scenario expects food insecurity issues to impact affected populations throughout the eight-county region, in varying degrees.

The United States Department of Agriculture (USDA) defines *food security* as "access by all people at all times to enough food for an active, healthy life" (Coleman-Jensen et al. 2017, 2). *Food insecurity* can similarly be defined as when these conditions are not met. Food security in a community is threatened when a disaster occurs to a population vulnerable to a hazard, regardless of whether it is a broad segment of the general population or its socially vulnerable members (Paci-Green and Berardi 2015).

For modern households, food security is now defined by the availability of nearby prepared food products for purchase through "fast-food" chains, take-out ordering, or prepared hot-food products available at nearby markets—rather than by home pantry storage as it was in the 20th century (Guthrie et al. 2013; Paci-Green and Berardi 2015). Therefore, households have far fewer staples, canned goods and supplies readily available for emergencies. These changes in household food consumption patterns make emergency management planning assumptions that households in a community might remain self-sufficient (in terms of food and water) for a week or more after a disaster, increasingly unrealistic (Paci-Green and Berardi 2015).

Food security during a disaster serves several long-term goals. Most importantly, food security prevents individuals and communities from declining into emergency health crises and

civil unrest. Food security also reduces the likelihood of population "out-migration" from the impacted area, which is inevitable if basic life-sustaining resources are not available (Paci-Green and Berardi 2015). Emergency managers therefore plan for the general population to be self-sufficient in food for only three days, as the OPLAN indicates (CalOES and FEMA 2011). However, as the literature notes (e.g. Juntunen 2006; Philips et al. 2010; Gillespie and Zakour 2013; Lindell 2013), socially vulnerable populations will require more initial resources and for longer times—and so even these assumptions are tenuous. While healthy adults may be more resilient if confronted by a week or more of food insecurity, socially vulnerable groups (e.g. young children, pregnant and nursing women, disabled, sick and elderly) may be especially vulnerable (WHO 2000).

The (M) 7.8 San Andreas Earthquake ShakeOut Scenario will be a "no-notice" event, so damage to food supply and distribution will be unexpected and severe (CalOES and FEMA 2011). An event like the ShakeOut scenario will directly impact food access for households at all income levels to some degree. However, food insecurity will not impact households equally, as the literature suggests (Paci-Green and Berardi 2015). These issues of social vulnerability and their relation to food insecurity and logistical resource requirements are further investigated in Section 3.3.

While it is noted that resource demand in the affected area may be stochastic and unpredictable (Camacho-Vallejo et al. 2014), the OPLAN and other studies suggests that impact to food security in the ShakeOut scenario can indeed be predicted through the interconnection to infrastructure functionality (CalOES and FEMA 2011). In a large no-notice earthquake, power outages will cause perishable foods to spoil, leaving only non-perishable food stores (CalOES and UASI 2015). Businesses (including supermarkets and restaurants) are highly dependent on

power, water and transportation to function (CalOES and UASI 2015) and will be closed and have limited resources until power and water are restored (CalOES and FEMA 2011). As CalOES and FEMA (2015) indicates, significant damage to the food supply chain (because of damage to buildings, stores, warehouses and food distribution centers) in combination with interruptions to lifeline transportation infrastructure (Jones et al. 2008; Paci-Green and Berardi 2015), will reduce the amount of food available in the impacted area. These infrastructure damages can therefore be considered as *indicators* for food insecurity and logistical resource requirements and are further investigated in Section 3.4.

In conclusion, the complex supply chain and distribution network of food brought into the region, along with a decline in household food storage, means food security is interconnected with power, water, transportation and business interruption and the complex supply chains affecting delivery of food products. With individual preparedness for emergency food storage estimated at only three days of supplies, social vulnerability then amplifies these food insecurity issues. Planning for these resource requirements before the (M) 7.8 San Andreas Earthquake Scenario occurs can mitigate against resource scarcity and food insecurity in the affected communities when disaster strikes.

As the main motivation for the current study, a modeling methodology has yet to be developed that identifies locations of affected populations and summary estimates of their emergency logistical resource requirements and resource requirements over time. In consideration of this, the OPLAN is therefore limited in its capacity to address these issues. The current study proposes to begin to fill this gap in the literature and in emergency management planning capabilities with a novel methodology for modeling emergency logistical resource requirements in the (M) 7.8 San Andreas Earthquake Scenario.

Chapter 3 Model Background

This chapter introduces the components of the *risk* equation, which guides the entire framework of the current study to develop a probabilistic risk model for emergency logistical resource requirements of affected populations in the (M) 7.8 San Andreas Earthquake Scenario. This includes methodologies for estimation of *population* impacts for disaster response and an investigation of at-risk populations, social *vulnerability* and their relation to food insecurity in disasters. The final section investigates the *hazard* component of the *risk* equation as determined by specific indicators of infrastructure impact and restoration and how these indicators can be used to model emergency logistical resource requirements, develop a relative risk ratio and to estimate resource requirements over time.

3.1. The Risk Equation

This study identifies populations "at-risk" for emergency logistical resource requirements in the (M) 7.8 San Andreas Earthquake Scenario. *Risk*, or the expected population "at-risk", is defined as:

$$Risk = Hazard \times Vulnerability \times Population \quad (1)$$

This equation is based on the definition from Dwyer et al. (2004) to define *risk* in the management of a disaster. In general, *risk* is defined as the probability or expectation of loss. *Hazard* is a condition of probability posing the threat of harm to populations, infrastructure, property, the environment or the economy. *Vulnerability* is the degree of susceptibility to which populations or infrastructure are likely to be affected. *Population* is the affected population in the current study but more generally is a component of the *elements exposed*, which can also include infrastructure, building stock and/or socioeconomic factors in more general applications of the

risk equation. The resulting at-risk *population* in the *risk* equation is then multiplied by a resources-per-person multiplier to determine the total *resource* requirements (Cova 1999; Dwyer et al. 2004).

This *risk* equation guides the entire framework for the current study and is computationally implemented to develop a probabilistic risk model of the affected at-risk population and their emergency food and water requirements. These requirements are based on the Southern California Catastrophic Earthquake Response Operational Plan (OPLAN) assumptions that 2.5 million to 3.5 million people require initial emergency logistical resources in the eight-county region at three-days post-event (t = 3 days). These components of the *risk* equation are introduced below with the rest of Chapter 3 dedicated to investigating them in detail for application in the current study.

3.1.1. *The Risk Equation in the Current Study*

The *hazard* component of the probabilistic risk model is based on modeled ground-motion data for the (M) 7.8 San Andreas Earthquake Scenario, developed by the United States Geological Survey (USGS) for the "ShakeOut" exercises and the OPLAN (see Figure 7). The USGS provides modeled ground-motion spatial data as Modified Mercalli Intensity (MMI), Peak Ground Acceleration (PGA), Peak Ground Velocity (PGV) and 1.0 Second Spectral Acceleration (SA10) over the eight-county study area (Jones et al. 2008). This is then evaluated in combination with six damage functions from the FEMA Hazards United States (HAZUS-MH) Technical Manual and ATC-13 (1985) to estimate probability of damage for six infrastructure indicators (FEMA 2003). It is shown from the literature (e.g. Jones et al. 2008; CalOES and FEMA 2011; CalOES and UASI 2015; Paci-Green and Berardi 2015) that these six damage functions, which model probability of electric power system damage and outages, water and

natural gas pipeline infrastructure damage and transportation infrastructure damage, provide the most comprehensive set of indicators representing food insecurity in the *hazard* component of the *risk* equation.

For *vulnerability*, this study concentrates on social vulnerability through the social vulnerability (SoVI) index originally developed by the University of South Carolina, Hazards and Vulnerability Research Institute in Cutter et al. (2003). "Socially Vulnerable" populations are defined by the social, economic, demographic and housing characteristics that influence a community's ability to respond to and recover from environmental hazards (HVRI 2018). In the SoVI index, social vulnerability in the 2010 U.S. Decennial Census is identified through inductive indices of seven socioeconomic and demographic variables by Principal Component Analysis (PCA). The resulting composite factor scores for social vulnerability from the SoVI study are normalized and rescaled for computational implementation as an amplification factor in the probabilistic risk model, matching community recovery rates from a key study in social vulnerability research (Hobor 2015). This result preserves the relative relationships from the original data in computational determination of initial resource requirements and the length of time of resource need (HVRI 2018).

To estimate at-risk *populations* in the eight-county study region, the probabilistic risk model includes LandScan 2015 "global" (~1 km, 30 arcsecond) population raster grid cells over the eight-county study region. LandScan 2015 is a product of Oakridge National Laboratories (ORNL), with licensing to the University of Southern California (USC), that uses a dasymetric mapping technique to model populations based on underlying aggregated data from 2010 U.S. Decennial Census blocks, National Landcover Data (NLCD), transportation, water and other demographic and commercial datasets (Bhaduri et al. 2007).

Oakridge National Laboratories, in coordination with the United States Department of Homeland Security (U.S. DHS) has also developed LandScan USA 2012 "conus_night", a high-resolution (~90 m, 3 arcsecond) version of the population data for emergency management application (Bhaduri et al. 2007), which has been approved for use in this study. High-resolution (~90 m, 3 arcsecond) data from LandScan USA 2012 is used in application of the probabilistic risk model to the Los Angeles County study region to investigate initial community level emergency resource requirements and resources requirements over time.

Resources are then defined as *population* multiplied by two meals per person/day and three liters of water per person/day. These multipliers are standard emergency management planning assumptions and are used in the OPLAN (CalOES and FEMA 2011). The final results are the total resource requirements for the at-risk populations over the study region, which are calculated discretely through each respective grid cell in computational implementation of the *risk* equation.

3.2. Estimation of Population Impacts

Estimation of the total population impacted by an event and identification of their demographic characteristics and location are the first steps in mounting an effective humanitarian response (NRC 2007). Assessments of at-risk populations involve the connection between population within the Area of Impact (AOI), magnitude of the hazard impact and the resilience of the community and built environment. Therefore, the quality and resolution of population datasets used to estimate population impacts have a direct relationship to response operations and correspondingly to the effectiveness of life-saving and life-sustaining missions.

For international humanitarian relief impact assessment, the main system that incorporates earthquake event information with "exposed" population (defined as all populations

in the AOI) is the Prompt Assessment of Global Earthquakes for Response (PAGER) system (Earle et al. 2009). PAGER is developed by the USGS as an automated system that produces reports and messaging concerning the impact of earthquakes. PAGER summarizes the population per cell, based on LandScan 2015 "global" population data at given MMI intensity values estimated by ShakeMap to produce a population exposure table. This is currently the best indication of the potential initial population impact of an earthquake event.

The PAGER system is the most general approach to estimate exposed populations and economic impacts following significant earthquakes worldwide using LandScan "global" population data with MMI as a key indicator for severity (Earle et al. 2009). In the current study, the LandScan 2015 "global" population data is also used to investigate affected populations. While PAGER uses an algorithm that is different than the current study, LandScan "global" population data is becoming a standard baseline for population impact assessment in the disaster response community—so it is also appropriate for use in the current study.

3.2.1. *LandScan Population Data and Dasymetric Mapping Techniques*

Los Angeles County, with 88 incorporated cities, is the most populous county in the nation with over 10.17 million people (exceeded only by eight states), based on 2015 United States Census Bureau estimates. The eight-county Southern California Region, the basis for the OPLAN, has a population estimated at 23.6 million (2015). In order to map these populations at a community level, and to identify spatial patterns in emergency logistical resource requirements, dasymetric-mapping techniques through the Landscan 2015 "global" population database and the LandScan USA 2012 "conus_night" population database are employed in the current study.

In dasymetric mapping, data is transformed from an arbitrary spatial extent in the original source data (e.g. 2010 U.S. Decennial Census block geography) to standardized zones (e.g.

LandScan "global" (~1 km) based raster grid cells) that incorporate the use of additional data sets representing the variation in the underlying statistical surface (Aubrecht et al. 2013). The LandScan 2015 "global" (~1 km) and the LandScan 2012 "conus_night" (~90 m) population datasets both employ dasymetric mapping techniques by utilizing ancillary data to disaggregate coarse 2010 U.S. Decennial Census geography to areas which expose the distribution of the underlying population density (Bhaduri et al. 2007). An important benefit of using these techniques is that LandScan data in comparison with the 2010 U.S. Decennial Census block (or higher) level results in virtually equivalent total population counts. The total population for the census block can then be recovered by summation of the populations of the individual cells divided by the sum of the weights for all of the cells within it.

The LandScan dasymetric-mapping algorithm (Equation 2) is based on a ten-factor weighting process (as $W_{Cell\ i,j}$) for each of the respective ~1 km or ~90 m cells (as $Population_{Cell\ i,j}$), based on the proportional 2010 U.S. Decennial Census block population (as PC_{Block}) from Bhaduri et al. (2007):

$$\boldsymbol{Population}_{\mathbf{Cell\ i,j}} = \mathbf{PC}_{\mathbf{Block}} \times \mathbf{W}_{\mathbf{Cell\ i,j}} \tag{2}$$

$$\mathbf{W}_{\mathbf{Cell\ i,j}} = \mathbf{LC}_{\mathbf{i,j}} \times \mathbf{PR}_{\mathbf{i,j}} \times \mathbf{PRR}_{\mathbf{i,j}} \times \mathbf{S}_{\mathbf{i,j}} \times \mathbf{LC}_{\mathbf{i,j}} \times \mathbf{LM}_{\mathbf{i,j}} \times \mathbf{PRKS}_{\mathbf{i,j}} \times \mathbf{SCH}_{\mathbf{i,j}} \times \mathbf{PRSN}_{\mathbf{i,j}} \times \mathbf{ARPT}_{\mathbf{i,j}} \times \mathbf{WTR}_{\mathbf{i,j}}$$

LC = Weight of National Landcover Database (NLCD)
PR = Weight for Proximity to Roads
PRR = Weight for Proximity to Railroads
S = Weight for Slope factor
LM = Weight for Landmark polygon feature
PRKS = Weight for Parks and Open Space
SCH = Weight for Schools (K-12)
PRSN = Weight for Prisons
ARPT = Weight for Airports
WTR = Weight for Water Bodies
i,j = The Vertical and Horizontal Index for Each Raster Cell

One of the key weighting factors used by LandScan is the National Landcover dataset (NLCD), which can exclude unpopulated places in the dasymetric mapping results (Bhaduri et al. 2007). Using a 90-meter spatial sensitivity filter, a cross validation sensitivity analysis (Cai et

al. 2006) resulted in 72.5 percent accuracy in predicting the populated cells over residential locations and a 99 percent accuracy in predicting unpopulated areas in comparison with U.S. Census estimates and high resolution ortho-photography. The result is that Landscan dasymetric algorithm can identify where populations actually are, and where they are not, located in a study area which is essential for identifying affected populations and supporting emergency resource distribution.

A significant level of correlation between LandScan USA and the U.S. Decennial Census block populations in Los Angeles County also results with an R-squared statistic of .93 as shown in Figure 8 from the study by Bhaduri et al. (2007). In the current study, this is an important consideration, as social vulnerability modeled by SoVI uses 2010 U.S. Decennial Census tracts to aggregate the cumulative factor scores, and so this correlation minimizes uncertainty in the SoVI weighting calculation of the probabilistic risk model.

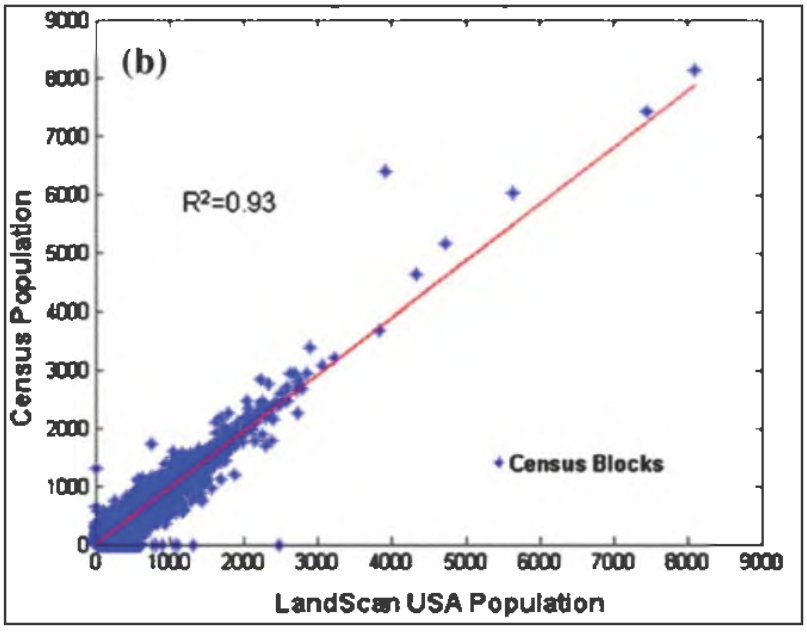

Figure 8. Landscan USA and U.S. Census population in Los Angeles County. Graph from Bhaduri et al. (2007).

LandScan USA 2012 “conus_night” (Figure 9) is the highest resolution population data available, and also the first to model diurnal population dynamics at a high-resolution (Bhaduri et al. 2007). These dynamics are important in the current study, as nighttime populations are the most accurate representation of when populations are most stable and where long-term emergency logistical resource requirements are most likely needed for affected populations.

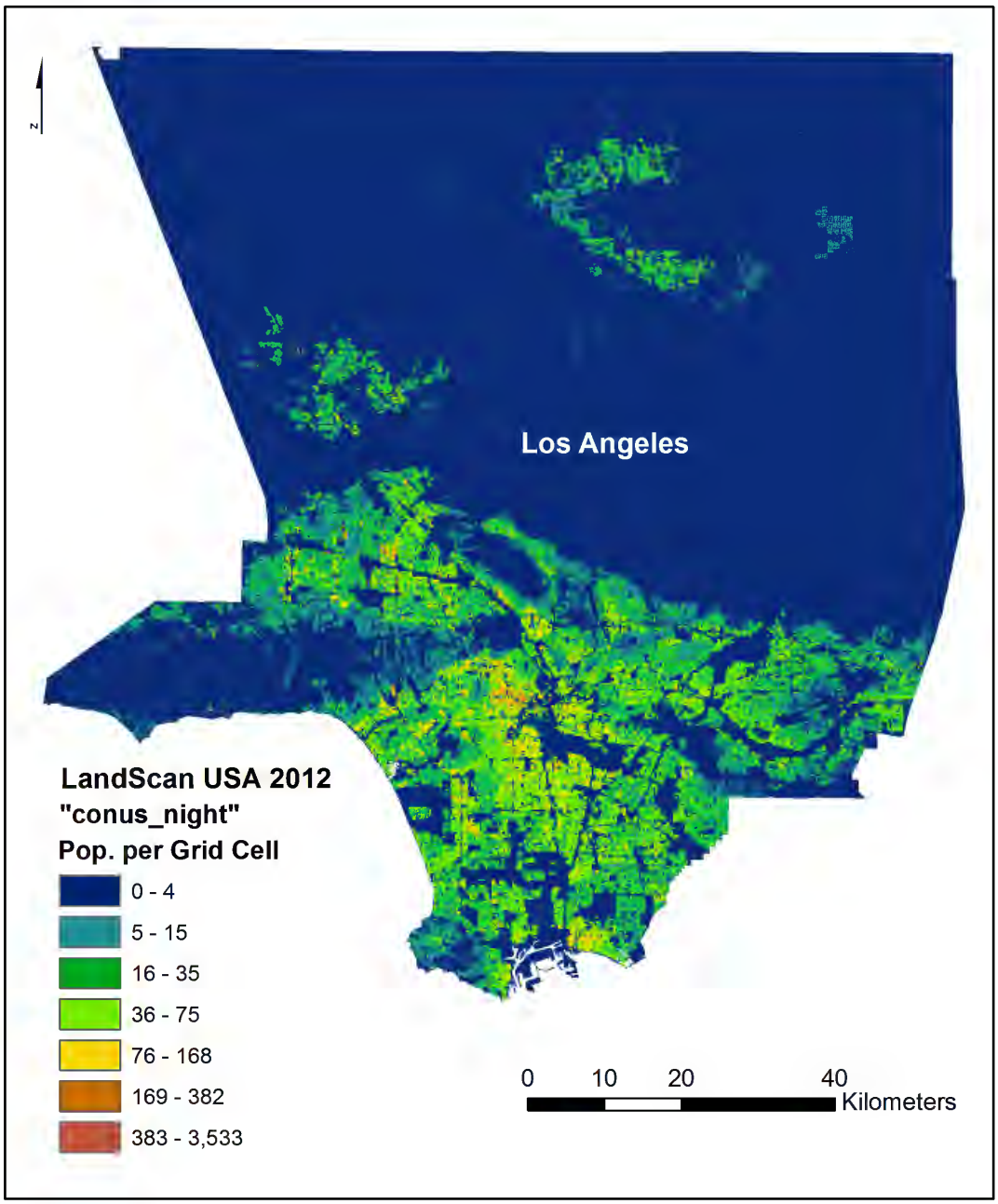

Figure 9. LandScan USA 2012 “conus_night” population in Los Angeles County

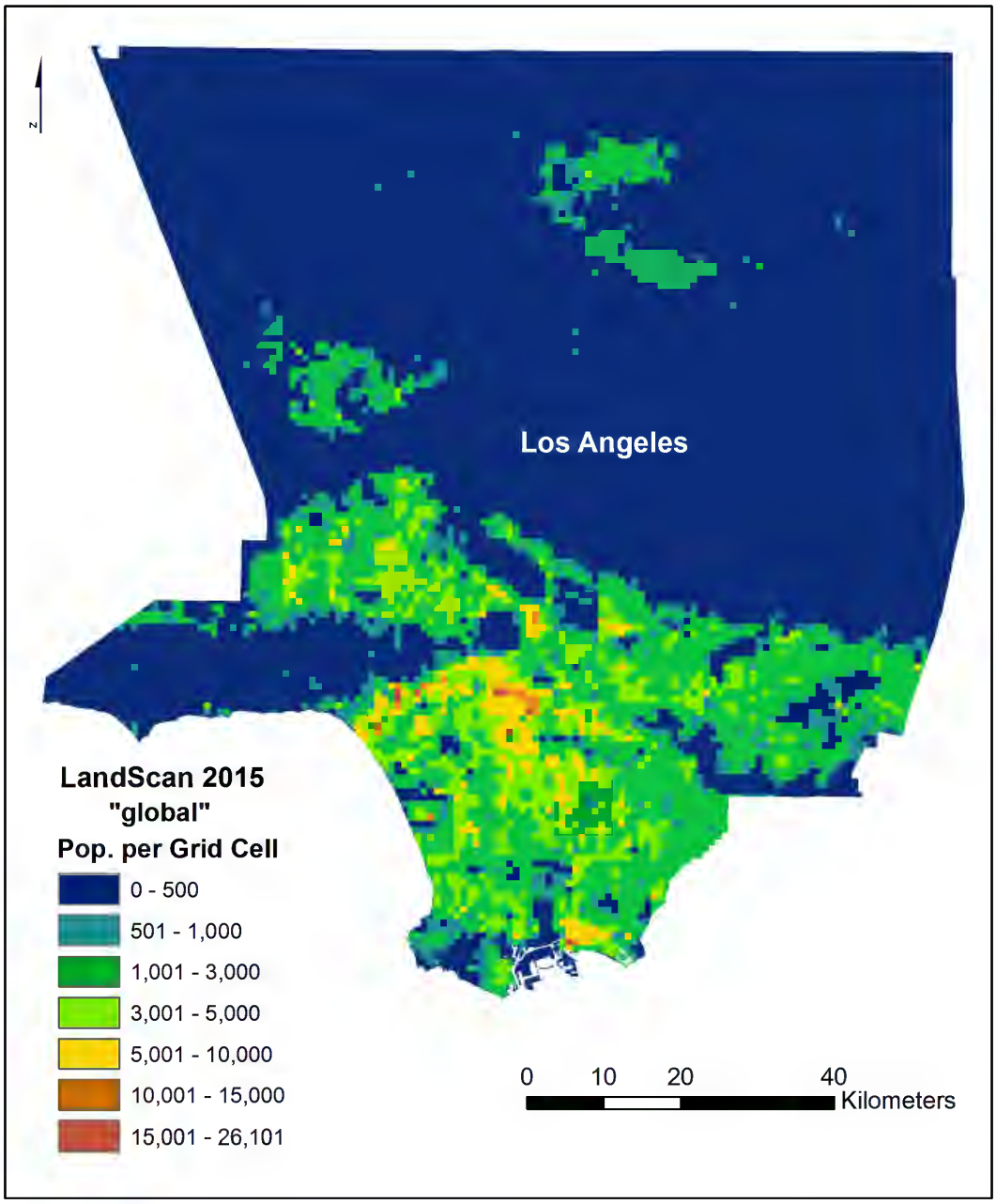

Figure 10. LandScan 2015 "global" population in Los Angeles County. Coverage in the eight-county study region is similar.

For the LandScan USA 2012 "conus_night" population data used in the current study, nighttime population is defined by Bhaduri et al. (2007) as:

$$\textit{Nighttime Population} = \textit{Nighttime Residential Population} + \textit{Nighttime Workers} + \textit{Tourists} + \textit{Business travelers} + \textit{Static Population} \quad (3)$$

For Los Angeles County, this results in a study area with 1,440,225 raster grid cells and a population of 9.66 million from the LandScan USA 2012 (~90 m) population dataset. For the eight-county study region 180,380 raster cells result for LandScan 2015 "global" (~1 km) population data (Figure 10, previous page) with a population of 22.36 million. These results can then be tractably converted to point centroids for analysis, which is investigated further in Chapter 4.

Some limitations to the LandScan population datasets do exist, however. As a dasymetric model, model validation is impractical and can only be achieved in comparison to the original aggregated data, rather than with ground truth studies (Bhaduri et al. 2007). Another limitation of the LandScan datasets are that they do not incorporate any other socioeconomic or demographic population characteristics found in the aggregated U.S. Decennial Census data other than the total population count. These characteristics, as the next section investigates, are critical in identifying the vulnerability associated with the lack of emergency food and resources in a disaster (NRC 2007; Paci-Green and Berardi 2015).

Another approach using LandScan 2015 "global" population data is the method recommended by Hansen and Bausch (2007) for extension of the HAZUS-MH loss estimation methodology in international applications. This method provides the added benefits of dasymetric mapping techniques for identifying population locations at a high-resolution, which extends the HAZUS-MH loss estimation methodology beyond its default 2010 U.S. Decennial Census geography-based approach. This method is similar to that proposed in the current study for modeling affected populations and connects the HAZUS-MH loss estimation methodology with the LandScan 2015 "global" population database.

For the current model design, LandScan data are used to represent the baseline population in the study areas without any modification and are identified by raster cell as:

$$\mathbf{[LandScan_{Population}]} \quad (4)$$

This notation is used for computational implementation of the *risk* equation as the *population* component. The bracket notation implies an Esri featureclass or raster dataset, with associated attribute (in one-to-one relationships) used in the computation of a single new raster grid cell ($Cell_{i,j}$) attribute or centroid point data attribute. This is introduced as the standard notation used in the current study to represent GIS data, outside of a VBScript or Python-based computational context.

From this section, it has been shown that mapping and analysis of the locations of exposed populations forms an essential first step in assessment of population impacts and social vulnerability in an impacted area. However, as the literature notes (e.g. NRC 2007; Paci-Green and Berardi 2015), once an event occurs, demographic structure and socioeconomic characteristics play an increasingly important role in estimation of *vulnerability* and *risk* and (as in the current study) specifically in regard to the risk for emergency logistical resource requirements. In the next section, these social vulnerability characteristics are investigated along with their relationship to food insecurity in disasters.

3.3. Social Vulnerability

Within the last 30 years, and especially after Hurricane Katrina, disaster research has focused on the pre-disaster political and socioeconomic conditions creating uneven vulnerability to natural hazards in the general population (Fussell 2015). The "vulnerability model" theorizes that socioeconomic, demographic and political processes (along with hazard exposure) affecting

the distribution of *resources* among groups of people produce *vulnerability* to natural hazards and can lead to a "disaster" (Tierney 2007).

Vulnerability can be defined as the potential for loss of life, injury or property from hazards, in addition to the definition in the previous section. The "hazards-of-place" model from Cutter (1996) combines the "biophysical vulnerability" (from the hazard and the environment) and "social vulnerability" to define a "place vulnerability". The current study is concerned chiefly with social vulnerability, as elements of physical vulnerability are included in the modeling components proposed and their impacts to affected populations.

3.3.1. *The Social Vulnerability Index*

Social vulnerability is defined as: "the social, economic, demographic and housing characteristics that influence a community's ability to respond to, cope with, recover from, and adapt to environmental hazards" (HVRI 2018, 1). For the current study, a working definition can be used from Cutter and Finch (2008) that social vulnerability "identifies sensitive populations that may be less likely to respond to, cope with, and recover from a natural disaster" (Cutter and Finch (2008, 2301). With this definition applied in the current study, the focus is then on the identification of sensitive "at-risk" populations that may be more likely to have emergency resource requirements.

Several studies indicate that disasters disproportionately impact demographically and socioeconomically disadvantaged groups, both in their initial impacts and in their ability to recover from them in the long term (e.g. Fothergill et al. 1999; Cutter et al. 2003; Fothergill and Peek 2004; Juntunen 2006; Philips et al. 2010; Gillespie and Zakour 2013; Lindell 2013). Vulnerability to disasters is amplified by demographic characteristics and represented by indicators (Cutter et al. 2003). For example, people with physical or mental disabilities, the

elderly or young, families in poverty or those who speak English as a second language, can have a much more difficult experience than the general population in disasters (Juntunen 2006; Philips et al. 2010). Among the most vulnerable populations are low-income individuals and families that lack the economic or physical resources to purchase or store basic emergency provisions such as food and water; repair their home; replace their property; or support themselves for the long term during recovery (Gillespie and Zakour 2013; Paci-Green and Berardi 2015).

As a result, the poor are more likely to lack the basic resiliency (e.g. income and/or assets) needed to prepare for a possible disaster or to recover from one (Cutter et al. 2003). These studies suggest that specific socioeconomic and demographic indicators can be used to isolate this social vulnerability and investigate its risks independently from other components, such as physical vulnerability and hazard-of-place models.

In the current study, The Social Vulnerability Index (SoVI), developed by the University of South Carolina, Hazards and Vulnerability Research Institute (HVRI) is applied as a sophisticated social vulnerability model that incorporates these findings. The Social Vulnerability Index can then be incorporated into the current study to provide an amplification factor for social vulnerability in the probabilistic risk model for emergency resource requirements.

The Social Vulnerability Index (SoVI) is a place-based social vulnerability index that includes demographic factor indices for population growth, socioeconomic status, gender, race/ethnicity, age, family structure, occupation, social dependence and special-needs (Cutter et al. 2003). For the built environment, it includes factor indices from land use such as: value, occupation of housing units, density of medical facilities, extent of infrastructure and rental versus ownership status. These factor indices were developed from the 2010 U.S. Decennial

Census and the Five-Year American Community Survey, 06-10. Using a factor analytic approach and principal component analysis (PCA), 30 socioeconomic and demographic variables were reduced to seven independent factors that accounted for about 72.5 percent of the variance in the results (HRVI 2018) as shown in Table 1.

Table 1. 2006‑2010 Social Vulnerability Component Summary. Data from HVRI (2018).

Cardinality	*Name*	*% Variance Explained*	*Dominant Variables*	*Factor Loading*
+	Race and Class	16.599	% Families with female-headed households with no spouse present	0.863
			% African American (Black) population	0.752
			% Persons living in poverty	0.715
			% Housing units with no car available	0.615
			% Civilian labor force unemployed	0.612
			% Population over 25 with less than 12 years of education	0.547
			% Children living in married couple families	-0.837
-	Wealth	15.905	Median dollar value of owner-occupied housing units	0.891
			% Families earning more than $200,000 per year	0.854
			Median gross rent for for renter-occupied housing units	0.85
			Per capita income	0.805
			% Asian population	0.681
+	Age	13.196	Median age	0.889
			% Population under 5 years or age 65 and over	0.767
			% Households receiving Social Security benefits	0.763
			% Unoccupied housing units	0.718
			Average number of people per household	-0.596
			% Renter-occupied housing units	-0.669
+	Ethnicity (Hispanic)	9.479	% population without health insurance	0.744
			% Hispanic population	0.725
			% Employment in extractive industries (fishing, farming, mining etc.)	0.545
			% Population over 25 with less than 12 years of education	0.532
			% Female participation in the labor force	-0.621
+	Nursing Home Residents	7.471	% Population living in nursing facilities	0.666
			Community hospitals per capita	0.643
+	Ethnicity (Native)	5.042	% Native American population	0.892
+	Employment in Service Industries	4.809	% Employment in service occupations	0.739
			% Families with female-headed households with no spouse present	-0.660
	Cumulative Variance Explained	**72.501**		

The final results of the SoVI model are a nationwide dataset, updated for the 2010 U.S. Decennial Census tract geography, that establishes relative factor scores for each component's contribution to social vulnerability, which are applied to each 2010 U.S. Decennial Census tract in the SoVI index, as shown in Figure 11.

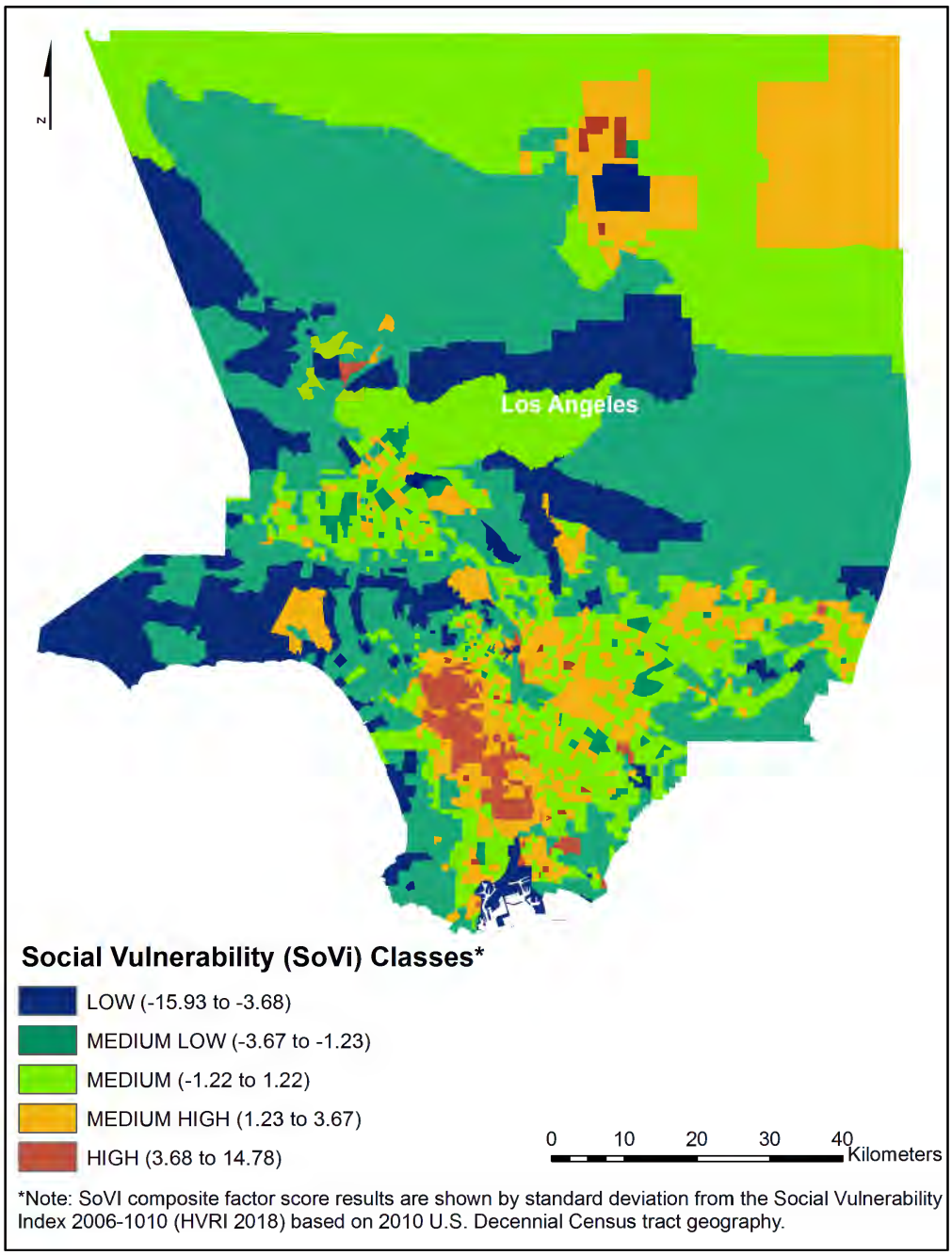

Figure 11. Modeled social vulnerability from SoVI in Los Angeles County. Data coverage in the eight-county study region is similar and is shown in Figure 37.

The authors summarize these factor scores as a new composite ranked distribution for each tract, which in the eight-county study region range from between -15.93 to 14.78 with an associated ordinal classification based on standard deviations, as shown in Figure 11 (HVRI 2018). The ordinal scheme ranges from: Low (-15.93 to -3.68), Medium Low (-3.67 to -1.23), Medium (-1.22 to 1.22), Medium High (1.23 to 3.67), and High (3.68 to 14.78) social vulnerability, based on the composite factor score. While the SoVI scores cannot be compared absolutely, the composite factor scores can be used to show the relative social vulnerability relationship of a census tract to others from its place on the continuum of values within the range.

3.3.2. *Social Vulnerability and Emergency Management*

The identification of socially vulnerable populations and the characteristics contributing to social vulnerability are critical elements of successful emergency preparedness, response, recovery and mitigation planning in disaster response (Cutter et at. 2006). As the literature notes (e.g. Juntunen 2006; Philips et al. 2010; Gillespie and Zakour 2013; Lindell 2013), socially vulnerable populations will require increased assistance (i.e. resources) throughout a disaster and have the most difficulty recovering.

It is this access to emergency life-saving and life-sustaining resources that exposes the main mechanisms through which hazards produce socioeconomic and demographic disparities—where socially vulnerable populations simply require more resources initially and for longer periods than the general population. These conclusions indicate that integration of social vulnerability models into the emergency management lifecycle should be a key priority. However, this has been difficult, as there have been few social vulnerability validation studies in the literature. Hobor (2015) is one of the few studies to have provided some validation of social

factors (i.e. indicators that are characterized through SoVI as "social vulnerability" in the current study) in relation to trajectories of recovery in New Orleans, Louisiana, and their correlation with long-term population fluctuations from 2000-2013 affected primarily by Hurricane Katrina recovery.

Hobor's results show that neighborhoods in New Orleans that have come back to around 75 percent of their pre-Hurricane Katrina population are the mean with those at 80 percent and above considered very successful and those below 60 percent are distressed. The study indicates that community recovery rates in New Orleans for Hurricane Katrina ranged from a standard deviation of approximately (±) 22 percent, with a mean rate of 75 percent, in consideration of social factors in the main trajectories of recovery (Hobor 2015).

As the best available validation of social vulnerability's influence in community recovery, these observations of (±) 22 percent range as amplification of initial resource requirements and recovery are taken as a key assumption in the current model design. This captures the findings from the literature that indicate socially vulnerable populations require a greater initial percentage of resources than the general population and take longer to recover, as identified above.

In order to computationally implement the Social Vulnerability Index (SoVI) with an amplification factor, the range of ranked factor scores from the original SoVI model are rescaled to a weighting that reflects the observations from Hobor (2015) of a (±) 22 percent range in standard deviation—which is calculated from 0.78 to 1.22, with 1 being the mean.

Standard statistical normalization procedures are used through feature scaling (Dodge 2003) to accomplish this in the model design as:

$$[SOVI_{Weight}] = a + \frac{(X - X_{min})(b - a)}{X_{Max} - X_{Min}} \quad (5)$$

a = .78
b = 1.22
X = [CA_Tract_SoVI_06_10]![SOVI0610CA]

The result is a *vulnerability* component of the computationally implemented *risk* equation that is combined with the *hazard* component as a product to represent social vulnerability amplification in the affected population. This also preserves the ranked social vulnerability relationships in the original data.

One final study by Noriega (2011) connects social vulnerability in cities within Los Angeles County to the (M) 7.8 San Andreas Earthquake Scenario in terms of economic losses and resources. The social vulnerability of cities in Los Angeles County "at-risk" from the (M) 7.8 San Andreas Earthquake Scenario was investigated with the intention of informing the distribution of resources before an event occurs. In relation to the current study, these findings suggest that in the event of the (M) 7.8 San Andreas Earthquake Scenario, communities with lower incomes, large minority populations and other social vulnerability characteristics may have a disproportionate impact, and therefore disproportionate resource requirement, from the general population.

Noriega's research in Los Angeles County concluded that the identification and location of socially vulnerable populations before a disaster can help target locations for initial resources after a disaster. Therefore, the objective to integrate social vulnerability amplification into the probabilistic risk model of emergency logistical resource requirements for affected populations in the (M) 7.8 San Andreas Earthquake Scenario is aligned with the recent research recommendations from Noriega (2011) in the Los Angeles County study region and so continues that work.

In conclusion, it is this access to emergency life-saving and life-sustaining *resources*—whether tangible resources in disaster response, recovery or mitigation, socioeconomic resources, or political—that leads to the most successful outcomes to all affected populations, and especially the socially vulnerable. In the current study, "resources" in the original *risk* equation are restricted to life-sustaining logistical commodities (e.g. food and water) and the resource requirements of disaster-affected populations—and so access to these resources is therefore the key determinant for *food security* in the disaster-affected populations.

As introduced in Section 2.2.3, food insecurity and its impacts in the ShakeOut scenario are directly related to social vulnerability and the complex interdependencies involved in food transportation, storage and commercial business networks that are interconnected with power, water and transportation infrastructure damage. Dwyer et al. (2004) also notes that vulnerability to food insecurity could not be determined by a single variable but, rather, through a combination of indicators, which is the approach to be used in the current model design.

Therefore, an appropriate research goal is to develop a modeling methodology for emergency logistical resource requirements and to estimate at-risk populations, by proxy, through using indicators from the infrastructure damage and restoration timelines along with social vulnerability factors in the (M) 7.8 San Andreas Earthquake ShakeOut Scenario.

3.4. Infrastructure Indicators and Modeling the Hazard Component of the Risk Equation

The United States Department of Homeland Security (U.S. DHS) and 42 U.S. Code § 519 define a *critical lifeline infrastructure (*or *lifeline infrastructure*s) as the systems and assets, whether physical or virtual, so vital that their disruption would have a debilitating effect on public health and safety. Components of lifeline infrastructure observed in the findings of the

previous sections include transportation, power and water systems. Different types of lifeline infrastructure systems and their components can be interconnected dependently on each other, which can be defined as *infrastructure interdependency.* Infrastructure interdependency is important in the current model design, as the components of the lifeline infrastructure, and their restoration timelines become increasingly connected as resource requirements are estimated over time (Bach et al. 2013).

An important factor for lifeline infrastructure in the United States is that privatization of utilities and their various proprietary service areas have resulted in a decentralized and often fragmented market with an increased number of actors operating in a single area (Bach et al. 2013). As the HAZUS-MH Technical Manual notes, detailed analyses and understanding of the interactions between components in a private sector lifeline utility requires their cooperation, data and an advanced system (network) analysis—which is difficult to coordinate and outside of the scope of the current study (FEMA 2003). This was also the conclusion in the ShakeOut scenario, as network analyses for most lifeline utility infrastructure sectors were not performed.

In the current model design, these issues limit the methodology for modeling lifeline infrastructure systems to established damage functions and supporting assumptions that relate infrastructure component distribution to population density. These assumptions are investigated further in Chapter 4. A simplified methodology is proposed for the current study using the established HAZUS-MH damage functions, with some extension, to align with the HAZUS-MH based ShakeOut scenario methodology.

In this approach, key components of the infrastructure systems are chosen that are sufficiently connected with population impacts and food insecurity. These are identified from the

literature (e.g. from Jones et al. 2008; CalOES and FEMA 2011; CalOES and UASI 2015; Paci-Green and Berardi 2015) as:

- Electric Power System Damage
- Natural Gas Pipeline Damage
- Water Pipeline Damage
- Bridge Damage
- Road Damage
- Rail Damage

The rest of this chapter investigates these infrastructure indicators as simplified independent components of the *hazard* in the *risk* equation through both the HAZUS-MH damage functions and through the ShakeOut scenario.

3.4.1. *HAZUS-MH Loss Estimation Methodology*

The Hazards United States Multi-Hazard (HAZUS-MH) loss estimation software is the FEMA standardized multi-hazard methodology that contains models for estimating potential losses from earthquakes and other disasters (Buika 2000; FEMA 2003; Kircher et al. 2006). It is considered the preeminent and authoritative loss-estimation methodology in the United States. The HAZUS-MH Technical Manual is a compilation of methodologies and data covering earth science, structural engineering, social science and economics and is the basis for the HAZUS-MH loss estimation methodology and software application, which itself is based on ATC-13 (1985). ATC-13 (1985) is the original study by FEMA and the Applied Technology Council used to estimate the economic impacts of a major California earthquake on the state, region and nation (FEMA 2003).

The HAZUS-MH Technical Manual has established general damage and restoration functions for lifeline infrastructure components, which can be implemented independently from

the HAZUS-MH software. The HAZUS-MH loss estimation methodology is one of the foundational components of the ShakeOut scenario and the OPLAN (Jones et al. 2008; CalOES and FEMA 2011). Therefore, it is an appropriate research goal to develop an approach to modeling emergency logistical resource requirements of affected at-risk populations that aligns with the HAZUS-MH loss estimation methodology. This methodology is employed, with some extension, using the HAZUS-MH Technical Manual and ATC-13 (1985) damage functions of the six indicators and infrastructure restoration timelines.

HAZUS-MH damage functions describe the probability (by lognormal cumulative distribution functions) of reaching or exceeding a specific damage state given ground-motion ShakeMap data (FEMA 2003). Restoration functions evaluate the loss of function and restoration sources (by normal cumulative distribution function) up to and including a specific time (in days) based on these same data sources. The damage states are identified as "minor", "moderate", "extensive" and "complete" and are used in both the probabilistic risk model and the estimation of resource requirements over time.

The damage functions used for computation of damage probabilities of the six infrastructure indicators are based on ground-motion parameters from the ShakeOut scenario (Jones et al. 2008). Most of these damage functions are formulated as cumulative distribution functions (CDFs) and are defined as:

$$CDF(X) = P\left(X \le x\right) = \int_{-\infty}^{x} P(t)\,dt \qquad (6)$$

X: A random variable $\quad x, t \in \mathbb{R}$

$P\left(X \le x\right)$: Cumulative probability that the random variable X is less than or equal to a number x

The normal CDF function represents the cumulative probability that the random variable X is less than or equal to a number x (Pitman 2006), which in the current study is used to

estimate restoration times up to and including a specific time (in days) for each damage state (FEMA 2003). The lognormal CDF function is the maximum entropy probability distribution for a random variable X and so in the current study this represents the cumulative probability of being in, or exceeding, each damage state given a specific level of ground motion. A *maximum entropy* probability distribution is defined as having entropy that is at least as great as that of all other members of a class of probability distributions, where entropy can be considered as a measure of information loss (Jaynes 2003). A CDF can be generated and evaluated with only two parameters: a mean, μ or log(μ) for the lognormal CDF, and a standard deviation, σ, through MATLAB statistics libraries.

3.4.2. *Limitations of the HAZUS-MH Loss Estimation Methodology and Extension*

In order to handle more complex approaches for modeling logistical resource requirements, the HAZUS-MH loss estimation methodology must be extended. For example, while HAZUS-MH provides some estimates for lifeline utility outages, which could be considered *prima facie* as the required indicators in the probabilistic risk model for modeling emergency resource requirements for affected populations at (t = 3), further investigation shows that those estimates use a methodology that is incomplete and subject to too much uncertainty (see Section 3.4.3 and Appendix B). Currently, HAZUS-MH neither has the built-in capability to model the disaster-affected population's emergency resource requirements after (t = 0) days, nor provide these estimates with enough precision and with a complex enough methodology for emergency managers to support community level emergency logistical resource planning for affected populations.

One of the more advanced studies to extend the capabilities of HAZUS-MH for modeling emergency resources is the MAE (2009) study for the New Madrid Seismic Zone developed by

the Mid-America Earthquake (MAE) Center and the Central United States Earthquake Consortium (CUSEC). In that study, the authors define at-risk populations as those displaced households (due to structural damage) and those without water and/or power for at least 72 hours. They provide estimates for affected populations up to (t = 3) days post-event, with similar application to the approach proposed in the current study. However, they do so completely within the HAZUS-MH loss estimation software platform, and so are limited by the inherent uncertainty within this methodology. Their estimates are made without considerations for social vulnerability and an advanced social vulnerability model. They also do not incorporate the indicators representing the interconnections between transportation infrastructure damage with water and power infrastructure restoration that the literature suggests drive food insecurity issues.

The MAE (2009) study identifies these issues as major gaps in the HAZUS-MH modeling capabilities for logistical planning support. In the "New Models and New Components" development recommendations of their study, they identify several gaps in the current capabilities for logistical planning support and situation awareness. These include modeling community level resource requirements, modeling mass care resource requirements in consideration of social vulnerability, and modeling resource requirements over time in logistical planning.

In summary, all of the literature points to the interconnections between critical lifeline power, water and transportation system infrastructure as indicators associated with food insecurity and business interruption, with amplification by social vulnerability factors. The current study, therefore, attempts to address some of these identified capability gaps through a probabilistic risk modeling methodology for emergency logistical resource requirements, with

some extension of the HAZUS-MH loss estimation methodology using the damage functions from the HAZUS-MH Technical Manual and ATC-13 (1985) study.

An overview of the narrative of impacts from the Shakeout scenario and connection with the HAZUS-MH loss estimation methodology provides the final justification for the choice of the six indicators and restoration functions.

3.4.3. *Electric Power System Damage and Restoration in the ShakeOut Scenario and HAZUS*

Throughout the eight-county region, energy lifeline infrastructure system impacts in the ShakeOut scenario include electric power system damage and outages as well as natural gas pipeline impacts. The scenario narrative indicates that:

> Electric power is lost throughout the distribution systems in the study area immediately, and it is restored to 90 percent of those capable of receiving it within three days. Los Angeles, San Bernardino, and Riverside Counties immediately lose all electric power. Gas pipeline damage reduces the ability to produce power within the affected areas of those counties. Within 24 hours, repairs restore 30-50 percent of service; within three to ten days, 75-90 percent of those capable of receiving power have service restored; and in one to four months virtually all power is restored (Jones et al. 2008, 94).

The HAZUS-MH Technical Manual estimates electric power system outages in the region to be dependent on the functionality of medium voltage substations (FEMA 2003). An electric substation is a facility that operates as the source of power supply for the community in the local service area. These components of electric power systems are among some of the most vulnerable in an earthquake. Damage to medium voltage substations can impact large areas. However, many of the substations in California have been seismically retrofitted (Jones et al. 2008). These service areas, which are often proprietary business information, were not available for the ShakeOut scenario or for the HAZUS-MH loss estimation methodology in the current study.

To generate the CDF damage functions for medium voltage substations with seismic components (Figure 12) the following parameters are used from the HAZUS-MH Technical Manual: minor, ($\mu = 0.15$, $\sigma = 0.6$); moderate, ($\mu = 0.25$, $\sigma = 0.5$); extensive, ($\mu = 0.35$, $\sigma = 0.4$); and complete, ($\mu = 0.7$, $\sigma = 0.4$).

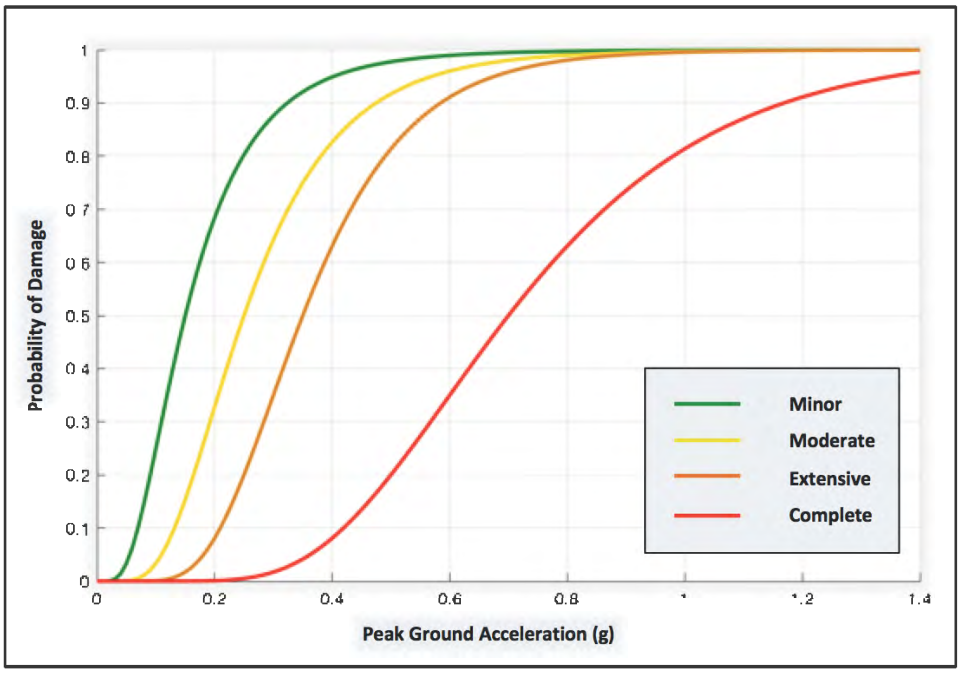

Figure 12. Probability of damage for medium voltage substations with seismic components

Restoration functions for electric substations and distribution circuits in the HAZUS-MH loss estimation methodology are based on empirical data from G&E (1994) and are shown in FEMA (2003) to mostly be vulnerable to Peak Ground Acceleration (PGA). Restoration functions (also called restoration curves or restoration timelines) determine the estimated timeframe for repair or replacement back to full capacity (100 percent) of the infrastructure systems, where the discrete time (in days) for complete restoration at each damage state are calculated or estimated.

Discrete power restoration timelines, based on the HAZUS-MH damage categories show for 100 percent restoration: minor (3-days), moderate (7-days), extensive (30-days) and complete (90-days). Power restoration timelines from the ShakeOut scenario are based on expert panel recommendations and are estimated at: minor (6-days), moderate (9-days), extensive (21-days) and complete (120-days). It should be noted that the ShakeOut estimates include a range of uncertainty in the narrative for the restoration timelines, which is not found in the HAZUS-MH Technical Manual restoration timeline curves.

To associate power damage and power restoration timelines with power outages (and affected populations) in the impacted areas, the HAZUS-MH Technical Manual recommends a performance evaluation methodology (shown in Equation 7). This methodology is employed in the current study to calculate the probability for power outages at day-three (FEMA 2003):

$$[POWER_{Damage}] = 1 - \sum_{i=1}^{5} [Restoration]_i \times P[Damage\ State_i \mid PGA] \quad (7)$$

Damage State ∈ {1 - minor, minor- moderate, moderate - extensive, extensive – complete, complete }

Restoration = (1, 1, .95, .49, .04)

Note: **Restoration** values are estimated based on both the ShakeOut Scenario and the HAZUS-MH 4.0 restoration functions

The default power restoration times from the HAZUS-MH Technical Manual are updated in the current study to include information from both the ShakeOut scenario and the empirical sources from the HAZUS-MH loss estimation methodology (FEMA 2003; Jones et al. 2008). In general, the ShakeOut scenario estimates a rapid infrastructure recovery at day-three, while the HAZUS-MH restoration times estimate a slower recovery. The “none”, “minor” and “moderate” damage states are estimated at near 100 percent recovered in both HAZUS-MH and the ShakeOut scenario at day-three and so these values are chosen to reflect this rapid recovery of minimally impacted areas. The “extensive” damage state is taken as the average of the HAZUS-

MH and the ShakeOut scenario restoration time as 49 percent. In this case, due to the large range of uncertainty in the ShakeOut estimates for restoration times, the timelines diverge from the HAZUS-MH loss estimation methodology estimates significantly—therefore an average is chosen to account for both sources. Finally, the "complete" damage state is taken from the HAZUS-MH restoration times, as 4 percent—which also captures the observation from the ShakeOut scenario that a maximum 120-day restoration timeline will be expected in the most severely impacted areas. These values are then used to calculate [$POWER_{Damage}$] at day-three.

In general, the HAZUS-MH loss estimation methodology is primarily focused around estimation of discrete infrastructure damage and restoration and so population impact estimation is much less advanced. An extension of the methodology is therefore required, as the current HAZUS-MH loss estimation methodology for populations affected by power utility outage is subject to a large degree of uncertainty. This is, in part, due to the *modifiable areal unit problem* (MAUP) in the variation of real world service area extents. The MAUP is a source of significant statistical bias and can significantly impact the results of calculations (Fotheringham et al. 1991). MAUP effects result when spatial phenomena, such as populations, are aggregated into areas. The resulting summary values are influenced by both the shape and scale of the aggregation unit (Openshaw 1984).

The HAZUS-MH loss estimation methodology for power utility outage is to average the probability of damage for all of the discretely located substations. A single "percentage-of-impact" weighting factor is then applied to the population of the entire study area such that every 2010 U.S. Decennial Census tract gets the same impact weight (FEMA 2003). Populations in the most severely impacted regions will be systematically underestimated and those in the least impacted regions will be overestimated based on that method and variably sized service areas as

an additional weighting factor (and the MAUP effect) are not even considered—so this methodology is not appropriate for determination of real-world population locations with emergency resource requirements.

To extend and improve this methodology for the current study, the assumption is made that the substations are more-or-less evenly distributed in the study region at the LandScan cell resolution, proportional to population density. The probability of outage is calculated, as the HAZUS-MH Technical Manual suggests using Equation 7 (FEMA 2003). Affected populations are then directly calculated based on the discrete Landscan raster cell population. This addresses the MAUP problem, within the uncertainty range inherent in the original method.

To validate this extension of the HAZUS-MH loss estimation methodology, it is sufficient to show that in the current study region this assumption and calculation of power outage affected population decreases the uncertainty of the original HAZUS-MH method, or that it is at least as good as the current standard. This conclusion is confirmed by further investigation provided in Appendix B.

3.4.4. *Natural Gas and Water Pipeline Damage and Restoration in the ShakeOut Scenario and HAZUS-MH*

Infrastructure indicators and food insecurity, as the literature has shown, are interconnected to business restoration because without electricity, gas, water and a transportation system, businesses are unable to function. Water utility service loss is a key factor in business interruption, as water loss can affect eight out of ten businesses in a disaster-impacted region (Jones et al. 2008).

As the ShakeOut scenario and OPLAN indicate, in some of the most heavily impacted areas the number of pipe breaks will be so severe the entire system will need to be recreated (Jones et al. 2008). These areas may not have residential, commercial or industrial water supplies

(and so also severe business interruption and food insecurity) for up to six months. Some of the more moderately impacted areas may expect up to two months without functioning water utilities. The lack of water conveyance (i.e. functioning pipelines) "becomes the largest factor in business interruption losses for the ShakeOut scenario, resulting in $50 billion in lost economic activity" (Jones et al. 2008, 9).

Business interruption has cascading negative effects throughout the community, whether businesses are specifically related to food security (e.g. grocery stores, restaurants and supermarkets) or are peripherally interconnected through the supply-chain and the regional economy (Rose et al. 2012). These factors inevitably affect the most vulnerable populations in a greater amount and for longer periods, as the literature has shown.

The ShakeOut scenario narrative continues for pipeline damages and their restoration timelines:

> Pipeline damage causes the loss of piped drinking water in much of the most strongly shaken areas (with MMI VIII+ shaking) for a week or more (Jones et al. 2008, 95)

> Communities within about 10 miles of the fault and small communities in isolated regions have pipeline damage so severe as to impair piped water supply for up to six months, with repairs proceeding in some prioritized fashion. Perhaps 5 percent of customers in small regions throughout Los Angeles, Riverside, and San Bernardino Counties have pipeline damage requiring between one week and two months to repair, before piped water supply is available (Jones et al. 2008, 150).

The HAZUS-MH methodology calculates water and gas pipeline damage based on Peak Ground Velocity (PGV) or Peak Ground Deformation (PGD) and assumes an 80 percent brittle pipeline ratio (FEMA 2003). Therefore, there is some divergence from the ShakeOut methodology, which estimates restoration timelines through the water utility expert panel by MMI, liquefaction and landslide potential (Jones et al. 2008). In the current study, the brittle pipeline damage function is assumed for all pipelines in the model design as a cautious approach

to avoid underestimation and is based on Peak Ground Velocity (PGV) only, as ground deformation data for liquefaction and landslide were not available.

The brittle pipeline damage function is based on the empirical data of O'Rourke and Ayala (1993). The data correspond to empirical brittle pipeline damage observed in six historic earthquakes in the United States and Mexico, where the diameter of the pipe is not considered in modeling the damage function. The following equation is provided for the repair rate (in repairs/km which can also be considered as the damage rate) of brittle pipelines with PGV in cm/sec (FEMA 2003):

$$\mathbf{Repair\_Rate} \cong \mathbf{0.0001} \times (\mathbf{PGV})^{\mathbf{2.25}} \tag{8}$$

A study by Isoyama and Katayama (1982) defined the original probability function for pipeline failure, which was assumed to follow a Poisson distribution due to the inherent uncertainty in vulnerability assessment. The probability was then converted to the average break rate, as in (Figure 13) from O'Rourke and Ayala (1993).

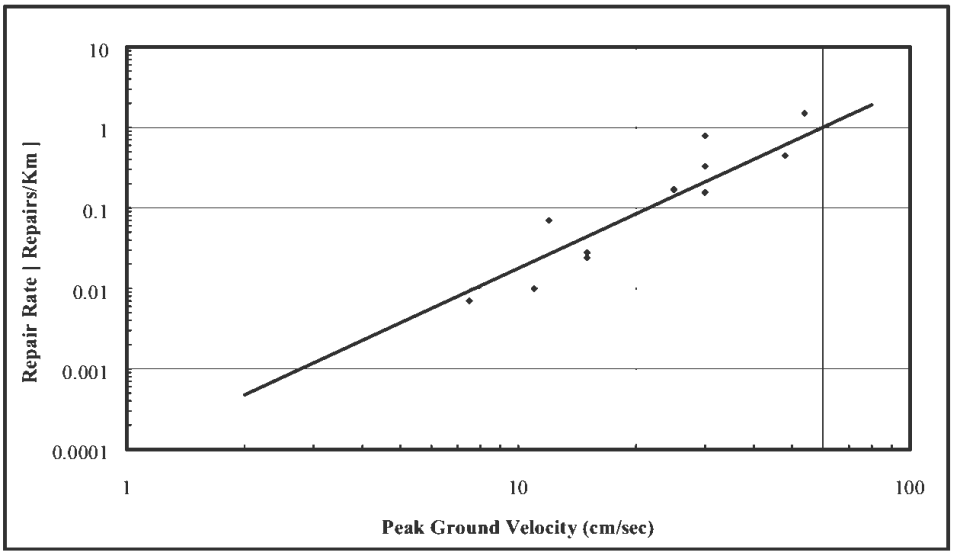

Figure 13. Repair rate per kilometer for pipeline damage. Graph from FEMA (2003).

In the current study, a simplified approach is applied, with results similar to the continuing work of Isoyama et al. (1998) and Sousa et al. (2012). These studies advance the original HAZUS-MH damage functions through the development of new rate curves for pipeline damage estimation with additional empirical data. The current study uses feature scaling (Equation 9) to normalize the fragility curve of the empirical data from O'Rourke and Ayala (1993), which results in a curve similar to Isoyama et al. (1998). Damage percentages are then directly calculated per discrete cell value, with the assumption that the maximum value can be taken as the upper bound for the percentage of complete damage:

$$[PIPES_{Damage}] = \frac{X - X_{Min}}{X_{Max} - X_{Min}} \tag{9}$$

Note: The range of values from evaluation of equation 8 are defined here as X, along with the X-minimum and X-maximum from these calculations in the study area.

This approach also has some intuitive results, as the units of repairs/km are generalized to a dimensionless measurement scale as the probability of repair to any random pipe per raster cell is calculated as a result of the percentage of damage per cell. This is founded on the assumption that the pipelines are more-or-less evenly distributed in the study, proportional to population density and randomly distributed per cell. The correlation of pipelines to population density can compensate for the variability of total pipelines per cell as the affected population increases proportionally to the population density and probability of pipeline damage.

Discrete water pipeline restoration timeline, based on the ShakeOut scenario panel estimates in Jones et al. (2008), shows: minor (7-days), moderate (14-days), extensive (60-days) and complete (180-days).

The HAZUS-MH loss estimation methodology uses the same damage functions for water pipes, natural gas and oil pipelines (FEMA 2003). While natural gas pipelines are modeled with the same damage function as water conveyance in Figure 13, their restoration timelines are different, as the ShakeOut narrative shows:

> For natural gas, damage to main distribution lines is caused by building damage and ground failure, with 50 percent of gas customers within the MMI VIII+ and in areas with landslide and liquefaction damage (MMI X) are without gas service for up to three weeks. Five percent of customers are without gas for between three weeks and two months (Jones et al. 2008, 148).

Discrete natural gas pipeline restoration timelines, based on the ShakeOut scenario panel estimates show: minor (7-days), moderate (14-days), extensive (21-days) and complete (60-days). The "minor" and "moderate" categories are estimated, based on the water pipeline restoration function, as no other data is available.

3.4.5. *Bridge System Damage and Restoration in the ShakeOut Scenario and HAZUS-MH*

The final narrative for the ShakeOut scenario is related to transportation, which includes rails, roads and bridges. The ShakeOut scenario notes that the Southern California road network consists of hundreds of thousands of "bridges", mostly on local roads, with many per square kilometer (Jones et al. 2008). A *bridge* is defined as a structure spanning and providing passage over a gap or barrier, such as a river or roadway. Whenever "a road is not poured literally on the ground it is considered a bridge" (Jones et al. 2008, 135).

For the ShakeOut scenario, a supplemental study by Werner et al. (2008) for bridge damage was developed that included a deterministic risk of ground-motion-induced damage and repair times to 6,719 interstate, national and California highway bridges from the National Bridge Inventory (NBI) and the National Highway Planning Network (NHPN). For all bridges in the study region, 92 percent are identified as concrete and 6 percent are steel (Yu 2015). The

model in Werner et al. (2008) uses the Spectral Acceleration (1.0 Second) ground-motion ShakeMap data, with the same damage functions as the HAZUS-MH methodology (FEMA 2003).

Werner et al. (2008) also notes that 24 percent of the major bridges in the region have completed some seismic retrofitting, while Jones et al. (2008) notes that most of the local bridges have not been seismically retrofitted and so proportionally more damage is expected to them. Finally, Werner notes the importance of bridge performance and restoration as an indicator in the overall resiliency of the transportation system in the region, which is interconnected with economic, disaster response and other lifeline infrastructure interdependencies in the ShakeOut scenario. The transportation damage narrative from the ShakeOut scenario continues:

> Many roads and highways will be impassable in the first few days after the earthquake because of debris on the roads, damage to bridges, and lack of power for the traffic signals. This will have a significant negative impact on the emergency response. Because of the major highway bridge retrofit program of the last 20 years, highway bridges are not expected to completely collapse, but some will not be passable. Many bridges on local roads have not been retrofitted and more damage is expected on those (Jones et al. 2008, 8).
>
> Shaking-related damage to highway bridges renders most freeways in Los Angeles, San Bernardino, and Riverside counties impassible at several locations, with some damages taking as long as 5-7 months to repair (Jones et al. 2008, 94).
>
> Irreparable bridge damage will take 5-7 months to rebuild, and one month to open the roads beneath the bridges. Extensive damage and moderate damage will take weeks and days to repair, respectively (Jones et al. 2008, 137).

The results of Werner et al. (2008) identify five zones with a high-degree of "complete" bridge damage where bridges are irreparably damaged and require total replacement (Figure 14).

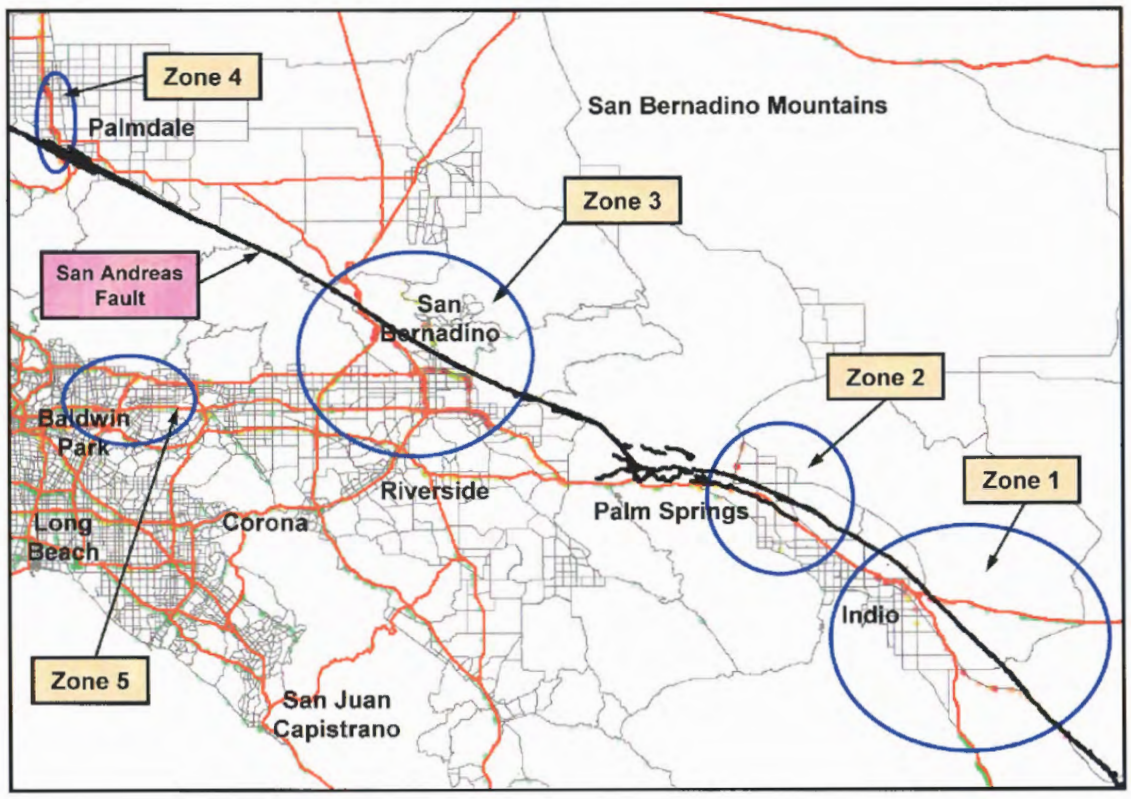

Figure 14. Complete bridge damage in the ShakeOut scenario. Map from Werner et al. (2008).

The HAZUS-MH Technical Manual uses 1.0 second peak spectral acceleration (SA10) ground-motion to evaluate structural damage to bridges, based on 28 bridge classes and a number of other parameters (FEMA 2003). From the literature (e.g. Yu 2015; Werner et al. 2008), more than 92 percent of the bridges in the region are concrete, and 6 percent are steel with 24 percent having been seismically retrofitted. Therefore, parameters are available to create a proportional weighted averaging model curve for characteristic bridges in the region. The average "probability of bridge damage" in the *hazard* component of the *risk* equation is then calculated based on the HAZUS-MH Technical Manual loss damage function parameters for bridge classes.

In the current study, all of the "non-CA" bridge classes were removed and the advanced HAZUS-MH parameters (e.g. shape, skew and factor shape) set equal to one. The associated

parameters for generation of the average impact CDF damage functions are: standard deviation, $\sigma = 0.6$ and mean, μ from the following proportional weighted mean equation:

$$\mu_{pavg} = \frac{\sum_{i=1}^{23} \mu_{HWB(i)} \times [Retrofit]_i \times [Type]_i}{\sum_{i=1}^{23} [Retrofit]_i \times [Type]_i} \quad (10)$$

For each "damage state", μ calculated : {slight, moderate, extensive, complete}

Highway Bridge (HWB) classes: Of 28 total 5 are non-CA and are excluded

Type = .92 for "concrete" or .06 for "steel" or .02 for "others"

Retrofit = .24 for "seismically retrofitted" or .76 for "no retrofitting"

This resulted in the following parameters for mean, μ to calculate CDF functions (Figure 15) for: minor, ($\mu = 0.5$, $\sigma = 0.6$); moderate, ($\mu = 0.7$, $\sigma = 0.6$); extensive, ($\mu = 0.8$, $\sigma = 0.6$); and complete, ($\mu = 1.2$, $\sigma = 0.6$);

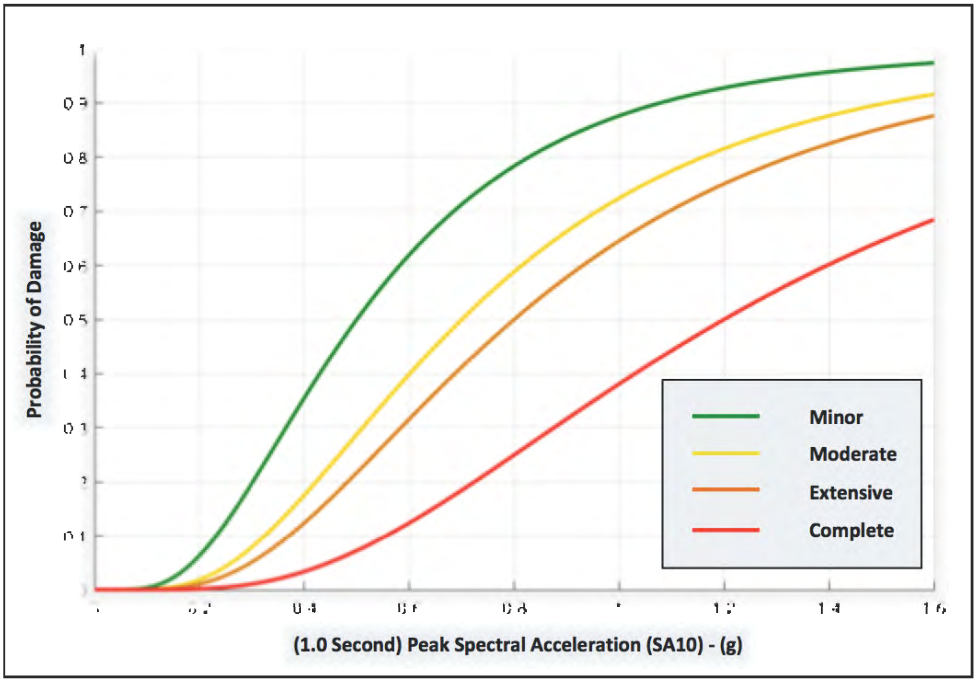

Figure 15. Probability of bridge damage based on weighted average method

The discrete probability of meeting or exceeding the "complete" damage category was then calculated as per the HAZUS-MH technical manual and evaluated as (FEMA 2003):

$$[\mathbf{BRIDGE_{Damage}}] = \mathbf{P[Complete\ Damage \mid SA10]} \quad (11)$$

This methodology was validated in Appendix C to ensure that it preserved the five complete bridge damage areas in its results in comparison to Werner (2008) identified in the ShakeOut supplemental study. The large numbers of bridges in the study region, too small for the NBI inventory but still subject to ground-motion-induced damages are assumed more-or-less evenly distributed in the study region (along with the other NBI bridges) proportional to population density and randomly distributed within each cell. This method is similar to the HAZUS-MH loss estimation methodology for averaging damage impacts from power system components as a general weighting to all of the 2010 U.S. Decennial Census tracts to calculate impact to the population (as discussed in Section 3.4.1).

Bridge restoration timelines from the Werner et al. (2008) supplemental study indicate: minor (3-days), moderate (12-days), extensive (49-days) and complete (140-days).

3.4.6. *Road and Rail System Damage and Restoration in the ShakeOut Scenario and HAZUS*

Roads and rails are subject to Peak Ground Deformation (PGD), which is associated with the surficial fault rupture, liquefaction and landslide potential (FEMA 2003). As Werner et al. (2008) noted, ground deformation data, other than the surficial fault rupture, was not provided for the study. Similarly, the current study is not able to use PGD, liquefaction and landslide potential to model these impacts. The Applied Technology Council-13 (1985) study, the seminal study that forms a core component of the HAZUS-MH loss estimation methodology, does provide an alternate method based on the Delphi model for expert opinion solicitations (Dalkey et al. 1970) to develop a road and rail damage curve, using high MMI values (VI+).

ATC-13 (1985) identified "Roadway and Pavements" motion-damage relationships for "Highways" as Facility Number 48 and "Rails" as Facility Type 47 in Appendix G, Table G.1 of

the study. To construct a trend curve based on the MMI levels a maximum, M, value of the best estimate and weighted standard deviation of the best estimates, σ, for both facility numbers were required. These are identified as MAXB and SDEVB respectively in the ATC-13 (1985) study. The road and rail damage probabilities were then directly calculated from the respective trend functions generated for the MMI values shown in Table 2.

Table 2. MMI based damage probabilities for highways and rails

	Highways		Rails	
MMI	M	σ	M	σ
VI	0.004	0.001	0.01	0.002
VII	0.01	0.004	0.05	0.005
VIII	0.1	0.02	0.1	0.013
VIX	0.15	0.029	0.25	0.045
X	0.2	0.046	0.29	0.063
XI	0.5	0.064	0.6	0.078
XII	0.8	0.081	0.8	0.15

Source: Data from ATC-13 (1985), Appendix G, Table G.1

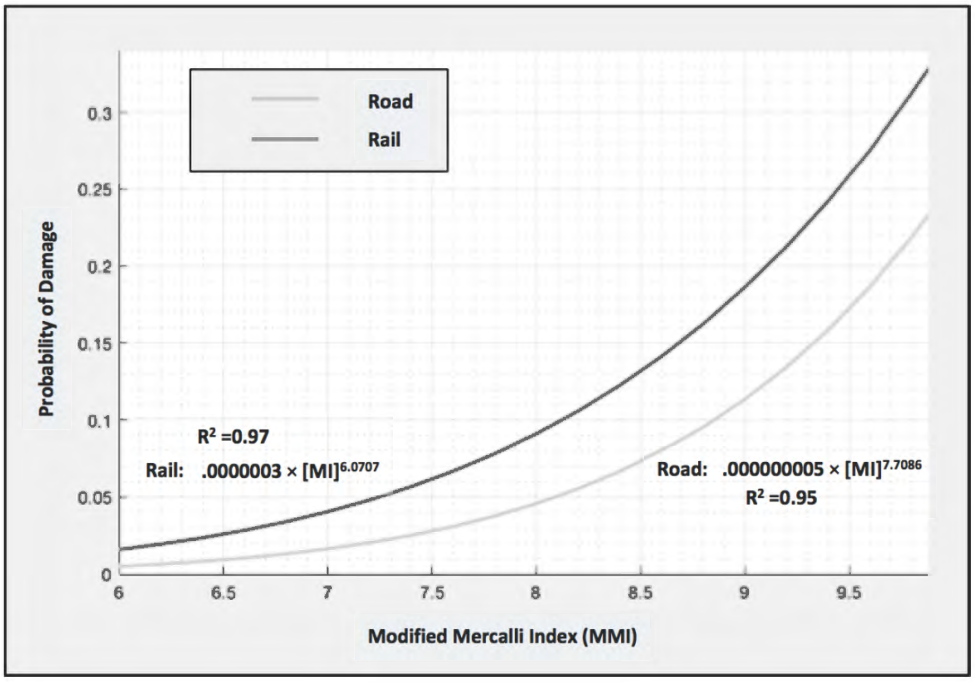

Figure 16. Road and rail damage probability from MMI. Data from ATC-13 (1985).

The discrete road system restoration timelines, based on the HAZUS-MH damage categories show: minor (2-days), moderate (7-days), extensive (62-days) and complete (62-days). Discrete rail system restoration timelines, based on the HAZUS-MH damage categories show: minor (2-days), moderate (11-days), extensive (49-days) and complete (180-days).

In summary, six damage functions have been identified from the HAZUS-MH Technical Manual and ATC-13 (1985), along with their associated restoration timelines, which have been incorporated into the model design (with some extension). These were combined into the *hazard* component of the probabilistic risk model, which is investigated in Chapter 4.

3.4.7. *Empirical Restoration Curves for Emergency Logistical Resources*

Most of the damage functions from the HAZUS-MH Technical Manual and results from the Shakeout scenario have restoration timeline curves associated with them. For the current study, a similar modeled curve for logistical resources requirements over time must be developed, in order to calculate resource requirements at specific discrete time intervals. From investigation of the tools used by the United States Army Corps of Engineers (USACE), and recent events in the commodity mission for Puerto Rico in Hurricane Maria, two very different restoration curves for resource requirements are found. These were used in the current study, in the methodology of Chapter 4, to create three possible simulations for resource requirements over time.

The USACE is identified as the lead agency for the commodity distribution mission, in coordination with FEMA and the Defense Logistics Agency (DLA) in the event of a catastrophic event. For the commodity mission, the USACE uses a strategic planning tool based solely on population impacted by power outage and the expected number of PODS to be activated in an impacted area (USACE 2008). This tool (an excel spreadsheet) then calculates the decreasing

amount of commodities for the entire incident. The model was originally designed to support emergency planning in suburban, rural and coastal areas in the southeastern United States and may have a large margin of error in urban areas (UASI 2014). This model also assumes a rapid timeline for infrastructure restoration, whether by repair or replacement of damage facilities or augmentation by emergency power generation capabilities—which as recent events have shown, may not be realistic.

For the current study, the USACE strategic planning tool was experimentally applied to estimate logistical resource requirements for 143 PODs in the Los Angeles County study area. The key information from this result are the graph and trend line shown in Figure 17. These trend equations and associated parameters for the affected categories in the four damage states are further investigated in Chapter 4 and were used as one simulation for resource requirements over time.

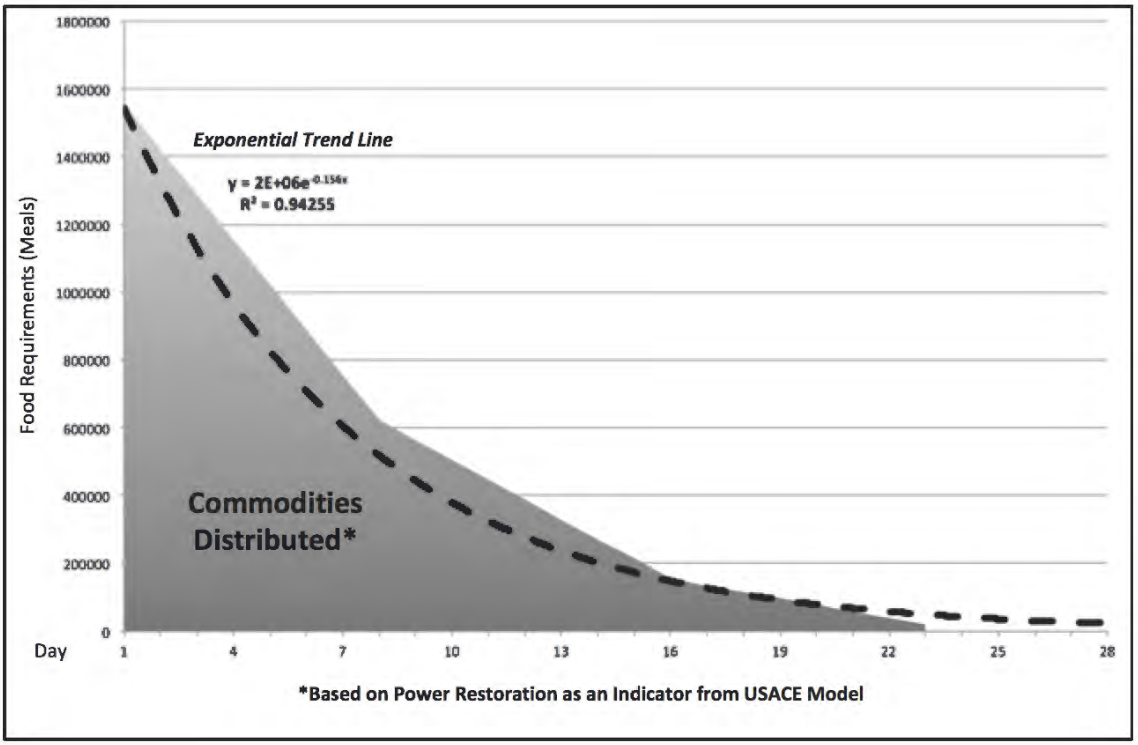

Figure 17. General resource requirements over time from the USACE model (USACE 2008)

The Puerto Rico logistical response for Hurricane Maria can serve as a model for the worst-case scenario, and so was chosen as a second possible restoration curve for emergency logistical resource requirements. The Puerto Rico logistical response is the largest commodity mission ever supported by the United States government, compounded with infrastructure restoration delayed for an extended period (FEMA 2018b). Figure 18 summarizes Puerto Rico commodity information from publicly available daily situation reports for six weeks (FEMA 2017). The total population affected is based on power service restoration estimates for an initial population of 1.5 million, which, it should be noted, is less than half of the population expected to have emergency logistical resource requirements in the (M) 7.8 San Andreas Earthquake Scenario.

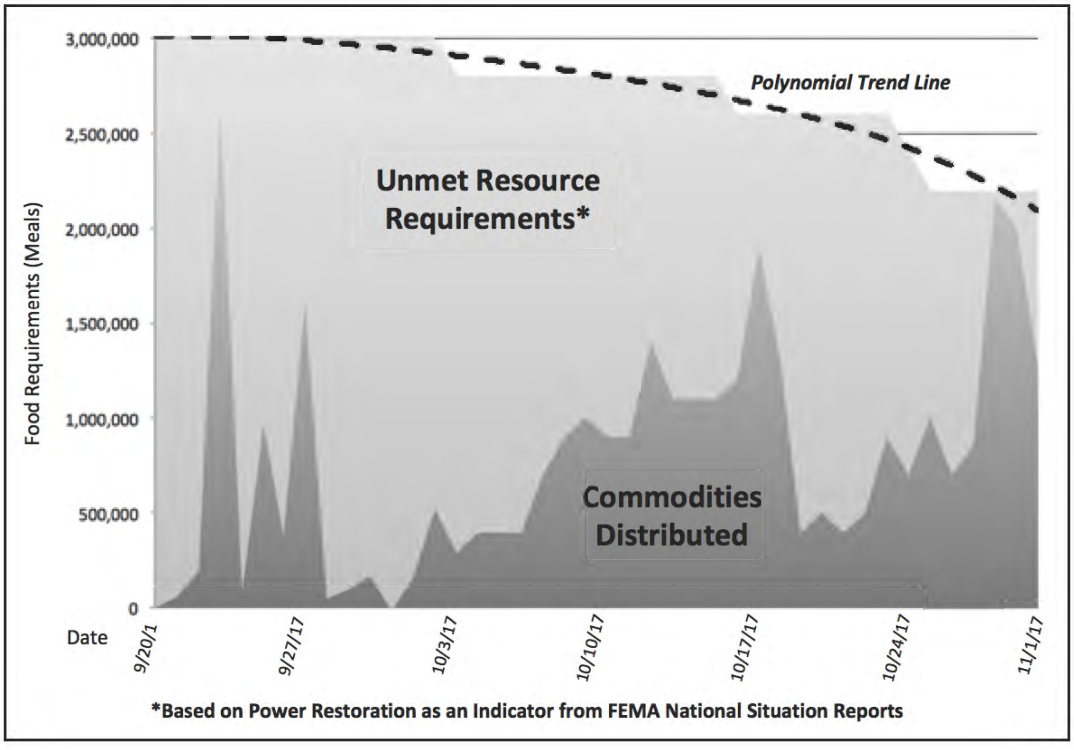

Figure 18. Puerto Rico commodity mission shortfalls in Hurricane Maria. Data from (FEMA) 2017.

The underlying trend lines of these empirically based resource requirement curves can be modeled as decreasing exponential functions, which are solutions to a set of Linear Ordinary Differential Equations (ODES). Linear ODEs are commonly used in population modeling (Boyce et al. 2017). These empirical sources and their trend lines are further investigated in Section 4.4.1 and were used to model emergency logistical resource requirements over time for three simulations which can provide logistical planning information for the OPLAN commodity mission.

In conclusion, all of the components of the probabilistic risk model have been presented and investigated as they are situated within their respective engineering and scientific disciplines. These components were then implemented in the methodology of the current study to estimate emergency logistical resource requirements for affected populations in the (M) 7.8 San Andreas Earthquake Scenario.

Chapter 4 Model Implementation

The practical aim of this study was to model the affected "at-risk" populations in the ShakeOut scenario, at three-days (t = 3) post-event for emergency logistical resource requirements using the general *risk* equation and assumptions from the Southern California Catastrophic Earthquake Response Operational Plan (OPLAN). This was accomplished through computational implementation of the *risk* equation from Chapter 3 (per each raster $Cell_{i,j}$) as:

$$[\mathbf{Risk_{Population}}] = [\mathbf{HAZARD_{Damage}}] \times [\mathbf{SOVI_{Weight}}] \times [\mathbf{LandScan_{Population}}] \quad (12)$$

The *Vulnerability* component has been established as $[SOVI_{Weight}]$ and the *Population* component as $[LandScan_{Population}]$ in Chapter 3. The *hazard* component of the model was computationally implemented, based on the results of Section 3.4 from the identification of the six indicators as:

$$[\mathbf{HAZARD_{Damage}}] = \mathbf{MAX}\left\{[POWER_{Damage}], [PIPES_{Damage}], [BRIDGE_{Damage}], [ROAD_{Damage}], [RAIL_{Damage}]\right\} \quad (13)$$

The components of infrastructure damage indicators, as independent probabilities, were combined as a "maximum", for each grid cell ($Cell_{i,j}$). The *hazard* component should be represented in a way that includes all the information that is known about the component functions without assuming anything that is not known. This can be considered a *maximum entropy* approach to modeling these infrastructure components in the probabilistic risk model.

A *maximum entropy* probability distribution is defined as having entropy that is at least as great as that of all other members of a class of probability distributions, where entropy can be considered as a measure of information loss (Jaynes 2003). The result is that the probability

distribution minimizes entropy subject to certain constraints—the maximum probability of damage value of the infrastructure indicator component, per cell. In summary, choosing the "maximum" of the probabilities of the component indicator functions agrees with everything that is known, avoids loss of information and avoids assuming anything that is not known (Philips et al. 2005).

Therefore, the "maximum" of the component probabilities has been chosen to computationally implement the *hazard* component of the *risk* equation. The resulting "maximum" function represents the final result of the probabilistic risk model computations for the [$HAZARD_{Damage}$] component.

Furthermore, total emergency logistical resources were calculated, and defined as the initial conditions (t = 3) for the modeling of resource requirements over time as:

$$\mathbf{[Risk_{Population}] \times [Meal_{Mutiplier}] = X_3} \quad (14)$$

$$\mathbf{[Risk_{Population}] \times [Water_{Multiplier}] = W_3} \quad (15)$$

In these equations, the resource multiplier was established from the OPLAN as 2 meals per person/day and 3 liters of water per person/day. These initial conditions were then used for establishing a relative risk ratio (which is investigated in Section 4.3) and for modeling decreasing resource requirements over time (which is investigated in Section 4.4). The steps for the development of the probabilistic risk model and its applications are presented in Figure 19 and are explored in the rest of the chapter.

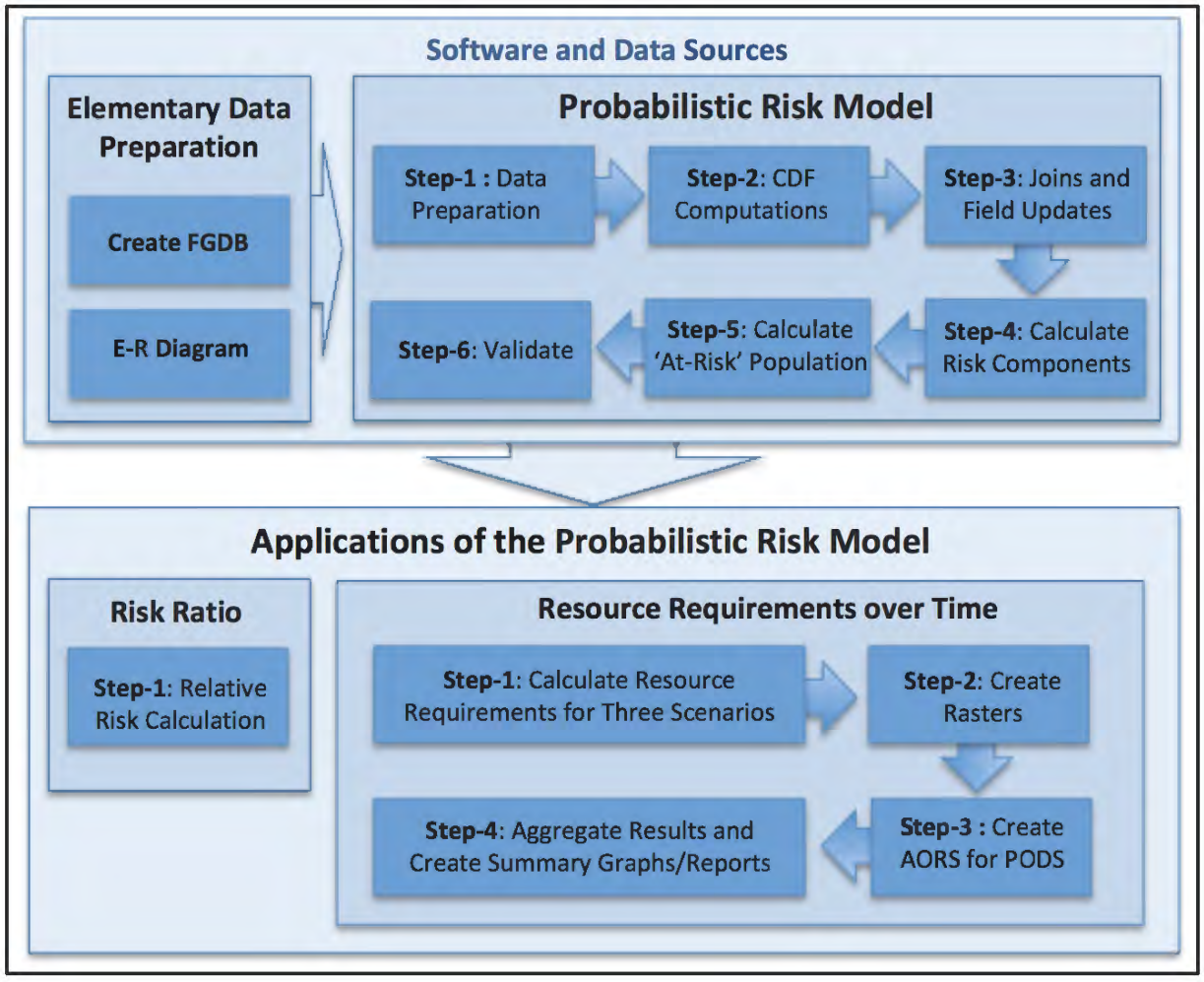

Figure 19. Development and applications of the probabilistic risk model

4.1. Global Assumptions

The current study incorporated a number of global assumptions required to develop a modeling methodology for emergency logistical resource requirements in the (M) 7.8 San Andreas Earthquake Scenario. Of these, the first set requires limited justification while individual assumptions that require more detailed justification or validation are provided immediately following their introduction. The first set of assumptions relate to the ShakeOut scenario and have already been established:

1. *The (M) 7.8 San Andreas Earthquake Scenario has occurred at night and impacted the*

eight-county Southern California region as identified in the OPLAN

2. *A disaster-affected population of between 2.5 million and 3.5 million require emergency food and water (emergency logistical resources) for a 45 to 90-day period*

3. *Points of Distribution (POD) sites with associated Areas of Responsibility (AORs) have been activated along with the emergency logistical resource commodity mission, per the OPLAN*

4. *AORs are determined by the Original Gravity Weighted Huff Model for probability of travel to a site location, bound by Los Angeles County boundaries, at the edges*

In Assumption 4, the Original Gravity Weighted Huff Model was used to identify AORs for the PODs, based on 2010 U.S. Decennial Census block population. These AORs were used to tabulate total resource requirements per POD and are based on a simple probability of travel model using the average nearest neighbor distance. This supplemental analysis is documented in Appendix A. The next two assumptions relate to the specific spatial and temporal resolution of the study:

5. *The populations in the respective LandScan 2015 "global" (~1 km) population database and the LandScan USA 2012 "conus_night" (~90 m) datasets are randomly dispersed within each raster grid cell and are represented by proxy at the centroid for calculations*

6. *The temporal variation between 2010 U.S. Decennial Census-based population, 2015 U.S. Census population estimates, and Landscan populations from 2012 and 2015 do not significantly affect the model's results (i.e. this is an acceptable range of uncertainty in population estimation)*

The next set of assumptions relate to calculations and data in the modeling methodology:

7. *The total disaster displaced population (from t = 0 to t < 3 days) of 542,000 from the OPLAN is included in the total (t = 3 day) disaster-affected population of between 2.5 million and 3.5 million (i.e. there is only one characteristic population to model resource*

requirements for).

The ShakeOut scenario provides estimates for initial displaced populations (t = 0) at 255,251 based on the FEMA Hazards United States (HAZUS-MH) multi-hazard loss estimation methodology in terms of the HAZUS-MH shelter model. However, it does not estimate emergency logistical resources or estimate (t = 3) affected populations (Jones et al. 2008). These estimates for (t = 0) are based on the 2010 U.S. Decennial Census tract population, demographics indicative of vulnerable populations with associated weighting factors established by the Red Cross (Harrald et al. 1992) and the damage functions for "extensive" and "complete" damage of single and multi-family residential occupancy classes represented in the building stock of the study area (FEMA 2003).

The OPLAN identifies an initial displaced population and estimates (t = 3) disaster-affected populations at 2.5 million, based on expert panel recommendation (CalOES and FEMA 2011). For this study, it is assumed that these initial displaced populations from (t = 0) of 542,000 are included in the (t = 3) disaster-affected population, which as the literature notes is affected more by social vulnerability, lifeline utility infrastructure impacts and restoration timelines.

In consideration of the outcomes over time for the displaced populations, it must be considered that a disaster emergency housing mission will be activated to stabilize these displaced populations (CalOES and FEMA 2011). These initial displaced populations are similarly affected by lifeline utility infrastructure damage and restoration. So, for all intents and purposes in the model, they are the same—as housing solutions also require full restoration of lifeline utility infrastructure. The result of this assumption ensures that there is only one

characteristic *population* to model initial resource requirements and resource requirements over time for, based on the ShakeOut scenario parameters and OPLAN.

8. *Infrastructure components and their damages are independent at (t = 3 days), but increasingly interconnected over time, represented by the averages for their functionality restoration timelines.*

The HAZUS-MH methodology assumes damages are independent when the earthquake occurs at (t = 0). For example, power infrastructure damage in the HAZUS-MH methodology is not related to any other factors and can be represented by the damage functions in the HAZUS-MH Technical Manual without feedback or lag mechanisms from other transportation, water or other lifeline utility sector components (FEMA 2003). However, as disaster recovery progresses, transportation impacts may delay infrastructure repair, power loss may delay water restoration, etc. It is outside the scope of the current study to develop network system analyses of infrastructure interdependencies. Therefore, these damage functions must be utilized in a simplified manner without a systems analysis approach to model these interdependencies.

To address this, it is assumed that the infrastructure components in the model, being independent at (t = 0) remain independent at (t = 3). As the HAZUS-MH loss estimation methodology uses this simplified approach to model component lifeline utility restoration throughout the restoration timeline, the current study is justified in applying the same assumption (FEMA 2003). This assumption is simply stating that at (t = 3) the damage and restoration of one infrastructure component does not relate to the others and, as such, that they can be independently combined in the model without consideration for interdependency (i.e. lag and or feedback mechanisms). The HAZUS-MH methodology recommends systems analysis for more detailed studies of lifeline utility interdependency.

A simplified model of lifeline infrastructure system interaction as increasingly interconnected over time ($t > 3$) is then applied, represented by the averages for functionality restoration timelines of the infrastructure components in the model. Absent any justification for assigning weights in the averaging of the components, it is assumed they are equally weighted. The average of the infrastructure components' restoration timelines is then used to create the restoration timeline intervals for the resource requirement curve for the associated impact categories. This assumption requires additional research to establish weights for the components and is a recommendation in the study's conclusion for future research.

9. *The literature shows that socially vulnerable populations require more resources and for longer periods of time. The probabilistic risk model represents this observation as a (±) 22 percent weighting factor, based on the ranked Social Vulnerability Index (SoVI), as the best available empirical data for social vulnerability's amplifying effects on resource requirements*

These are the direct conclusions from Section 3.2 which has shown that it is critically important to represent the effects of social vulnerability in relation to emergency logistical resource requirements. To be further calibrated, this assumption requires additional research and is a recommendation in the study's conclusion for future research.

These next assumptions use results from probability theory and statistical frequentist inference for applying (n) independent Bernoulli trials (for n = population value of LandScan cell) to result in the expected value of populations impacted (i.e. this assumption relates the probability of impact of populations within the grid cell to the proportion of the total population impacted within it).

10. *The total population impacted in a grid cell is the expected value of the probability of impact per grid cell and the total population impacted in the study area is the sum of the population impacted in all of the grid cells.*

This is the method used by the HAZUS-MH loss estimation methodology to calculate populations exposed to a hazard. Populations subject to outage are calculated directly from the discrete probability of impact to the substations (FEMA 2003). This is also the method used in the *risk* equation and for the other infrastructure indicator variables in the current study. The approach is based on classical frequentist inference assumption from probability theory to estimate expected values of indicator variables from the probabilities of success in a binomial distribution. This expected value is then used as the estimated population impacted per grid cell, and by the linearity of expectations, for the total population impacted in the study region (Pitman 2006).

The final three assumptions relate infrastructure density to population density and are simplifications or extensions of the HAZUS-MH loss estimation methodologies.

11. *The distribution of electric power system components that occur in each grid cell are regularly dispersed throughout the study area in proportion to population density and are randomly distributed within each raster grid cell, represented by proxy at the centroid*

This assumption is investigated in Section 3.4.3. The California Energy Commission substation data shows on average, there is one substation in every 6 sq. km in Los Angeles County and a higher density in urban areas. The HAZUS-MH methodology for calculating affected populations for outages is insufficient and does not account for the MAUP effect. The MAUP effect can be compensated for through the relationship of infrastructure components to population density.

As shown in Appendix B, in a sample of the current study region, this assumption and calculation of population affected by power outage decreases the range of uncertainty (or is at least as good as the current standard) in the original HAZUS-MH method, as explained in

Section 3.4.3. This approach can then be used to calculate the [$POWER_{Damage}$] component of [$HAZARD_{Damage}$]. The next assumption relates water and natural gas conveyance/pipelines to population density.

12. *The distribution of water and natural gas pipelines in each grid cell are regularly dispersed throughout the study area in proportion to population density and are randomly distributed within each raster grid cell, represented by proxy at the centroid*

This component in the HAZUS-MH loss estimation methodology is generalized to the census tract and associated with population density with 80 percent of the pipes assumed to be brittle (FEMA 2003). Therefore, just as there are more dwellings in areas of higher population density, there are similarly more residential and community pipelines. Using the equations of Section 3.4.4, the [$PIPES_{Damage}$] component of [$HAZARD_{Damage}$] can then be calculated. The final assumption is related to transportation infrastructure component distribution.

13. *The distribution of transportation infrastructure components (e.g. bridges, roads, rail) in each grid cell are regularly dispersed throughout the study area in proportion to population density and are randomly distributed within each raster grid cell, represented by proxy at the centroid value*

It is plausible to associate more roads with a higher population density, similar to the above methodology for pipe damage. Similarly, in addition to the 6,719 interstate, national and California highway bridges identified in the ShakeOut supplemental study, Jones et al. (2008) identifies that there are hundreds of thousands of structures also considered as bridges in the region, which can be associated with population density.

As shown in Appendix C, the areas of probability of "complete" bridge damage that dominate the *risk* equation (Equation 1) fall within the expected regions for complete bridge

damage in the study by Werner et al. (2008). This approach can then be used to calculate the [$BRIDGE_{Damage}$] component of [$HAZARD_{Damage}$] using the equations of Section 3.4.5.

To implement the model, the current study used the Esri ArcGIS Desktop 10.6 suite of software and tools for spatial analysis and database management, MATLAB (2017) and RStudio ver. 1.1 for statistical analyses and advanced computations.

4.2. Implementation of the Probabilistic Risk Model

For computational implementation of the *risk* equation, this section focuses on the translation of the modeling methodology into an Esri ArcGIS 10.6 compatible data structure (e.g. tables, attributes, relationships, featureclasses and domains) and the development of the associated database architecture and Entity-Relationship (E-R) schema. To illustrate the steps used for computational implementation of the probabilistic risk model, process flow diagrams with descriptions are provided.

4.2.1. *Data requirements and preparation*

For the current study, eight GIS raster and vector datasets were identified in Chapters 2 and 3 that are required for developing a model of emergency logistical resource requirements in the (M) 7.8 San Andreas Earthquake Scenario. These datasets are shown in Table 3.

Table 3. Eight datasets used for development of the probabilistic risk model

Name	File Name	Source Scale/Resolution	Format	Source
OPLAN POD Sites	PODS_OPLAN_2011.shp	1:50,000	Shapefile, Vector (Point)	California Governor's Office of Emergency Services (Digitized from OPLAN)
M7.8 San Andreas Earthquake scenario, Modeled Ground-Motion Data	mi.shp	1:24,000	Shapefile, Vector (Polygon)	USGS Pasadena
	pga.shp	1:24,000	Shapefile, Vector (Polygon)	USGS Pasadena
	pgv.shp	1:24,000	Shapefile, Vector (Polygon)	USGS Pasadena
	sa10.shp	1:24,000	Shapefile, Vector (Polygon)	USGS Pasadena
Los Angeles County Social Vulnerability (SoVI) Census Tracts	CA_Tract_SoVI_06_10	1:24,000	Feature Class, Vector (Polygon)	University of South Carolina, Hazards Research Institute
LandScan 2015 "Global" Population Database	Population (GRID)	~1 km, (30 arcsecond)	Grid, Raster	Oak Ridge National Laboratories
LandScan USA 2012 "Conus_Night" Population Database	Conus_Night (GRID)	~90 meter (3 arcsecond)	Grid, Raster	Homeland Infrastructure Foundation Level Data Workgroup/U.S. DHS
*Note: all data projected to WGS 1984 UTM Zone 11S				

The first step in development of the probabilistic risk model was elementary data preparation with the creation of an Esri File Geodatabase (FGDB) data structure and loading of the eight datasets identified above. Elementary data preparation steps for the Entity-Relationship schema also included:

- Created FGDB: RISK_MODEL_2018.fgdb
- Imported/loaded and projected data sources: WGS 1984 UTM Zone 11S
- Clipped LandScan 2015 "global" to eight-county study area (global.grid)
- Clipped LandScan 2012 "conus_night" to Los Angeles County study area (conus_night.grid)
- Created subset of Social Vulnerability (SoVI) 2010 U.S. Decennial Census tracts for study regions
- Created all new attributes in [FINAL_RISK_CALC], [PODS_OPLAN_2011] and [CA_Tract_SoVI_06_10]
- Created attribute domains and Entity-Relationship (E-R) structure. These data structures are presented in Figure 20.

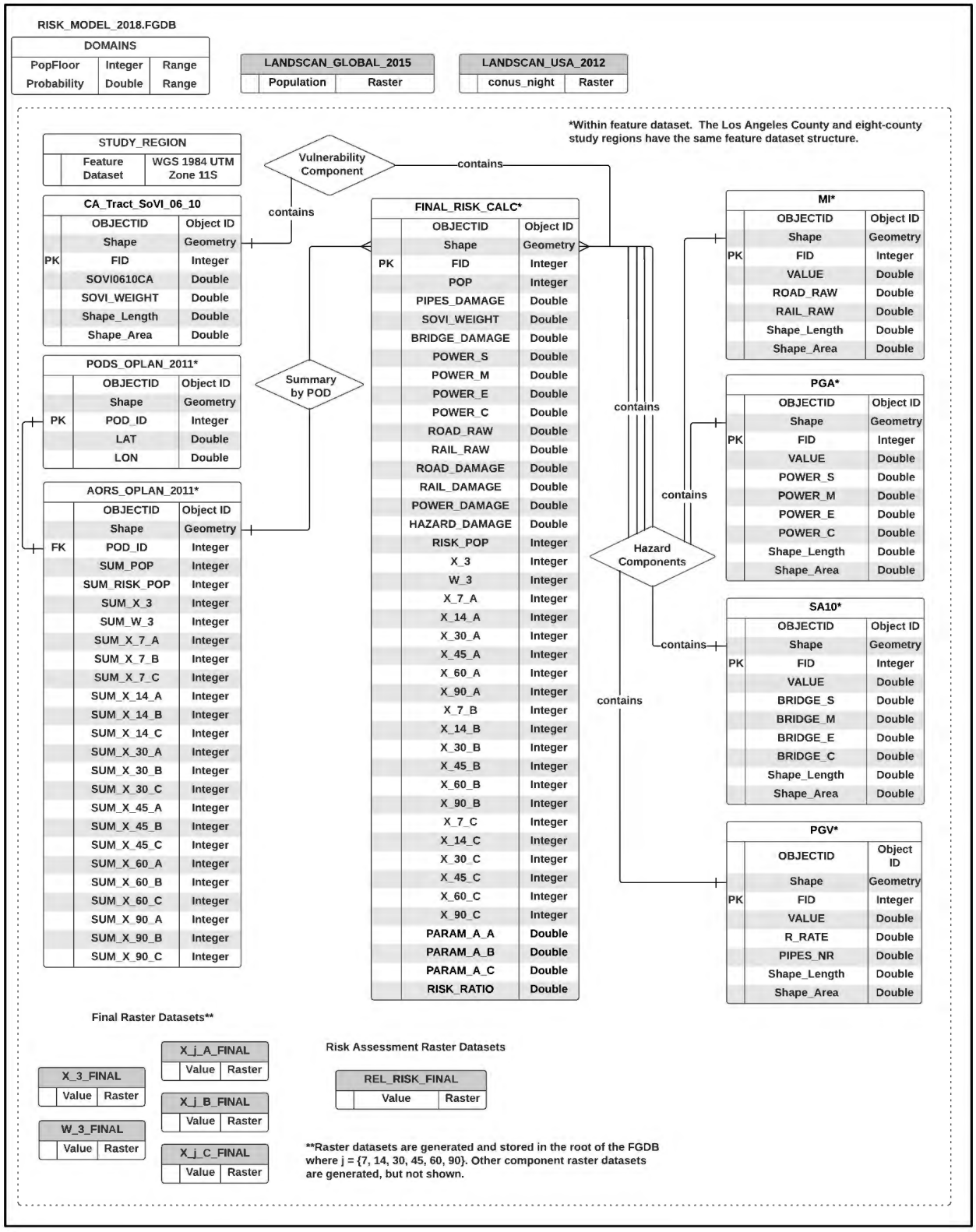

Figure 20. Database Entity-Relationship diagram

A vector-based (point) approach for analysis was chosen due to the large number of stored floating-point calculations. The need for interoperability between multiple software platforms running advanced calculations and statistical analysis made using a vector attribute table, rather than a raster data structure, a more flexible approach. The spatial resolution for the model was based on the cell size of the respective LandScan Raster datasets, which were clipped to the study region and converted to a point centroid dataset for analysis through the "raster-to-point" function in ArcGIS 10.6. These centroids were converted back to raster through the "point-to-raster" function in ArcGIS 10.6, without any loss of fidelity, when needed.

As indicated in Figure 19, at the beginning of the chapter, the implementation of the probabilistic risk model was accomplished in a sequence of six steps. In Step 1 (detailed in Figure 21), advanced data preparation for the datasets was initiated, with the "raster-to-point" calculation. This step produced the table [FINAL_RISK_CALC], which was used to store all risk calculation results. The rescaling of the social vulnerability weighting-factor, which results in the final *vulnerability* component of the *risk* equation, was also calculated. Note that a key for the color coding used in all process diagrams shown in this chapter is included in Figure 21.

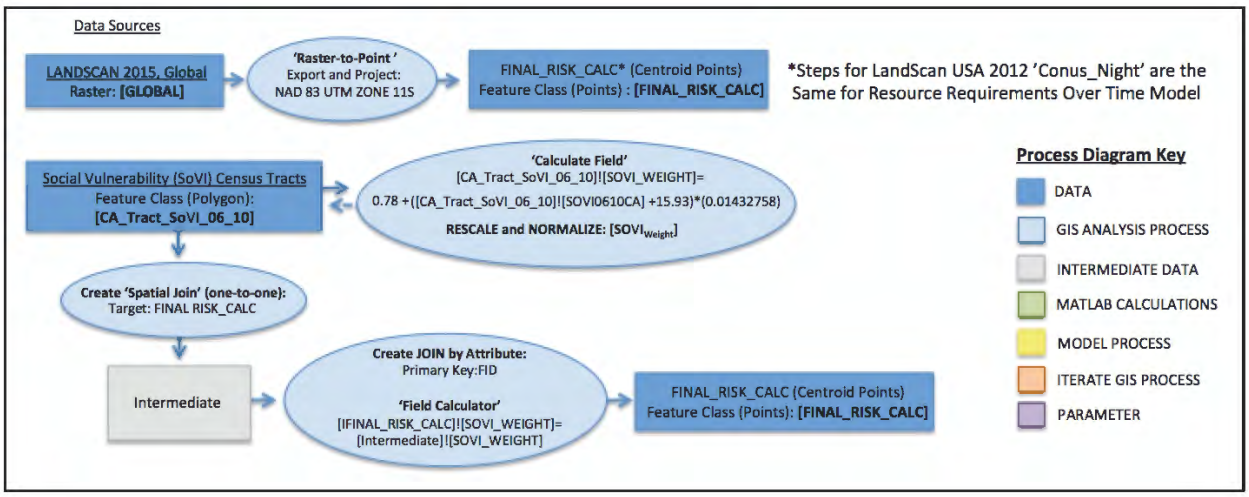

Figure 21. Step 1: Advanced data preparation

In Step 2, shown in Figure 22, all unique values in each of the four ground-motion vector polygon datasets were extracted to look-up tables that could be exported to MATLAB for calculation of the CDF functions. Once the calculations were completed, the tables were then joined back to the original ground-motion data sources and new attributes were created. This resulted in the raw probabilities of damage, which were associated with their respective ground-motion polygons, available for use in further calculation.

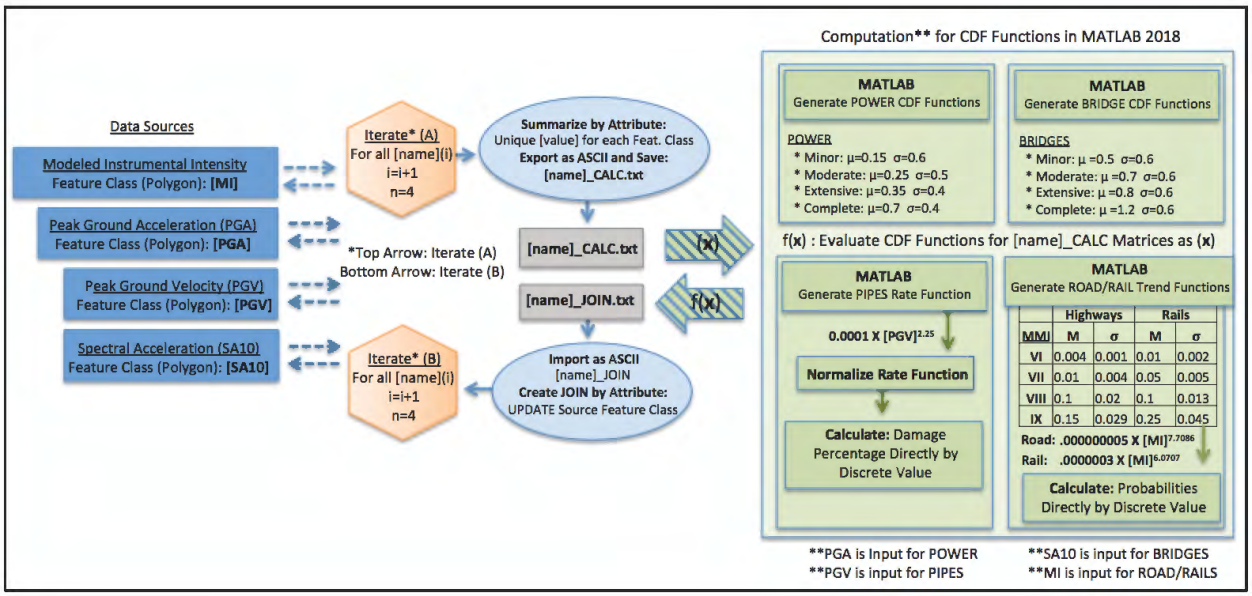

Figure 22. Step 2: Computations in MATLAB for the probabilistic risk model

In Step 3, shown in Figure 23, the results from the calculations in the respective ground-motion polygon feature classes were each spatially joined to the vector points feature class [FINAL_RISK_CALC]. At the end of this step, all data for calculation of the probabilistic risk model were stored as individual columns in the [FINAL_RISK_CALC] attribute table.

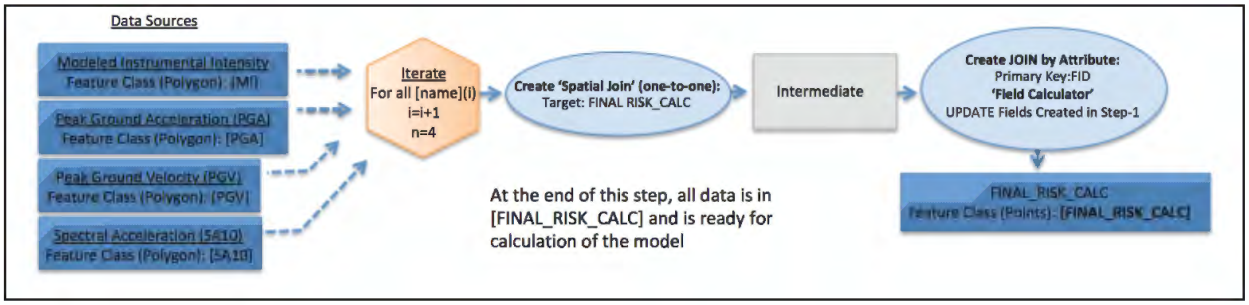

Figure 23. Step 3: Results from the CDF calculations

In Step 4, shown in Figure 24, each of the probability of damage functions for the five unique infrastructure indicators was calculated within the [FINAL_RISK_CALC] featureclass, based on the methodologies identified in Chapter 3. Finally, the *hazard* component of the *risk* equation was calculated by a python expression for the "maximum" of each of these damage functions, per each centroid point.

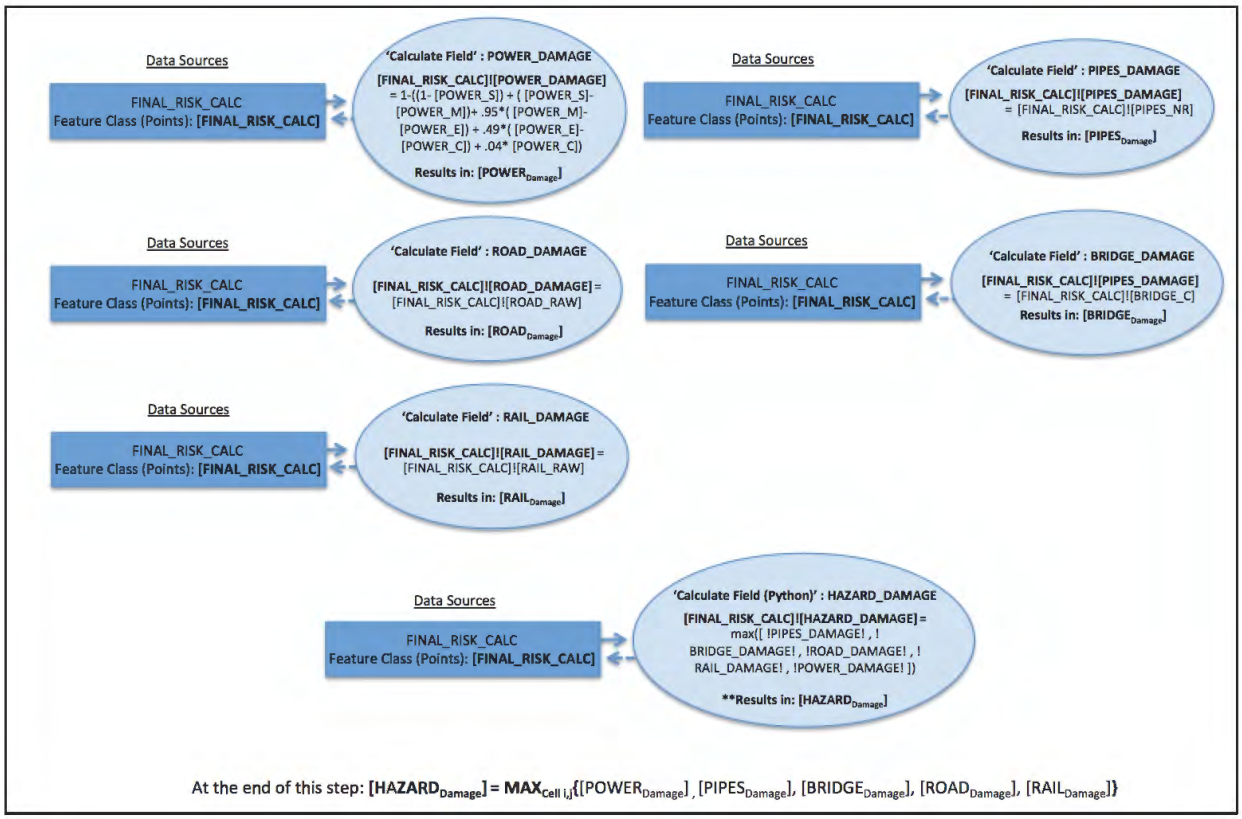

Figure 24. Step 4: Probabilistic damage functions and maximum probability are computed

In Step 5, shown in Figure 25, the final calculations of the probabilistic risk model, which included the weighting for social vulnerability, resulted in the total "at-risk" disaster-affected population and their emergency logistical resource requirements. Finally, for visualization purposes, all of these results for the six component probabilities were then converted into raster grids. At the end of Step 5, the probabilistic risk methodology for modeling emergency logistical resource of day-three post-event disaster-affected populations was completed.

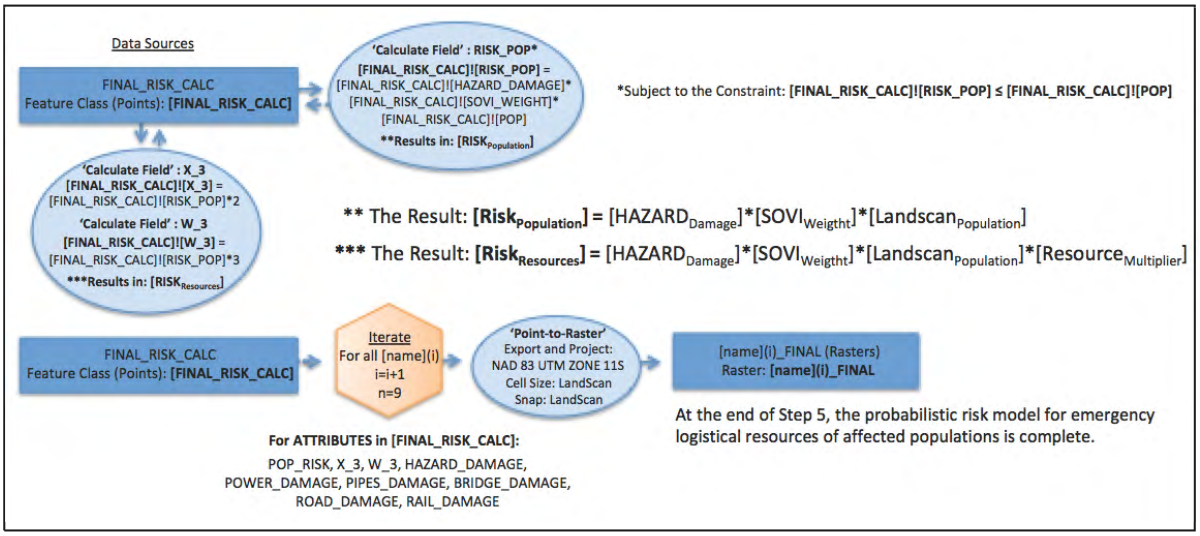

Figure 25. Step 5: Calculation of "at-risk" populations and their resource requirements, plus conversion back to raster for visualization purposes

4.2.2. *Validation of Results with Regression Analysis*

In order to validate the results of the probabilistic risk model before emergency management application, the current study quantified the distributions and relationships of the underlying indicator variables in the model results. Logistic regression analysis and associated statistical tests was undertaken in Step 6 for analysis of variable contributions in the results and to determine a confidence interval for these estimates. To do this, generalized linear model (GLM) regression analysis was applied in RStudio to statistically investigate the resulting *risk*

probability as the dependent variable. The independent variables were the respective five infrastructure indicator probabilities along with the SoVI weight parameter and ground-motion data.

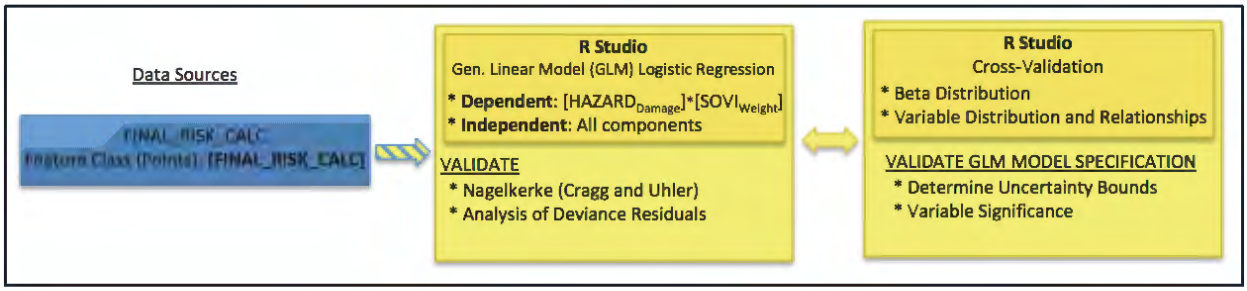

Figure 26. Step 6: Validation of the model

The GLM for logistic regression is best specified for models of dependent variables as a proportion of "successes" using logistic curves as link functions for the family of binomial data distributions (Cribari-Neto and Achim 2010). R statistics libraries were utilized to run and evaluate the GLM with the 180,380 raster-cell centroid point data-frame in the eight-county study region. The Nagelkerke (1991) pseudo R-squared metric was used, along with analysis of the deviance residuals. These results provided a quantification of the underlying indicators in the significance of their contribution to the resulting maximum *risk* probability and provided a range of uncertainty for the model from each of the components.

This concludes the implementation of the probabilistic risk model for emergency logistical resource requirements. These results were next applied in calculation of a relative risk ratio and to estimate the logistical resources needed over time in the Los Angeles County study area.

4.3. Methodology for Calculation of the Relative Risk Ratio

In the current study, a methodology similar to Bithell (1990) for estimation of relative risk to the general population was employed in the eight-county study region. This approach used the emergency logistical resource requirements as determined from the results of the probabilistic risk model as the "cases" and the background population from Landscan 2015 as the "control". The resulting *relative (universal) risk ratio* was then directly calculated as the quotient of the two raster surfaces of population "control" versus resource needs "cases", which effectively cancels out the "per-unit of area" term in the numerator and denominator. In general, a *relative risk ratio* is the ratio of the probability of an event occurring in an exposed population to its occurrence in the general population.

The final results were a raster grid based on the cell size from LandScan 2015 "global" (~ 1 km) that represented the relative risk to any member of the population in the study area. This can be used by emergency managers for planning purposes and to target resources to communities with a high probability of emergency logistical resource requirements in support of mitigation planning and preparedness.

4.3.1. *Computational Implementation of the Relative Risk Ratio*

Calculation of the relative risk ratio was accomplished in one step, based on application of the results from the probabilistic risk model (Figure 27). Two attributes were used to directly calculate the quotient as the resulting relative risk ratio, per the methodology of Bithell (1990).

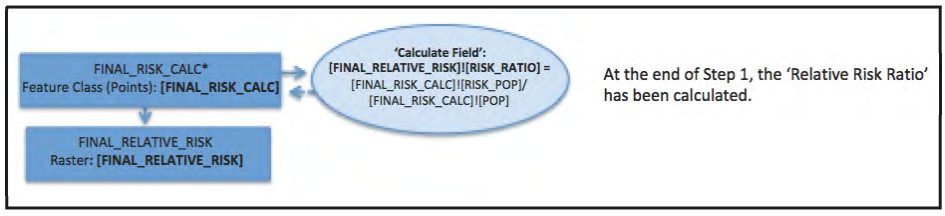

Figure 27. The final relative risk ratio calculated for the study area

The final result was a raster grid based on the cell size of LandScan 2015 "global" (~1 km) that represents the relative risk of any member of the population in the study area.

4.4. Methodology for Modeling Resource Requirements Over Time

The final part of the methodology investigated modeling emergency logistical resource requirements over time. The initial resource requirements (t = 3) of at-risk populations resulting from the probabilistic risk model were used to model recurring resource requirements over a 90-day period. This provided an estimate of at-risk populations for emergency resource requirements in Los Angeles County at six future operational periods (e.g. at t = 7, 14, 30, 45, 60 and 90 days) using the high-resolution LandScan USA 2012 "conus_night" (~90 m) population dataset. Emergency managers can utilize these results in planning for long-term community resource requirements issues in the commodity mission.

To do this, three factors were investigated which are involved in developing resource requirements curves, similar to the restoration timelines of the individual infrastructure components of the probabilistic risk model. The first factor focused on the development of an equivalent set of four impact categories for the probabilistic risk model's results and establishment of a restoration timeline point (i.e. when no further resources are required) for each of the four impact categories, within the "minor", "moderate", "extensive" and "complete" requirement ranges. These restoration timelines are based on the averages of the respective components restoration timelines as in Assumption 8.

The second factor was to model the form of the curve based on the empirical curves found at the end of Chapter 3. The four impact categories and their curves were then fit to the restoration timeline values where resource requirements are equal to zero on the y-axis for each of the respective "minor", "moderate", "extensive" and "complete" categories (FEMA 2003).

Curves for three simulations were generated to represent the maximum, mean and minimum dynamic resource requirement ranges in the current study. Respectively these were: (1) a minimum decay curve trend, for rapid recovery based on the United States Army Corps of Engineers (USACE) mission planning tool as Simulation A (Minimum); (2) a maximum decay curve trend representing long-term infrastructure restoration issues, such as in recent events in Puerto Rico, as Simulation B (Maximum); and (3) a linear decay curve trend as Simulation C (Average).

Finally, these curves were computationally implemented and evaluated at specific time intervals in the study region and summary results per POD site were calculated for emergency resource requirements in the three simulations, with consideration for social vulnerability per the probabilistic risk model developed in the current study. This part of the study concluded in display and summary results of the three simulations and in Appendix D.

4.4.1. *Impact Categories and Restoration Timelines*

From the results of the probabilistic risk model, the range of data values for $[HAZARD_{Damage}]\times[SOVI_{Weigtht}]$ were statistically evaluated to separate the ranked set into four natural breaks, based on the maximum, minimum and mean. The four damage categories were defined as: “minor”, as the range from the minimum to the (mean – minimum)/2; “moderate”, as the range between (mean – minimum)/2 and the mean; “extensive”, as the range between the mean and the (maximum – mean)/2; and “complete”, as the range between the (maximum – mean)/2 and the maximum. This is a simple way to define these impact categories using natural breaks in the data and is similar (within a standard deviation) to a nested means approach. The only assumption used in the approach is that areas with higher probability of impacts also take longer to recover, which the ShakeOut scenario indicates (Jones et al. 2008).

The next step in modeling emergency logistical resource requirements over time was to establish a restoration timeline point (i.e. the point where 100 percent of resource needs are met) for each of the four impact categories. From Assumption 8, it was proposed that the average of restoration timelines for the respective infrastructure indicators can be used to calculate resource requirement restoration points for each of the four categories. From the ShakeOut scenario (Jones et al 2008) and the HAZUS-MH Technical Manual (FEMA 2003) in Section 3.3, these observations have been summarized in Table 2:

Table 4. Average restoration timelines for resource requirements curve

	Category			
Component	**Minor**	**Moderate**	**Extensive**	**Complete**
POWER (ShakeOut)	6	9	21	120
POWER (HAZUS)	3	7	30	90
GAS (ShakeOut)	7	14	21	60
WATER (ShakeOut)	7	14	60	180
BRIDGE (ShakeOut)	3	12	49	140
ROAD (HAZUS)	2	7	62	62
RAIL (HAZUS)	2	11	49	180
AVERAGE (Days)	**4**	**11**	**42**	**119**

Source: FEMA (2003) and Jones et al. (2008)

These results were used to find the parameter (a) for fitting the resource requirement curve equations for each of the damage categories to zero values on the y-axis in the three simulations of the study.

4.4.2. *Dynamic Resource Requirements Curves*

The form of the curve in Figure 17 for the USACE resource restoration timeline was approximated by an exponential trend line. A *trend line is* created by a modeling function that represents the behavior of a set of data by identifying its underlying pattern (Dodge 2003). Equation 16 shows resource requirements over time as a function of time (days) with X_3 as the

initial conditions resulting from the probabilistic risk model, the parameter (a) as the damage category, and parameter (b) as the associated SoVI weight in the cell.

$$X(t) = X_3 e^{\frac{-(t-3)}{ab}}$$

a = Damage Category $\quad t$ = time, $t \in \mathbb{Z}_{\geq 3}$

$b = [SoVi_{Weight}] \quad X_3 = [Risk_{Population}] \times [Meal_{Mutiplier}]$ (16)

Equation 17 is then the linear ordinary differential equation that is solved by the equation above (Boyce et al. 2017):

$$X'(t) = \frac{-X(t)}{ab} \quad (17)$$

This was graphed (Figure 28) where X_3 is an arbitrary resource requirement calculated from the probabilistic risk model, for an arbitrary ($Cell_{i,j}$) in the study area. For the example below, (b=1) was chosen and can be considered as no social vulnerability amplification.

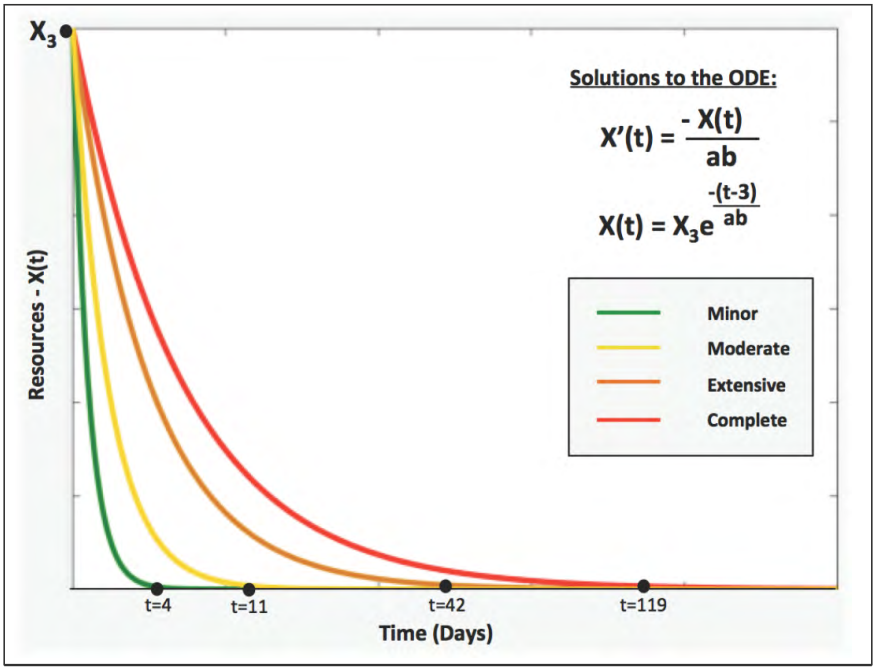

Figure 28. Simulation A (Minimum)—Dynamic resource requirements curve, based on the USACE model trend line

This rapid recovery curve can be considered as Simulation A (Minimum). Similarly, Figure 18 for the delayed infrastructure restoration in Puerto Rico suggests the following exponential trend line equation, with the same variables and parameters as the first:

$$X(t) = \begin{cases} X_3 & , t = 3 \\ -e^{\left[\frac{\log(X_3) \times (t-3)}{ab}\right]} + X_3 & , t > 3 \end{cases} \quad (18)$$

a = Damage Category t = time , $t \in \mathbb{Z}_{\geq 3}$

b = $[SoVi_{Weight}]$ $X_3 = [Risk_{Population}] \times [Meal_{Mutiplier}]$

This equation was split for t = 3, and t > 3 to be computationally implemented in a non-autonomous fashion (Boyce et al. 2017). Equation 18 is then the solution to the linear ordinary differential equation below, of the form:

$$X'(t) = \frac{\log(X_3) \times X(t)}{ab} - \frac{\log(X_3) \times X_3}{ab} \quad (19)$$

This was graphed (Figure 29) where X_3 is an arbitrary resource requirement, calculated from the probabilistic risk model, for an arbitrary ($Cell_{i,j}$) in the study area. For the example below, (b = 1) was again chosen which can be considered as no social vulnerability amplification.

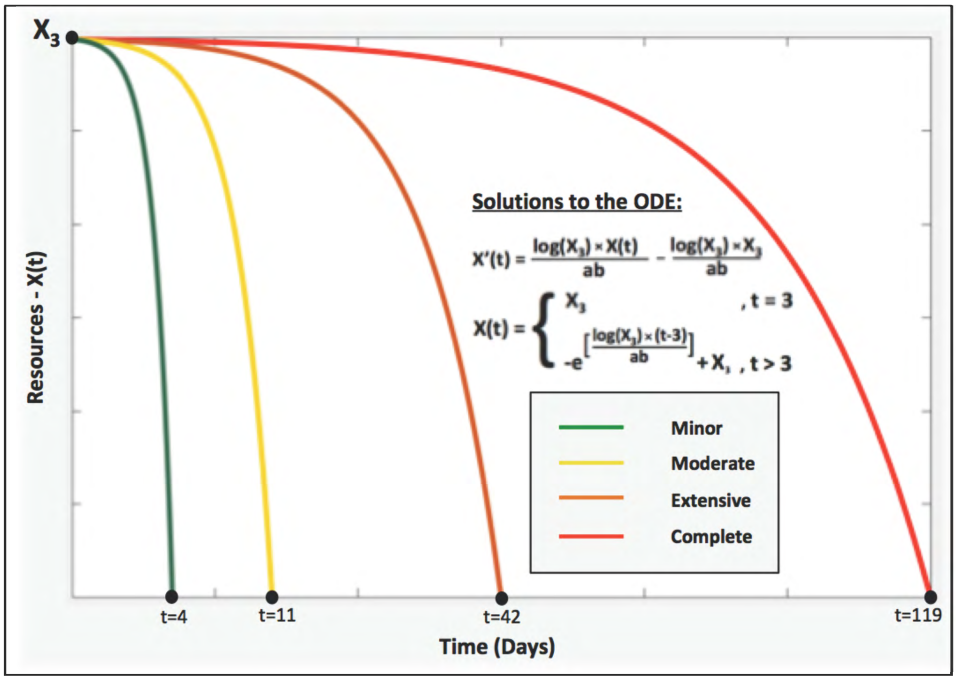

Figure 29. Simulation B (Maximum)—Dynamic resource requirements curve, based on delayed infrastructure restoration

This delayed restoration curve can be considered Simulation B (Maximum). The constant decrease scenario is the avaerage rate of the two simulation curves and can be similarly represented and graphed as:

$$X(t) = \frac{-X_3 \times (t-3)}{ab} + X_3$$

a = Damage Category t = time , $t \in \mathbb{Z}_{\geq 3}$

b = $[SoVi_{Weight}]$ $X_3 = [Risk_{Population}] \times [Meal_{Mutiplier}]$

(20)

Equation 20 is then the solution to the linear ordinary differential equation below, of the form:

$$X'(t) = \frac{-X_3}{ab}$$

(21)

This simple ODE results in linear trend curves, as graphed in Figure 30:

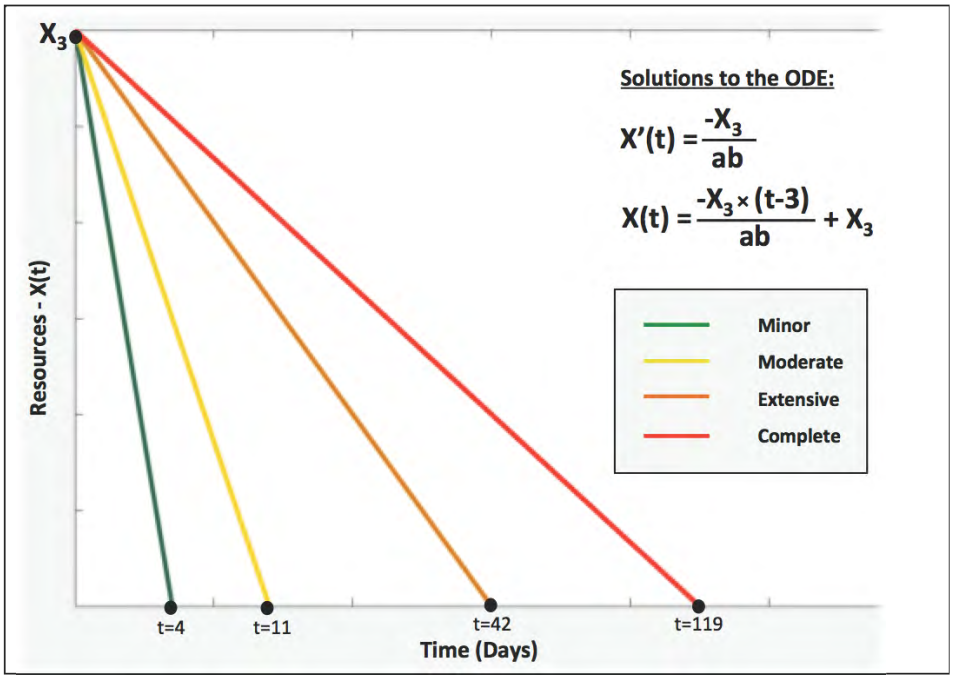

Figure 30. Simulation C (Average)—Dynamic resource requirements curve, linear trend

This linear trend can be considered Simulation C (Average). Together, three families of curves for modeling dynamic resource requirements over time have been presented. These three sets of curves were then implemented as the three simulations and evaluated (as functions) at the t = 7, 14, 30, 45, 60 and 90-day intervals to determine dynamic logistical resource requirements.

4.4.3. *Computational Implementation of the Dynamic Resource Requirements Curves*

The final application of the probabilistic risk modeling methodology was to computationally implement the resource requirement curves, identified in the previous section, in ArcGIS 10.6 to calculate resource requirements over time at t = 7, 14, 30, 45, 60 and 90-day intervals. First, the probabilistic risk model was applied to LandScan USA 2012 "conus_night" population database in the Los Angeles County study area, and initial conditions for calculating resource requirements over time (X_3) were defined as the (t = 3) day resource requirements

resulting from the probabilistic risk model. In the tabular data structure this field was stored as [FINAL_RISK_CALC]![X_3].

These results from the probabilistic risk model were then applied in four steps to calculate resource requirements over time in three simulations. In Step 1, all of the calculations as VBScript expressions using the exp() and log() functions were made for t = 7, 14, 30, 45, 60 and 90-days (Figure 31). This resulted in the total resource requirements at the six identified time intervals for the three simulations, with amplification for social vulnerability. The results of these 18 calculations were stored in the [FINAL_RISK_CALC] point featureclass.

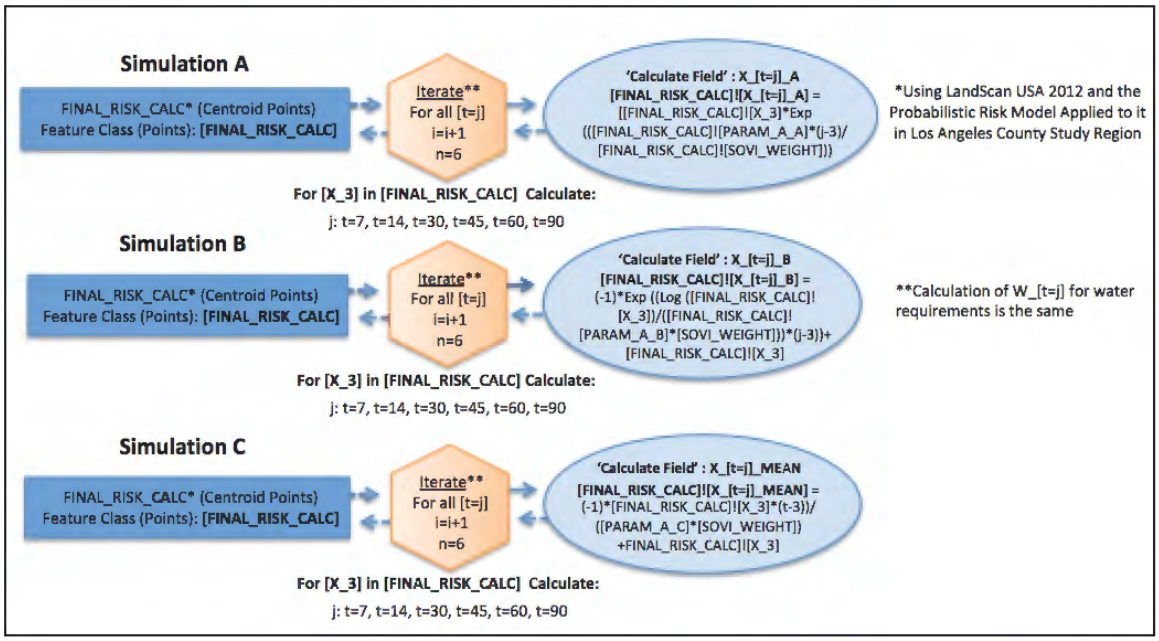

Figure 31. Step 1: Direct calculation of resource requirements over time

In Step 2, the "point-to-raster" tool was applied to generate the final results as 18 raster surfaces for presentation and display (Figure 32).

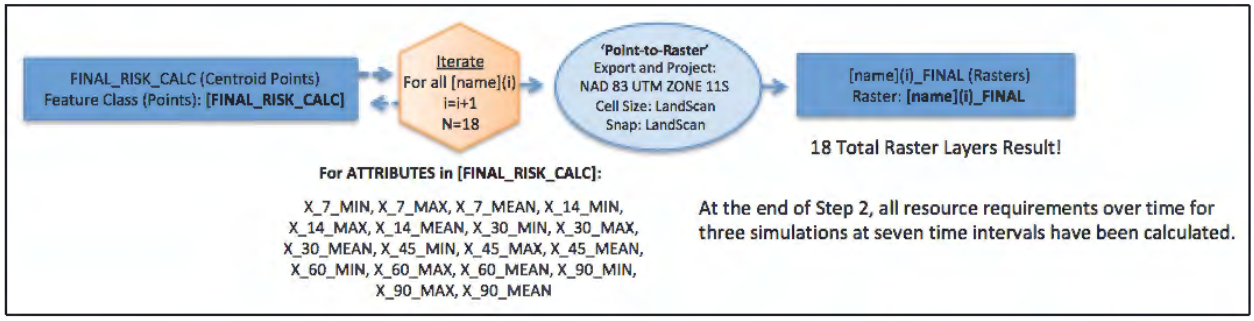

Figure 32. Step 2: Results of the calculations converted to raster surfaces

In Step 3, the results from Appendix A (Figure 33) were applied as the Areas of Responsibility (AOR) polygon featureclass, modeled from the Original Gravity Weighted Huff Model for probability of travel to facilities. This data was used to aggregate the results of the calculations into smaller units for reporting summary resource requirements over time for each POD throughout the Los Angeles County study area.

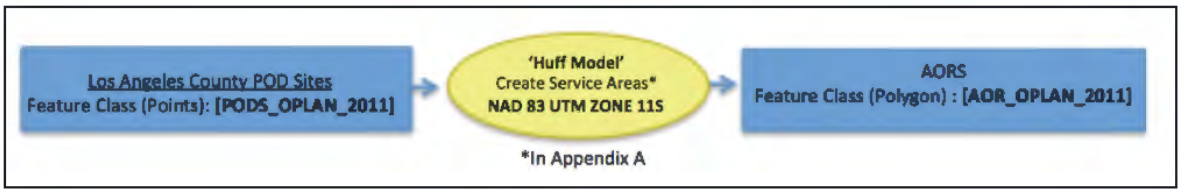

Figure 33. Step 3: AORS for summary resource requirements tabulation

In Step 4, the [FINAL_RISK_CALC] featureclass was spatially joined in a "many-to-one" relationship with the AORS, where all of the calculated resource requirements over time were summarized. Finally, [AORS_OPLAN_2011] and [PODS_OPLAN_2011] featureclasses were joined in a "one-to-one" relationship to update summary resource requirement fields (Figure 34), which were then presented as a report.

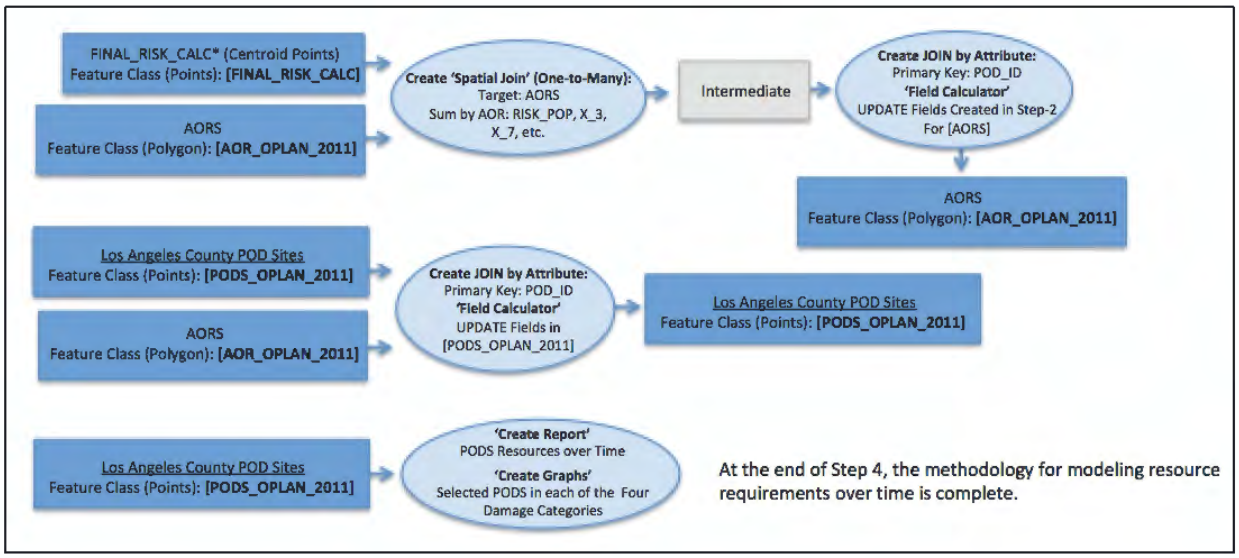

Figure 34. Step 4: Calculated resource requirements over time are summarized by AOR

The output of Step 4 is the Logistical Resource Summary Report, which is shown in its entirety in Appendix D, is a summary of the modeled resource requirements at each of the 143 Point of Distribution (POD) sites in Los Angeles County identified in the OPLAN (CalOES and FEMA 2011). For this report, truckloads and pallets of food and water for the seven operational periods in the recovery timeline were calculated, based on standard shipping formulas and established metrics used in humanitarian relief (Johnson and Coryell 2016).

The final result of this multi-step process was a comprehensive model for emergency logistical resource requirements supporting socially vulnerable disaster-affected populations affected by the (M) 7.8 San Andreas Earthquake Scenario in Los Angeles County.

Chapter 5 Model Results

The results for this study are presented in three sections. First, an overview of the probabilistic risk model development and results are provided along with the results from the logistic regression analysis. Second, results are presented from the application of the probabilistic risk model to calculate a relative risk ratio in the eight-county study area. Finally, emergency logistical resource requirements over time in Los Angeles County for the commodity mission in the Southern California Catastrophic Earthquake Response Operational Plan (OPLAN) are estimated and summarized by the Point of Distribution (POD) sites, for three simulations. These results are presented in their entirety in Appendix D.

5.1. Overview of the Probabilistic Risk Model Results

The computational implementation of the probabilistic risk model from Section 4.2.1 was successful, with a resulting "at-risk" population of 3,352,955 for emergency logistical resource requirements in the eight-county study region. These results are in alignment with the ShakeOut earthquake scenario and the OPLAN priority to provide meals and water to support disaster-affected populations of between 2.5 million and 3.5 million in the eight-county study region, from three-days post-event. Therefore, the model has produced preliminary results that can be used by emergency managers and community planners for planning assumptions in the support of affected population with emergency logistical resource requirements.

5.1.1. *Results from the Hazard Components of the Probabilistic Risk Model*

The calculations of the components in the probabilistic risk model were made without much deviation from the proposed six-step process shown in Figure 19. The hazard components were individually calculated according to the methodology in Figure 24, as shown in Figure 35.

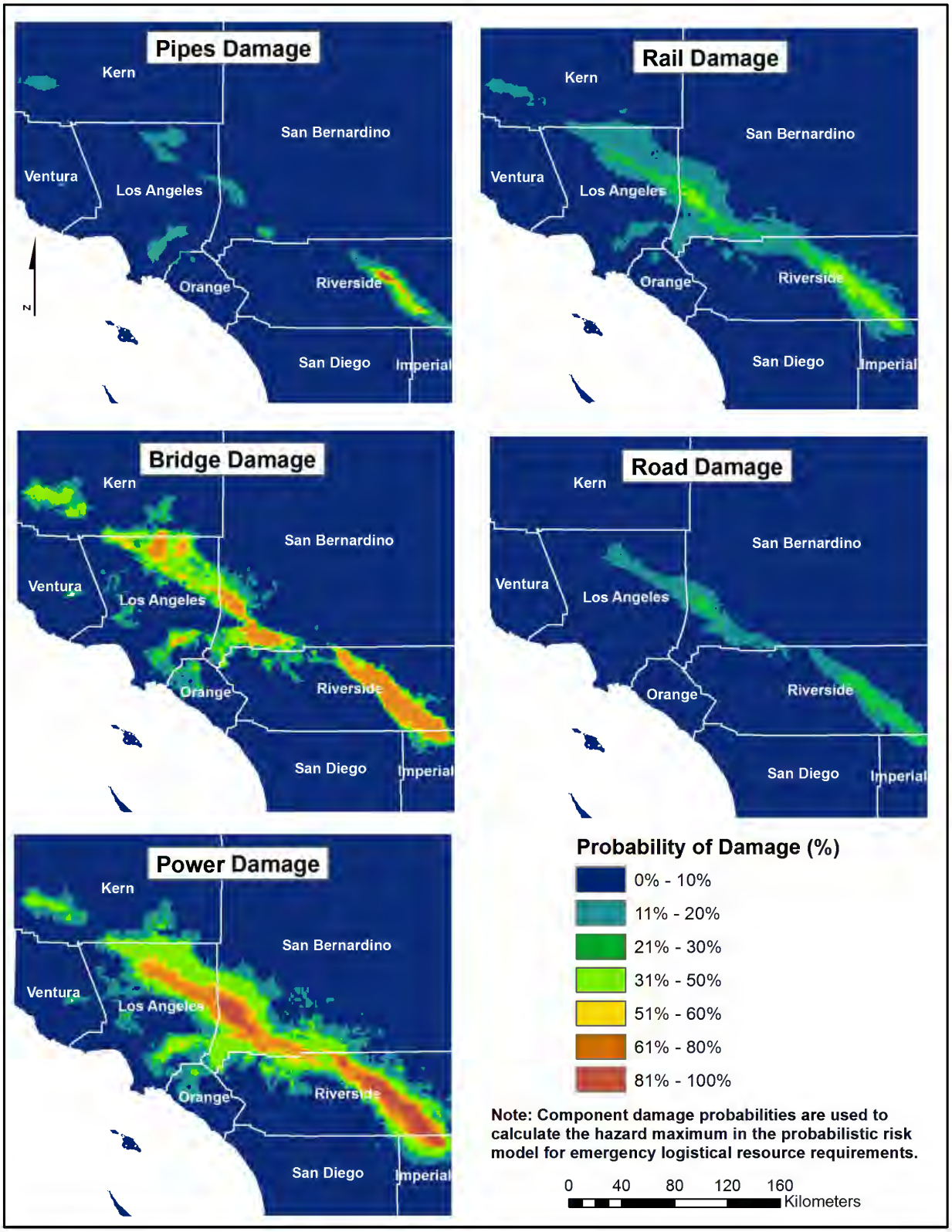

Figure 35. Probability of damage calculated for the infrastructure indicators

The final hazard damage "maximum" component of the probabilistic risk model, based on the identified infrastructure indicators, was then calculated as the "proxy" for the probability of emergency logistical resource requirements. These results are shown in Figure 36.

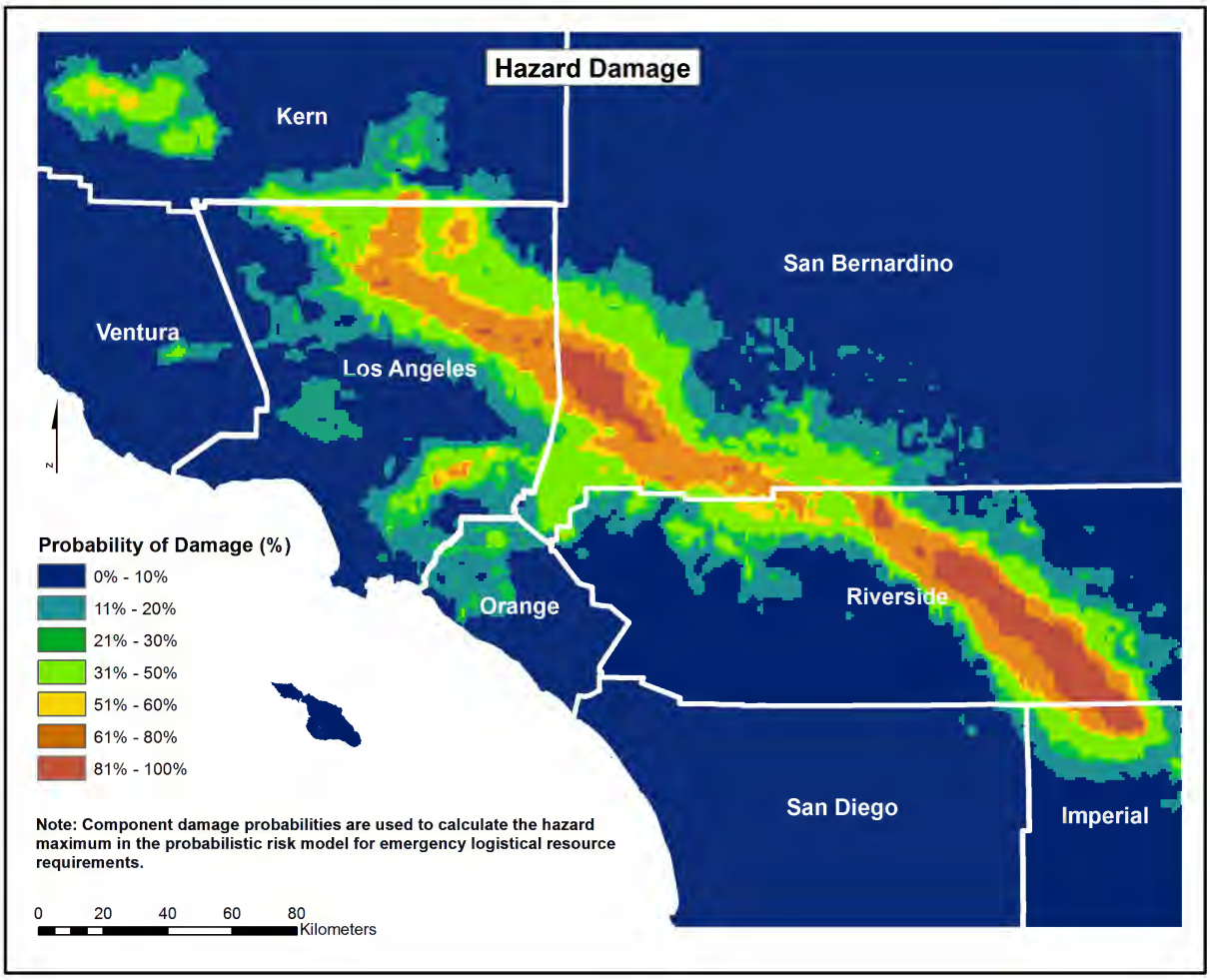

Figure 36. Results of calculation of the *hazard* component of the probabilistic risk model

Analysis of these results was performed to determine the contribution of each infrastructure damage component to the overall hazard in the study. Queries were used to identify the component that dominated the results of the hazard "maximum" calculation in each cell. The results of the analysis are presented in Table 5 for all of the grid cells.

Table 5. Summary of infrastructure component contribution to hazard results

Component	Total (%)*	Count*	Max Value
POWER	35.84%	43,728	0.958
RAIL	32.87%	40,098	0.078
PIPES	22.35%	27,261	0.963
BRIDGE	8.94%	10,906	0.793
HAZARD	**100%**	**121,993**	**0.963**

*Note: Cells in *Hazard* with component as highest value

These results using the Isoyama et al. (1998) damage functions for pipeline damage were also tested and compared with the normalized pipeline damage functions from O'Rourke and Ayala (1993) used in the current study—with only a small difference in the results. It was also found that bridge damage dominated the hazard calculation in the five expected areas from Werner et al. (2008), as shown in Appendix C.

It should also be noted that analysis of the infrastructure component contributions to the hazard indicated that road damage had a zero percent contribution to the final "maximum" hazard throughout the study area. This is because both the rail damage and road damage are based on Modified Mercalli Intensity (MMI). The rail damage curve dominated the road damage curve in each cell—and so the maximum excluded these values. The individual components of the model, and their quantitative contribution to the results, are further explored in the next section through validation with regression analysis.

One unexpected observation of boundary problems in the results required a slight adjustment to the methodology. Due to the smaller extent of the modeled ground-motion datasets, the entire eight-county region extent was not covered, so no damage probability values could be calculated for populations in these areas. However, analysis of the datasets indicated that there were likely very low ground-motion results in these sparsely populated areas. Therefore, all of the damage probability values were set to zero outside of the areas with

modeled ground-motion data, and the model was run with zero values in these regions. It is assumed this had no significant impact on the results.

The SoVI weight was also calculated as per the methodology, with no issues (Figure 37).

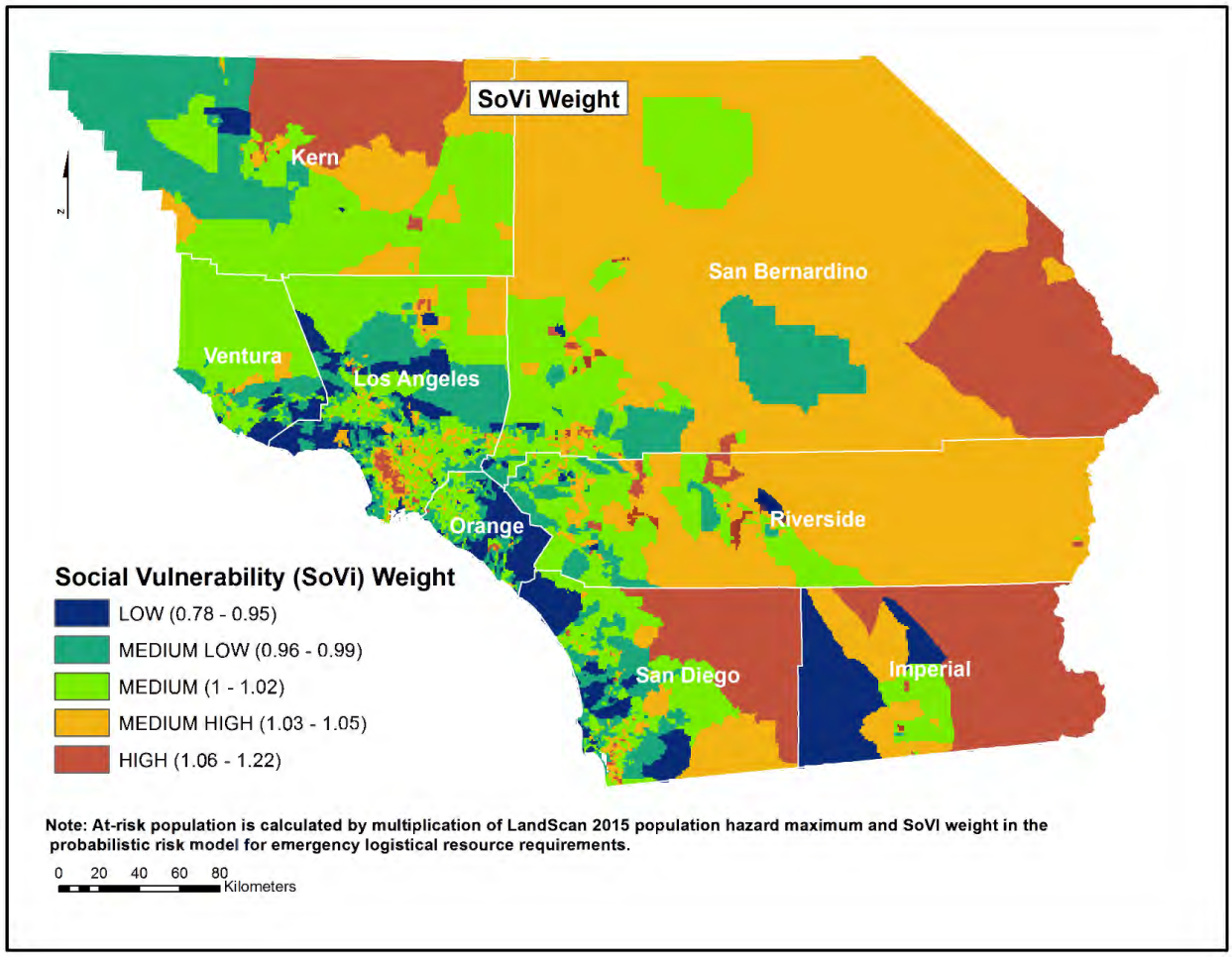

Figure 37. Results for the SoVI amplification factor calculation

The original range of composite factor scores for social vulnerability from the SoVI index (-15.93 to 14.78) were rescaled, as per the methodology in Chapter 4, to the new range (0.78 to 1.22) which preserved the ranked social vulnerability relation between census tracts in the computations. The social vulnerability classes and the resulting weights are presented in Figure 37 with the same standard deviation ranking as in the original data (HVRI 2018).

Finally, the computational implementation of the *risk* equation (Equation 12) was completed using the result of the *hazard* component calculations, social vulnerability weighting and the LandScan 2015 "global" population dataset. The final result, as presented in Figure 38, is a model of the "at-risk" population with emergency logistical resource requirements in the (M) 7.8 San Andreas Earthquake Scenario, throughout the eight-county study region, at day-three post event.

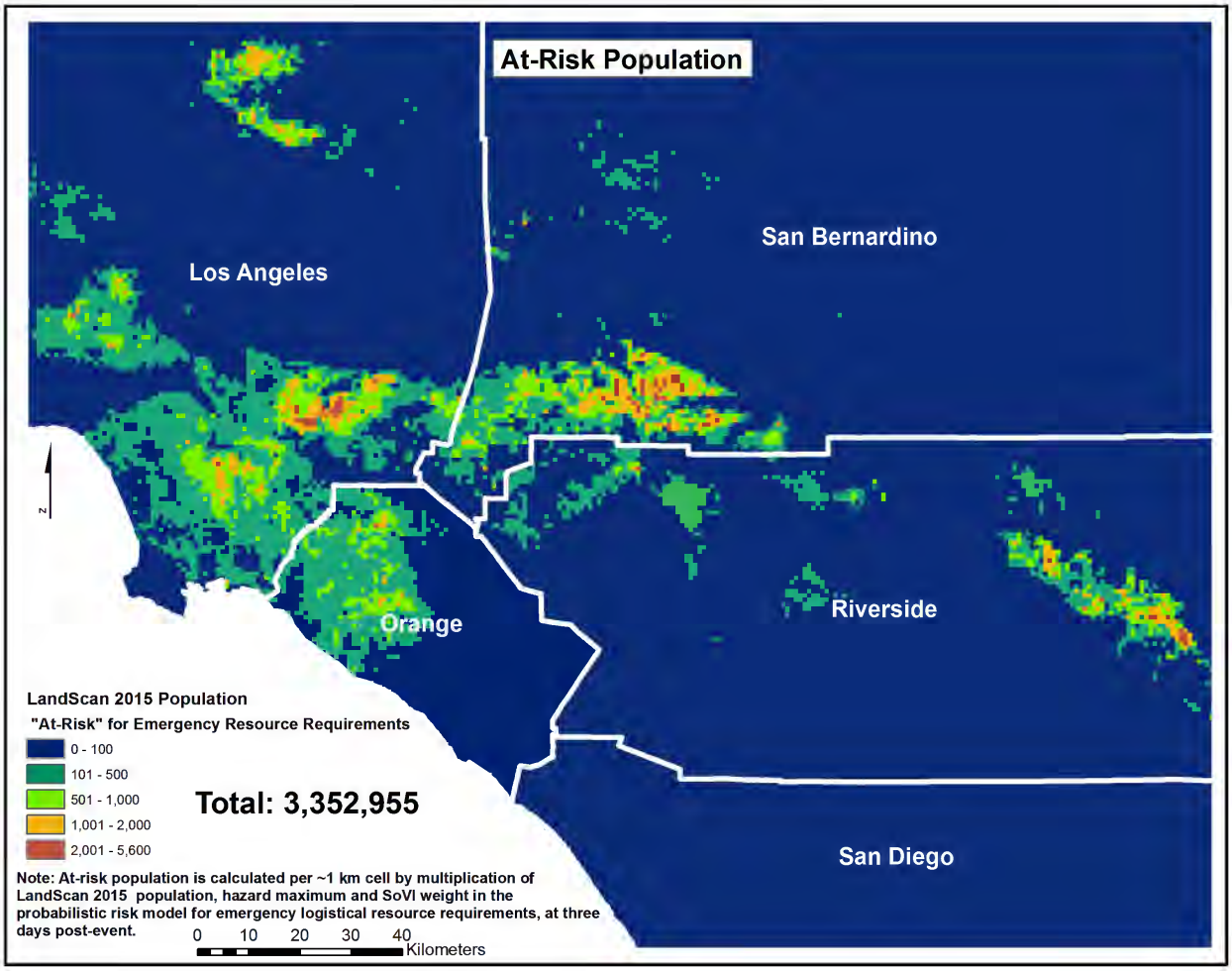

Figure 38. Final calculation of "at-risk" population

From these results, a summary of "at-risk" populations by county in the eight-county study region was calculated as well as the percentage of the total population from Landscan 2015

"global". These preliminary results and the percentage of the population "at-risk" versus the total population can be considered as a preliminary risk assessment by county, pending validation.

Table 6. Summary of "at-risk" populations in eight-county study area

COUNTY	POP (At-Risk)	POP (2015)*	POP (At-Risk) (% of Total)
SAN BERNARDINO	949,057	2,064,152	46%
RIVERSIDE	558,171	2,274,675	25%
LOS ANGELES	1,437,337	9,926,839	14%
ORANGE	356,528	3,098,579	12%
KERN	32,837	835,984	4%
VENTURA	15,950	828,307	2%
IMPERIAL	2,885	184,431	2%
SAN DIEGO	190	3,149,441	0%
TOTAL	**3,352,955**	**22,362,408**	**15%**

*Note: County population from LandScan 2015

5.1.2. *Validation with Regression Analysis*

The model was then validated to quantify the distributions and relationships of the underlying indicator variables in the model results. Logistic regression and associated statistical tests were performed for analysis of variable contributions in the results and to determine a confidence interval for these estimates.

The first step was to analyze the empirical distribution of the results from $[HAZARD_{damage}]\times[SOVI_{Weight}]$, which is the "proxy" for the probability of emergency logistical resource requirements calculated in Equation 12. A histogram was generated in RStudio which showed the distribution and frequency of these results. From this distribution, an empirical cumulative distribution function (CDF) was calculated, which represented the density (as a probability) of the modeled data less than or equal to any specific value in the dataset. From analysis of these results, it was found that the empirical distribution was most closely

approximated by the beta distribution with alpha = 0.1391879 and beta = .2605410. These graphs characterize the model results and are represented in Figure 39.

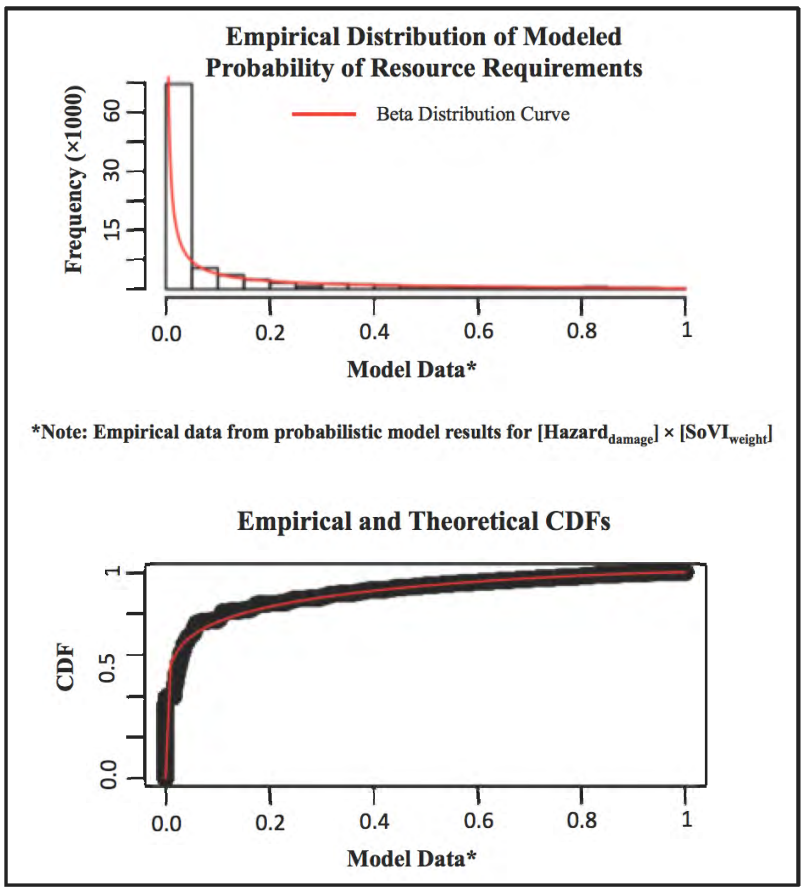

Figure 39. Empirical distribution of model results and beta distribution

The component variable distributions and relationships of the six infrastructure indicators and the four ground motion parameters were then analyzed individually in comparison to the model results. This analysis is presented in Figures 40 and 41, with a logistic trend curve approximating the relationship between each component and the results of the model, as the logistic curve serves as the link function for many forms of regression analysis with the family of binomial data distributions. This analysis of the components showed the distribution of each variable and the overall predictive trend for each variable in relation to the "proxy" for the

probability of emergency logistical resource requirements calculated in the methodology of the current study.

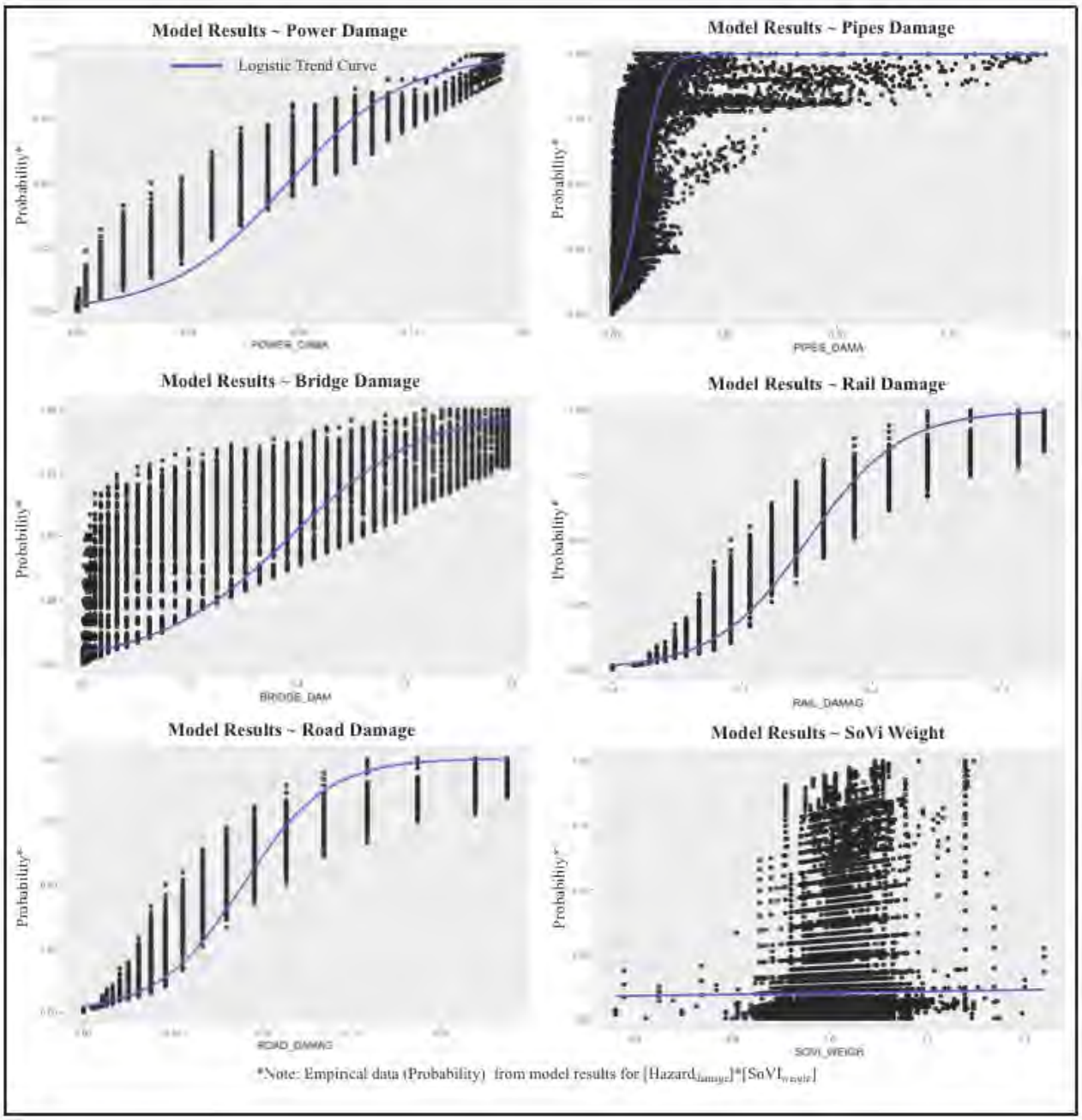

Figure 40. Variable distributions and relationships for model components

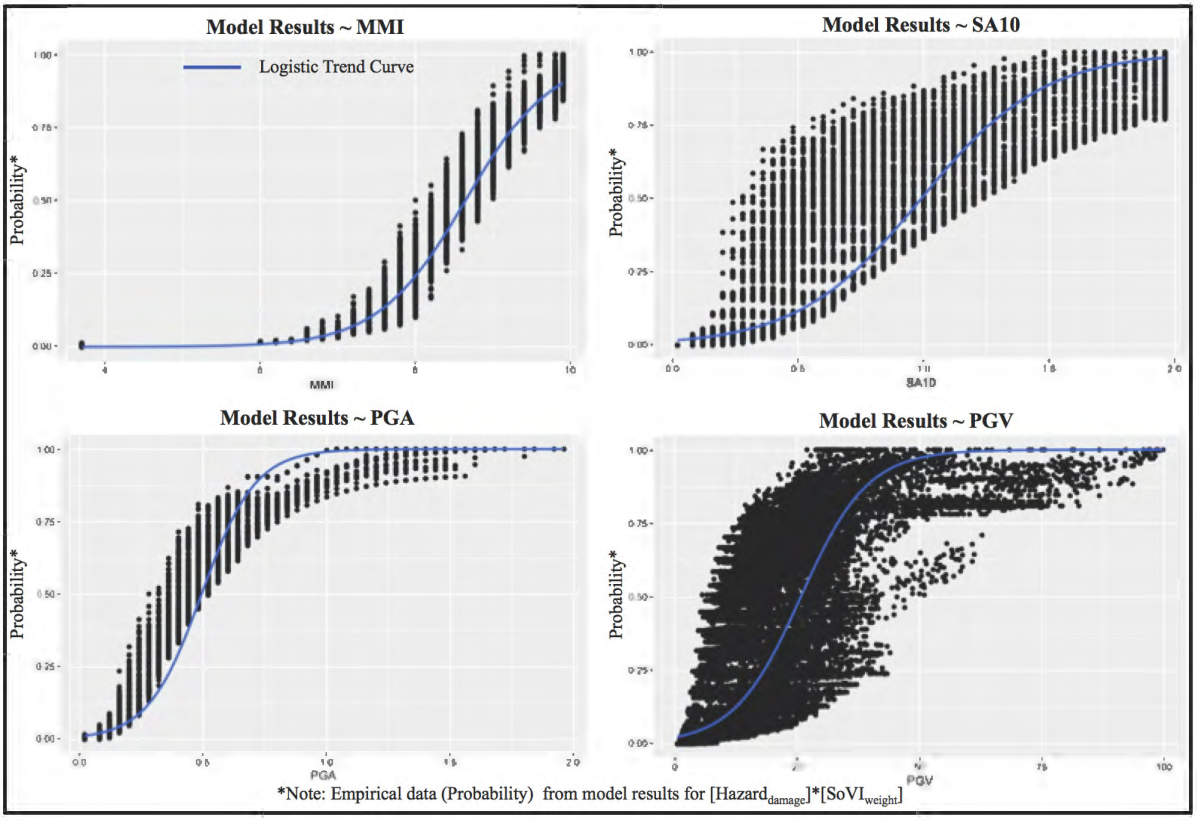

Figure 41. Variable distributions and relationships for ground-motion parameters

The range of each independent (predictor) variable is representative of independent conditional probabilities along the y-axis, given the probability on the x-axis, with the striated linear pattern resulting as an artifact from the discrete data values used in the model. In the current study, the probabilistic risk model results in a probability of emergency logistical resource requirements as a proportion of "successes" in the total population (as in Assumption 10 and 11). In this case, regression for a beta distribution is similar to a binomial generalized linear model (GLM) and so the GLM may provide useful information on the relative strength of the contribution of the variables in the model results (Cribari-Neto and Achim 2010).

Logistic regression was performed with the GLM for the binomial family using a "logistic" link function through RStudio core libraries. This was based on the ten independent variables as identified in Figures 40 and 41 and the dependent response variable as the "proxy"

for the probability of emergency logistical resource requirements resulting from the current study. Beta regression and GLM for the quasibinomial family were also tested, as Cribari-Neto and Achim (2010) indicated, with similar results to the binomial GLM for ranked significance of dependent variable contributions as measured by z values (or t values). A pseudo R-squared (Nagelkerke) value of .71774 resulted, which indicated that the binomial GLM model accounts for approximately 72 percent of the variance. The results are shown in Figure 42, sorted by the z values to indicate the relative strength of the contribution of the variables in the model results.

```
Coefficients:
             Estimate Std. Error z value Pr(>|z|)
(Intercept) -14.755724   0.735243 -20.069  < 2e-16 ***
MMI           1.515096   0.122644  12.354  < 2e-16 ***
POWER_DAMA    2.561044   0.400900   6.388 1.68e-10 ***
PGA           2.250138   0.452917   4.968 6.76e-07 ***
SOVI_WEIGH    1.275729   0.370410   3.444 0.000573 ***
SA10          0.544867   0.261311   2.085 0.037057 *
PIPES_DAMA    0.887830   0.616639   1.440 0.149928
BRIDGE_DAM    0.205491   0.475876   0.432 0.665875
ROAD_DAMAG    0.213728  10.736443   0.020 0.984118
PGV          -0.004020   0.004003  -1.004 0.315260
RAIL_DAMAG  -16.084941   9.282988  -1.733 0.083143 .
---
Signif. codes:  0 ‘***’ 0.001 ‘**’ 0.01 ‘*’ 0.05 ‘.’ 0.1 ‘ ’ 1

(Dispersion parameter for binomial family taken to be 1)

    Null deviance: 36179.94  on 121992  degrees of freedom
Residual deviance:   305.02  on 121982  degrees of freedom
AIC: 20414
```

Figure 42. Initial binomial GLM regression results

Further investigation of the binomial GLM with the removal of independent variables with statistical significance below the 95 percent threshold resulted in a similar AIC and pseudo R-squared value as the initial regression results. Therefore, all of the independent variables were left in the binomial GLM in the final regression results.

To evaluate these results and the goodness of fit of the binomial GLM regression model, an analysis of the residuals was performed and the deviance divided by the degrees-of-freedom

was calculated. Myers et al. (2002) states that lack of fit may be a problem when deviance divided by the degrees of freedom exceeds one. Deviance divided by the degrees-of-freedom showed a value of 0.296576, which did not indicate a lack of fit.

Residuals were examined to see if any systematic trends resulted. In summary, residuals plotted against predicted values showed a strong clustering near zero, with variance decreasing slightly as the absolute value of the predicted results increased—but overall the fit worked well. There were no signs of heteroscedasticity and no signs of significant outliers affecting results in plots of the standardized Pearson residual against the leverage. These results are shown in Figure 43.

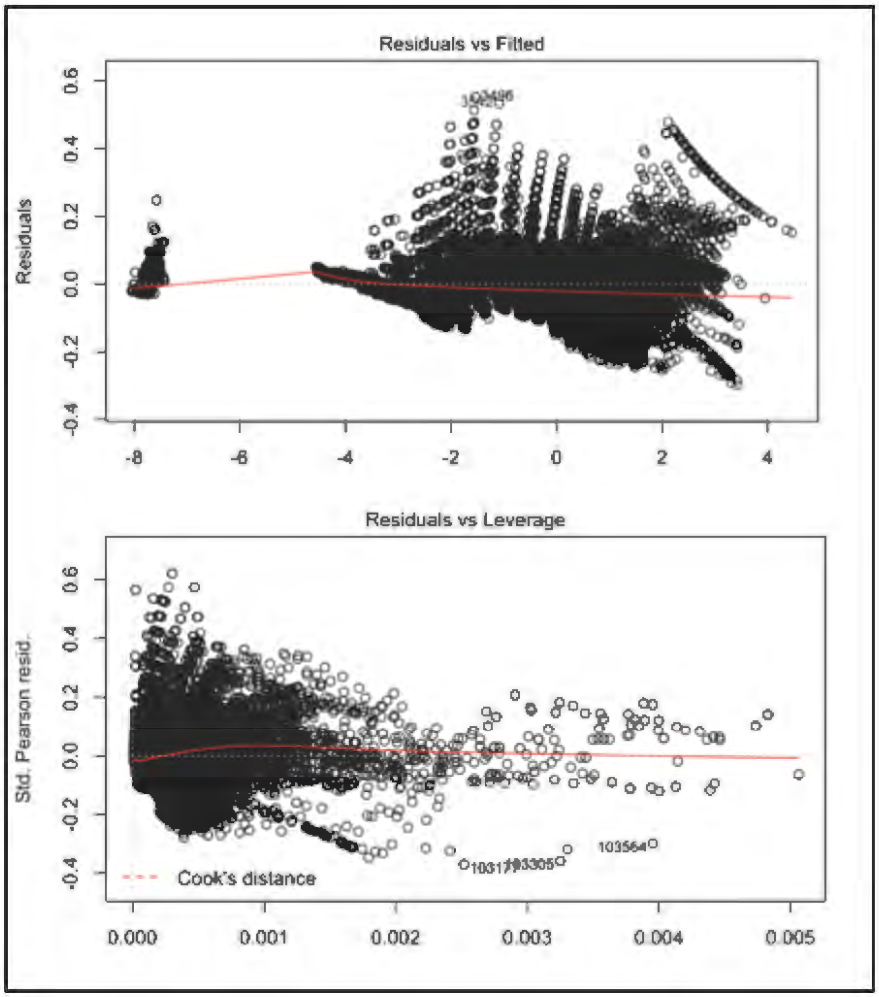

Figure 43. Analysis of residuals from the GLM regression results

Finally, the residuals were mapped over the study area, which showed some spatial autocorrelation, which is to be expected, but not a clear systematic trend. These results are shown in Figure 44.

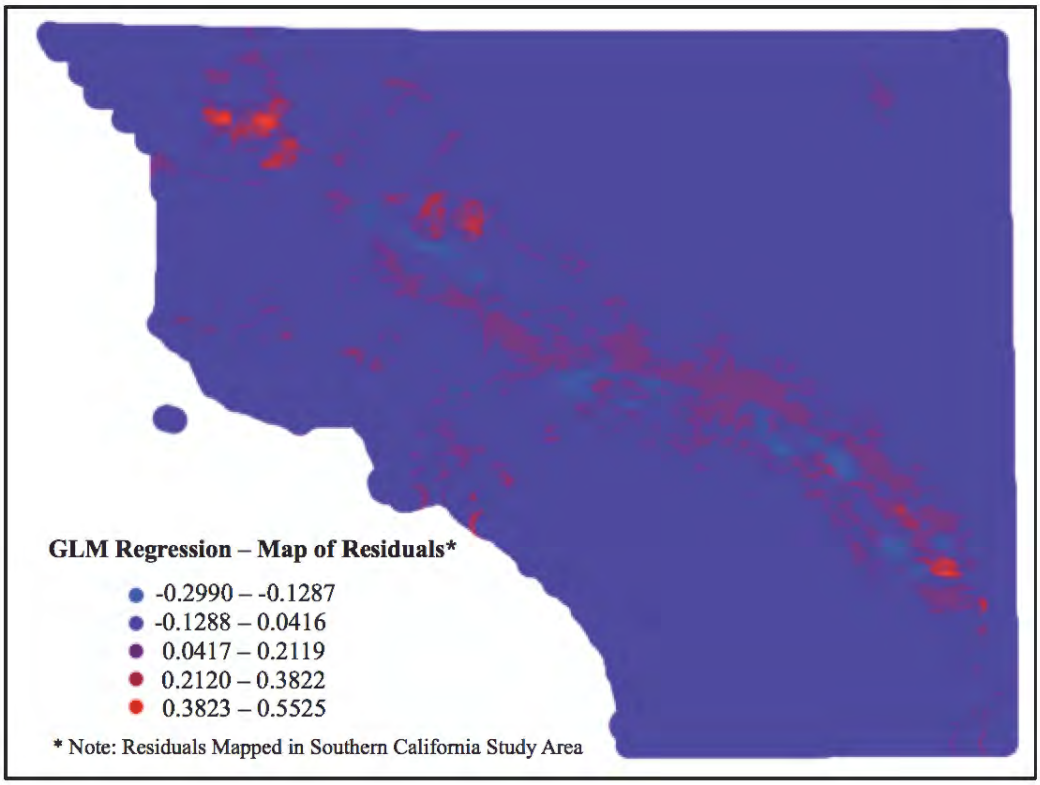

Figure 44. Mapping of residuals from the GLM regression results

The binomial GLM regression results showed that MMI and power damage were the two independent variables with the greatest contribution to the explained variance in the model. The power damage significance in logistical resource requirements was to be expected, as per USACE (2008) and UASI (2014) and so provided independent validation for the methodology of the probabilistic risk model—in particular for the choice of the maximum in the *hazard* component calculation of the risk equation.

The significance of MMI was an interesting result, as increased logistical resource requirements should be correlated with higher earthquake intensities—however the MMI data

cannot be directly related to damage probabilities for the majority of the infrastructure indicators, and so this is difficult to show. These results independently confirmed that MMI can be considered a global indicator for emergency logistical resource requirements, which is to be expected based on the literature (e.g. from NRC 2007; Earle et al. 2009, CalOES and FEMA 2011; CalOES and UASI 2015; UASI 2014). Therefore, the probabilistic risk model has produced viable results that can be considered validated for application by emergency managers and community planners.

5.2. Applications of the Probabilistic Risk Model

With the probabilistic risk model validated, the next step was to apply the results of the model in several applications for use by emergency managers and community planners. The development of a relative risk ratio in the eight-county study region proceeded according to the methodology of Chapter 4. The results are presented in Figure 45, where the extent is centered and scaled to an area that fits most of the relative risk ratio results.

The largest high-risk communities with over 50 percent risk for emergency logistical resource requirements identified were: El Monte, Baldwin Park, Glendora, Lancaster and Palmdale in Los Angeles County; San Bernardino, Rialto, Colton, Highland, Redlands and Yucaipa in San Bernardino County; and Palm Springs, Thousand Palms, Bermuda Dunes, Indio, Coachella, Thermal, Mecca in Riverside County.

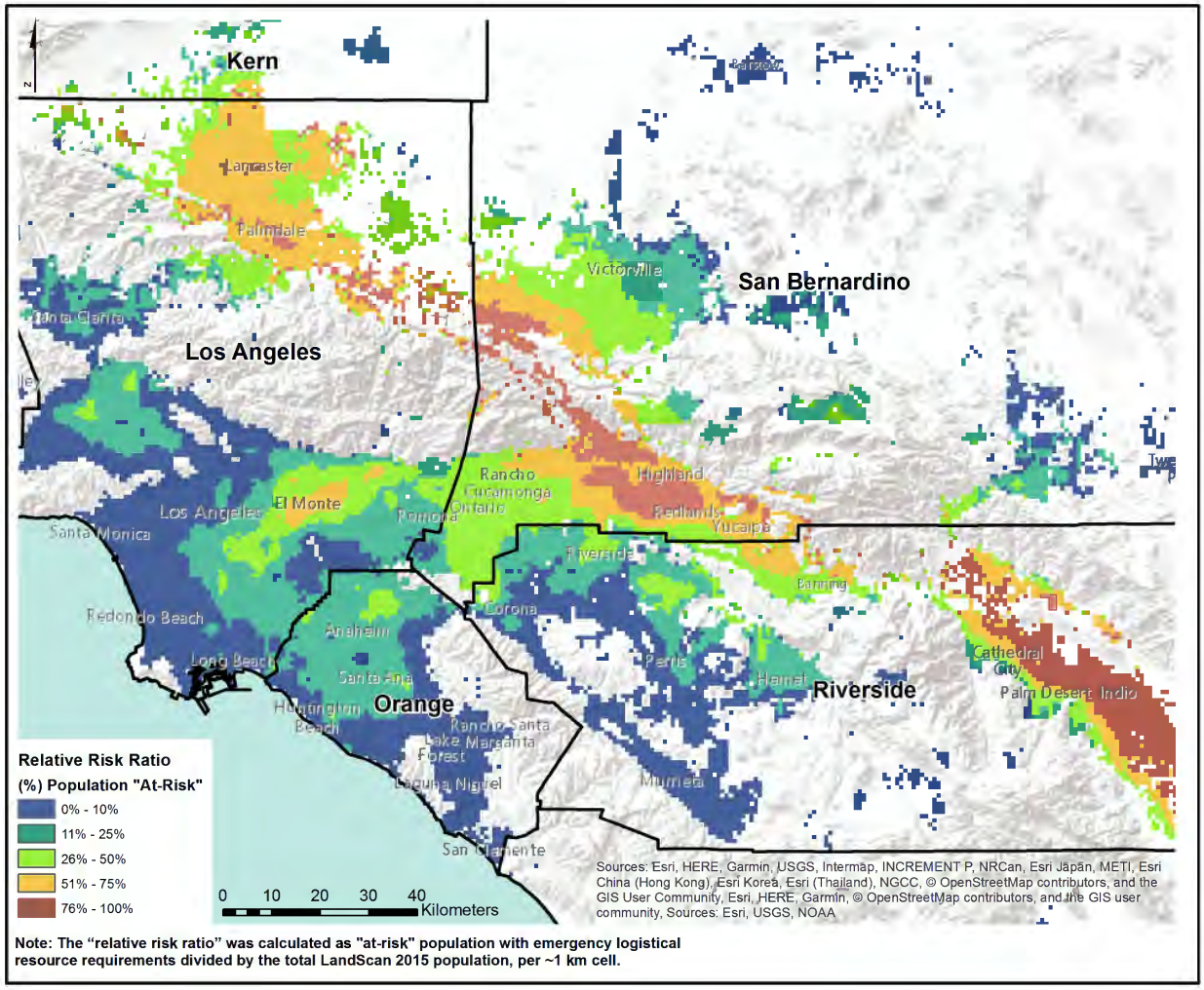

Figure 45. Results from calculation of the relative risk ratio to the general population

5.2.1. *Calculation of Resource Requirements Over Time in Los Angeles County*

To calculate the resource requirements over time in the Los Angeles County study area, the probabilistic risk model was applied with the LandScan USA 2012 "conus_night" population dataset, as per the methodology in Section 4.4. The results in Figure 46 show a total "at-risk" population for emergency logistical resource requirements of 1,421,415 at day-three, post-event—or approximately 14.7 percent of the population—with a total requirement of 2,832,830 meals and 4,264,245 liters of water. Population counts were calculated for each 90×90 meter cell.

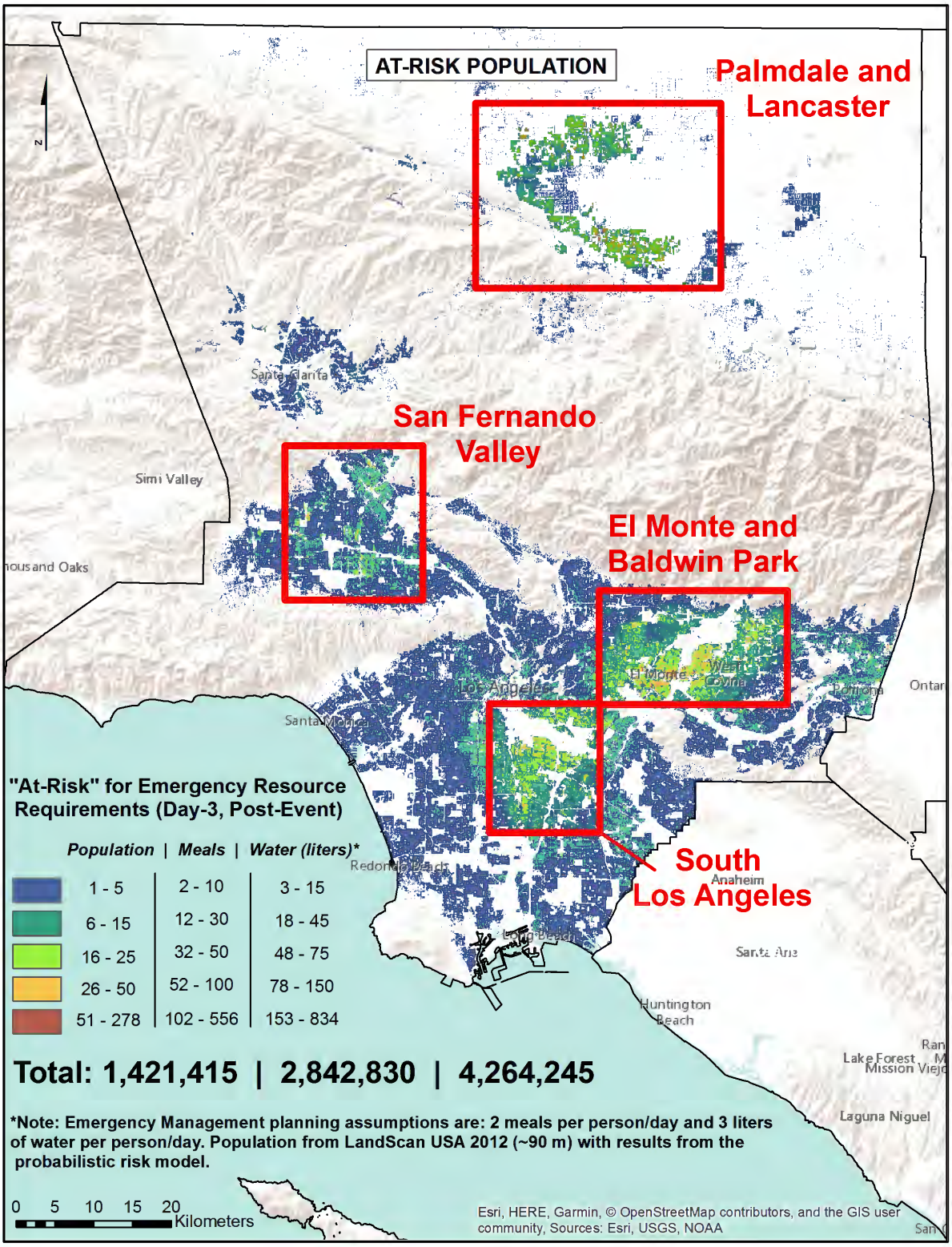

Figure 46. "At-risk" population and resource requirements at day-three, in Los Angeles County

These results had a small variation in summary population counts in comparison to LandScan 2015 because of differences in time and scale, as seen in Table 6. Four priority areas were identified in Figure 46 where the majority of the resource requirements were expected to arise. These areas are presented in detail in Figure 47 and 48, from the inset maps of Figure 46, with the same symbology and legend.

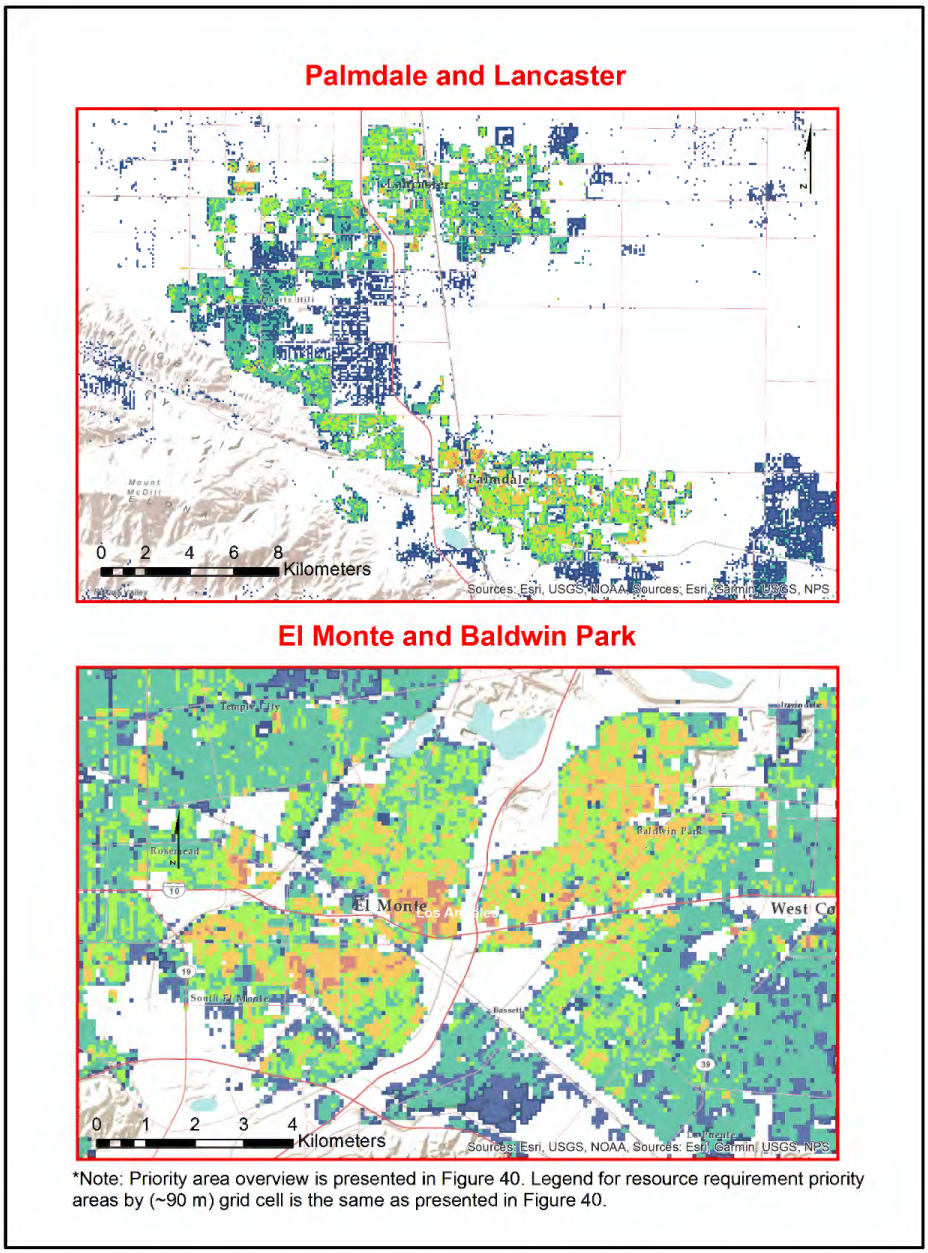

Figure 47. "At-risk" population and resource requirements at day-three, in Los Angeles County—Areas of Detail I

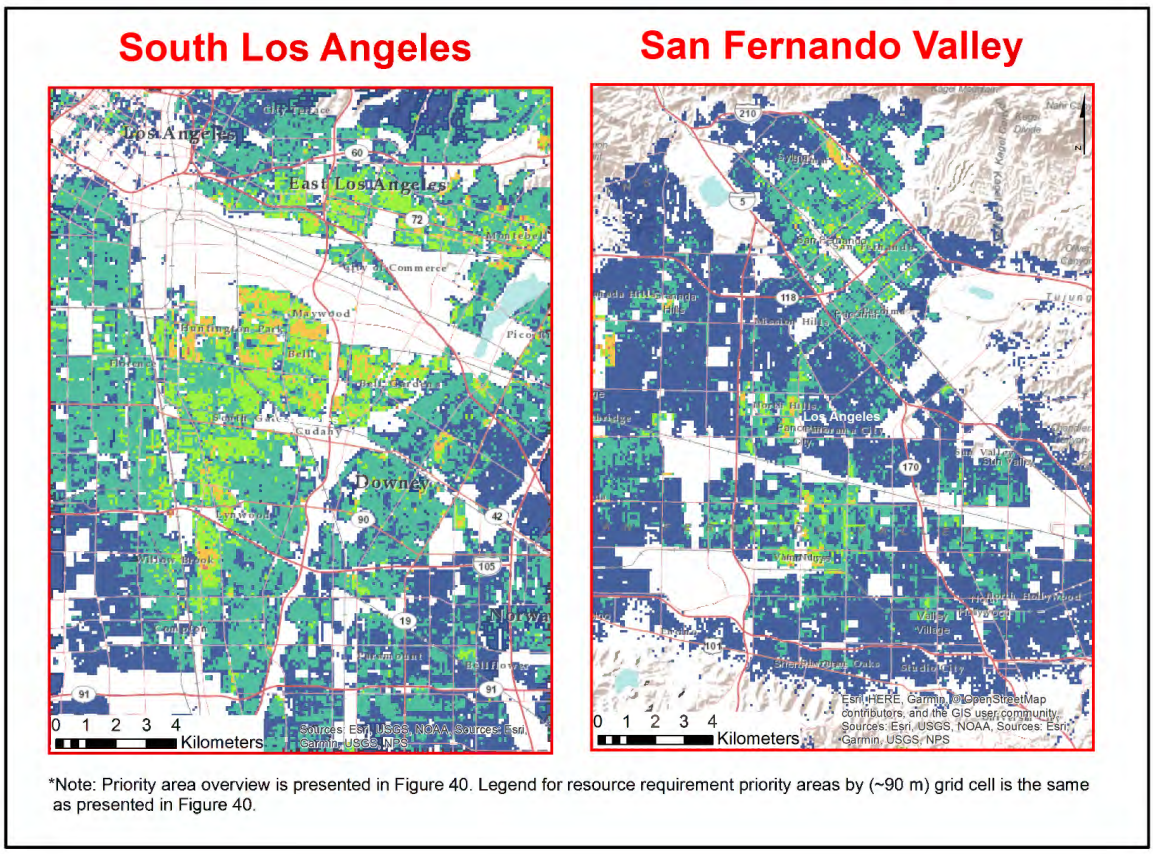

Figure 48. "At-risk" population and resource requirements at day-three, in Los Angeles County—Areas of Detail II

The next step in application of the methodology of Section 4.4 to determine resource requirements over time was to establish the classification breaks for the four damage categories from the results of the probabilistic risk model in Los Angeles County. Several methods were tested, including a quantile approach, equal interval, Jenks natural breaks and nested means, with varying results. However, natural breaks was chosen as per the methodology in Section 4.4.1 to best represent the naturally occurring groupings of resource requirements in increasing severity.

The results from $[HAZARD_{Damage}]\times[SOVI_{Weight}]$ were analyzed, and a maximum value of .8644, minimum of 0 and mean value of .2091 were found. From these values, the four damage categories were then defined as: "minor", as the range between 0 (minimum) and .1045; "moderate", as the range between .1046 and .2091 (mean); "extensive", as the range between

.2092 and .5367; and “complete”, as the range between .5368 and .8644 (maximum) probability of resource requirements.

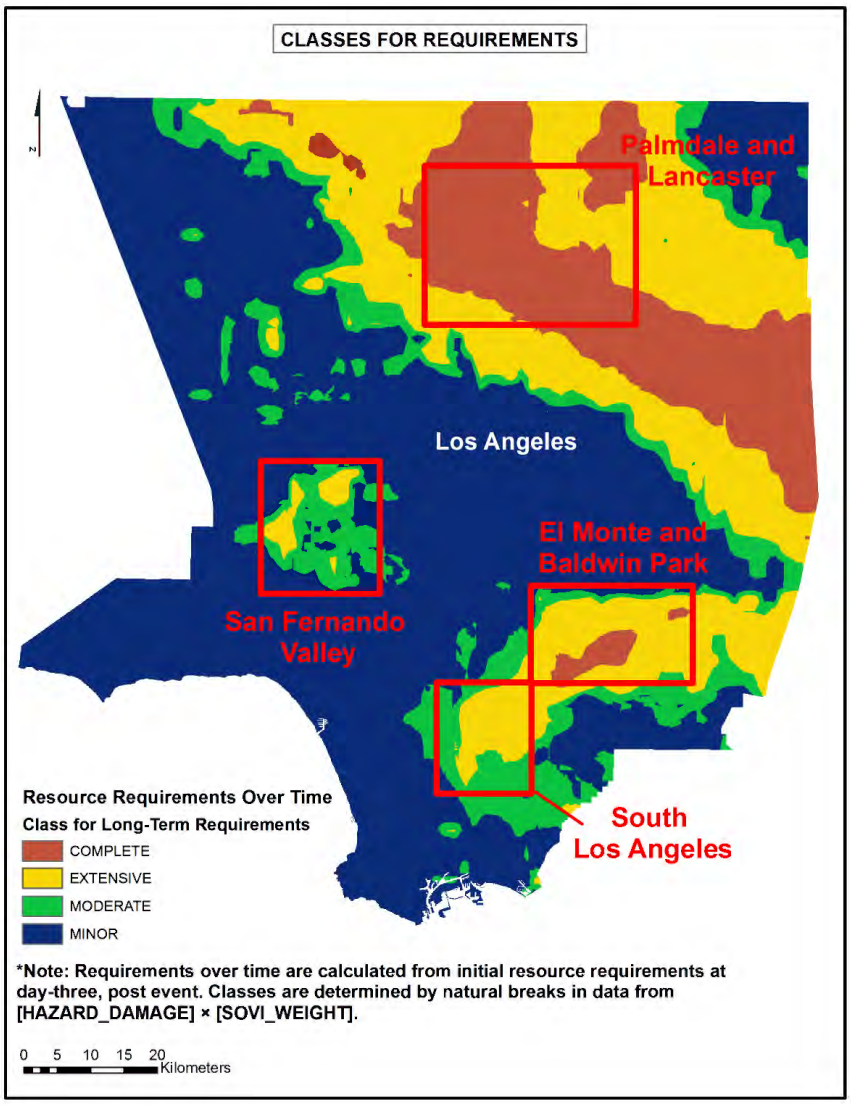

Figure 49. Establish classes for resource requirements over time

The next step was to fit the dynamic resource requirements curves from the three recovery simulations in Section 4.4.2 to a zero value on the y-axis (where no more resources are required) from Table 4. This resulted in values for computation of the resource requirements and their restoration timelines—identified as parameter (a) in Equations 16, 18, and 20. This was completed in MATLAB and using the online Wolfram Alpha calculator with no issues.

Table 7. Calculated results for the restoration timeline parameter

Category	SIMULATION A	SIMULATION B	SIMULATION C	Days Until Restored
COMPLETE	-0.05617	116.03	116.172	119
EXTENSIVE	-0.167044	39.0101	39.0579	42
MODERATE	-0.814339	8.0028	8.01187	11
MINOR	-6.51471	1.00026	1.00148	4

The parameter (b) in Equations 16, 18, and 20 was also calculated, for example, as shown in Figure 50 for recovery Simulation B (Maximum). This parameter increased or decreased the restoration timeline curve proportionally to the social vulnerability weighting based on [$SoVI_{Weight}$]. Results for the other two equations were similar for parameter (b).

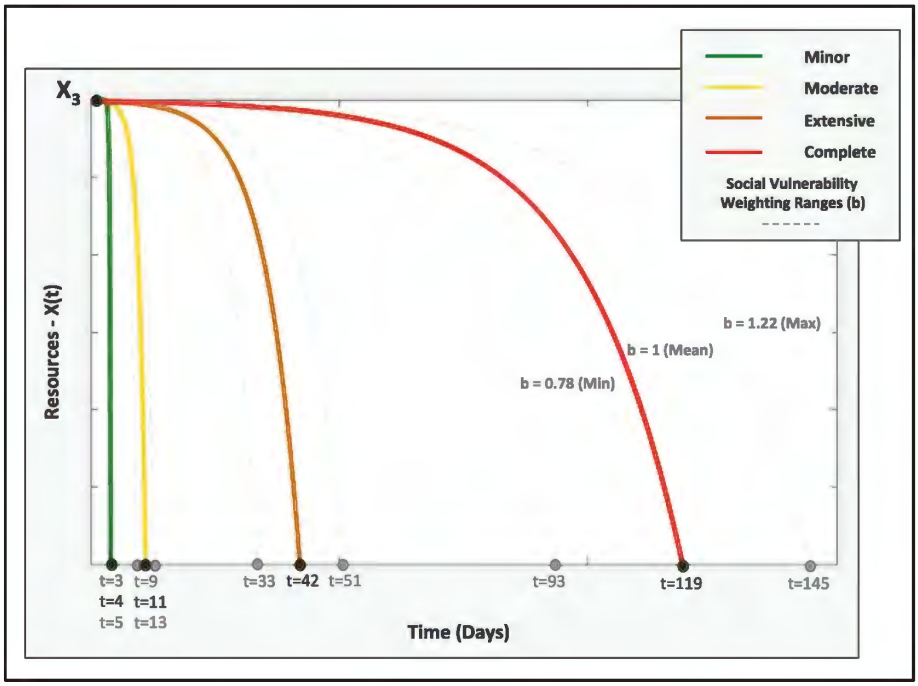

Figure 50. Equation 18 with social vulnerability weighting

Finally, resource requirements over time were directly calculated in ArcGIS 10.6 at t = 7, 14, 30, 45, 60 and 90-day post-event intervals for each of the three simulations. Equations 16, 18, and 20 were applied in ArcGIS 10.6 for direct calculation in each of the three simulations for resource requirements over time based on the four damage levels as per the methodology in

Chapter 4. The initial resource requirement level for each cell was based on the day-three post-event resource requirements as determined from application of the probabilistic risk model. The results are presented for each of the simulations in a summary table (Table 8), graph (Figure 51), and in three time series map compilations (Figures 52 to 54).

Table 8. Summary results for resource requirements over time for three simulations

FOOD (Meals*)									
	TOTAL POP.	AT-RISK POP	DAY-3	DAY-7	DAY-14	DAY-30	DAY-45	DAY-60	DAY-90
SIMULATION A (Minimum)	8,992,637	1,421,415	2,842,830	1,083,300	525,889	148,575	63,253	26,857	2,086
SIMUALTION B (Maximum)	8,992,637	1,421,415	2,842,830	2,090,919	1,552,876	1,255,080	573,555	538,974	390,077
SIMULATION C (Average)	8,992,637	1,421,415	2,842,830	1,912,160	1,350,590	843,284	417,159	334,682	173,170
WATER (Liters*)									
	TOTAL POP.	AT-RISK POP	DAY-3	DAY-7	DAY-14	DAY-30	DAY-45	DAY-60	DAY-90
SIMULATION A (Minimum)	8,992,637	1,421,415	4,264,245	1,624,950	788,834	222,863	94,880	40,286	3,129
SIMUALTION B (Maximum)	8,992,637	1,421,415	4,264,245	3,136,379	2,329,314	1,882,620	860,333	808,461	585,116
SIMULATION C (Average)	8,992,637	1,421,415	4,264,245	2,868,240	2,025,885	1,264,926	625,739	502,023	259,755

*Note: Emergency Management planning assumptions are: 2 meals per person/day and 3 liters of water per person/day)

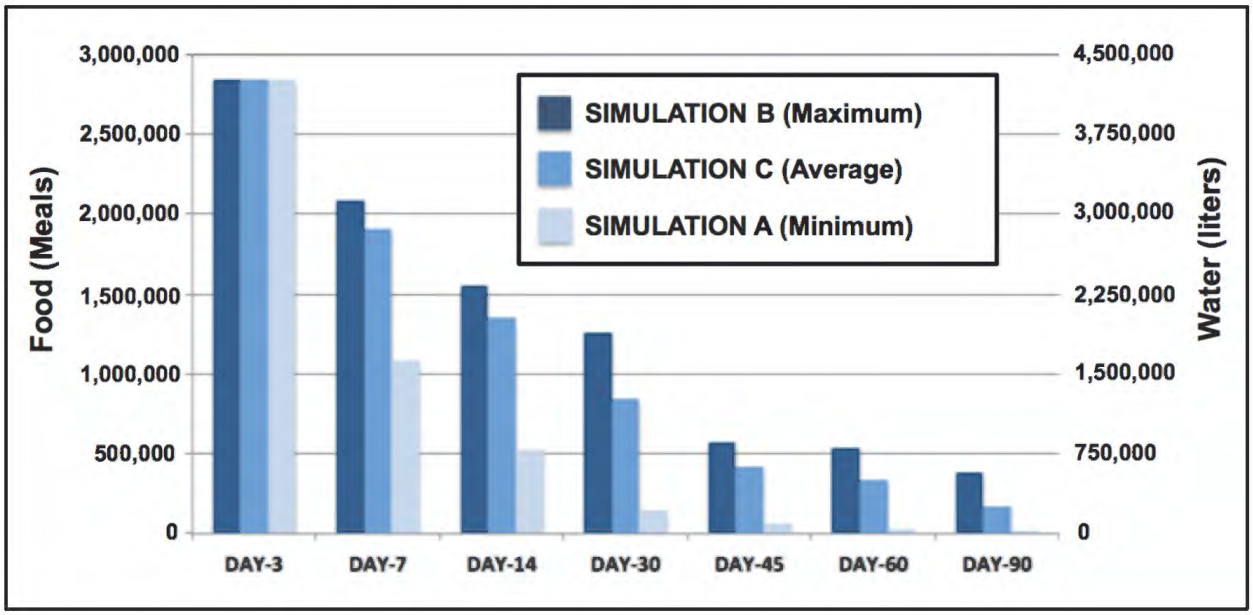

Figure 51. Summary resource requirements over time for three simulations

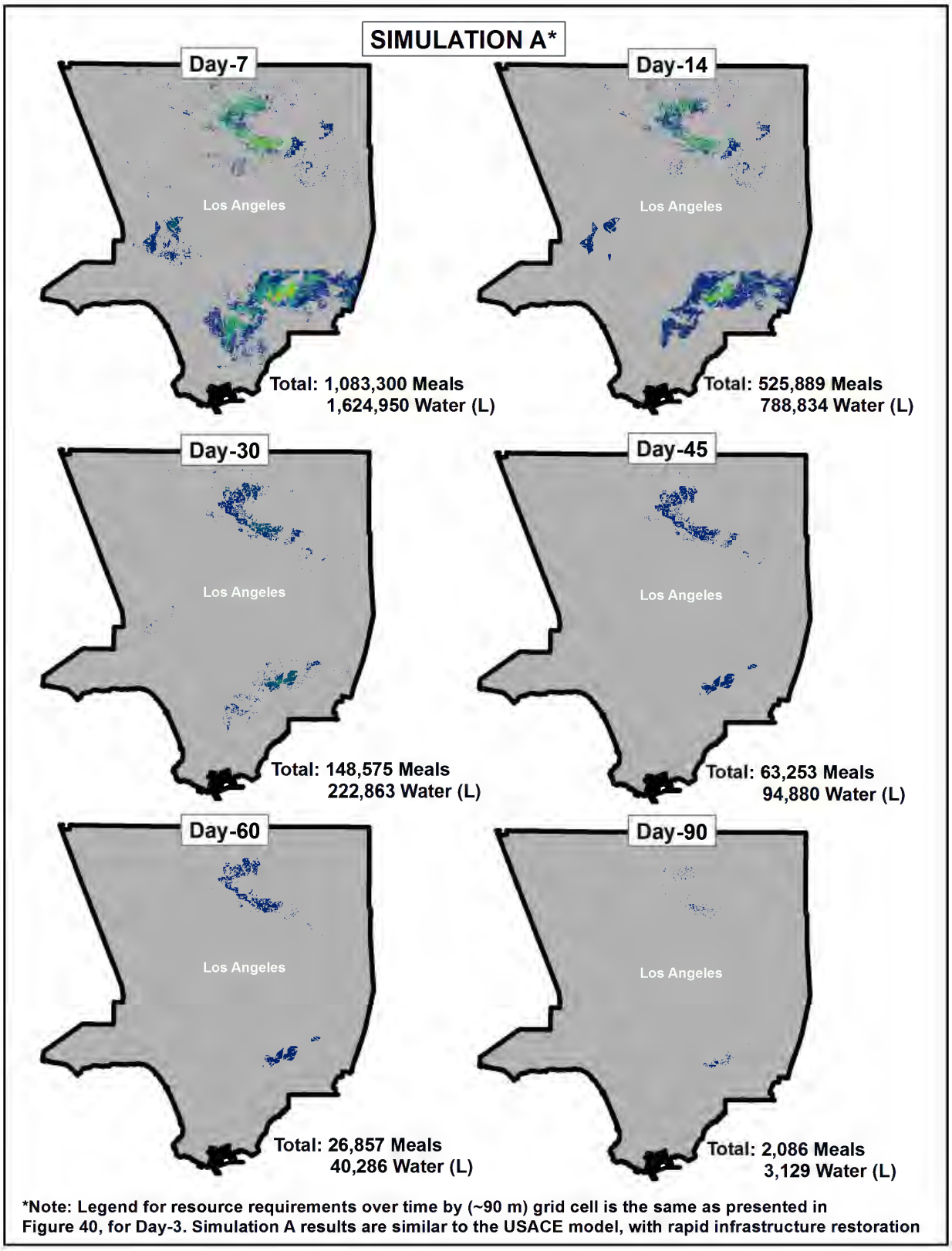

Figure 52. Resource requirements over time for Simulation A (Minimum)

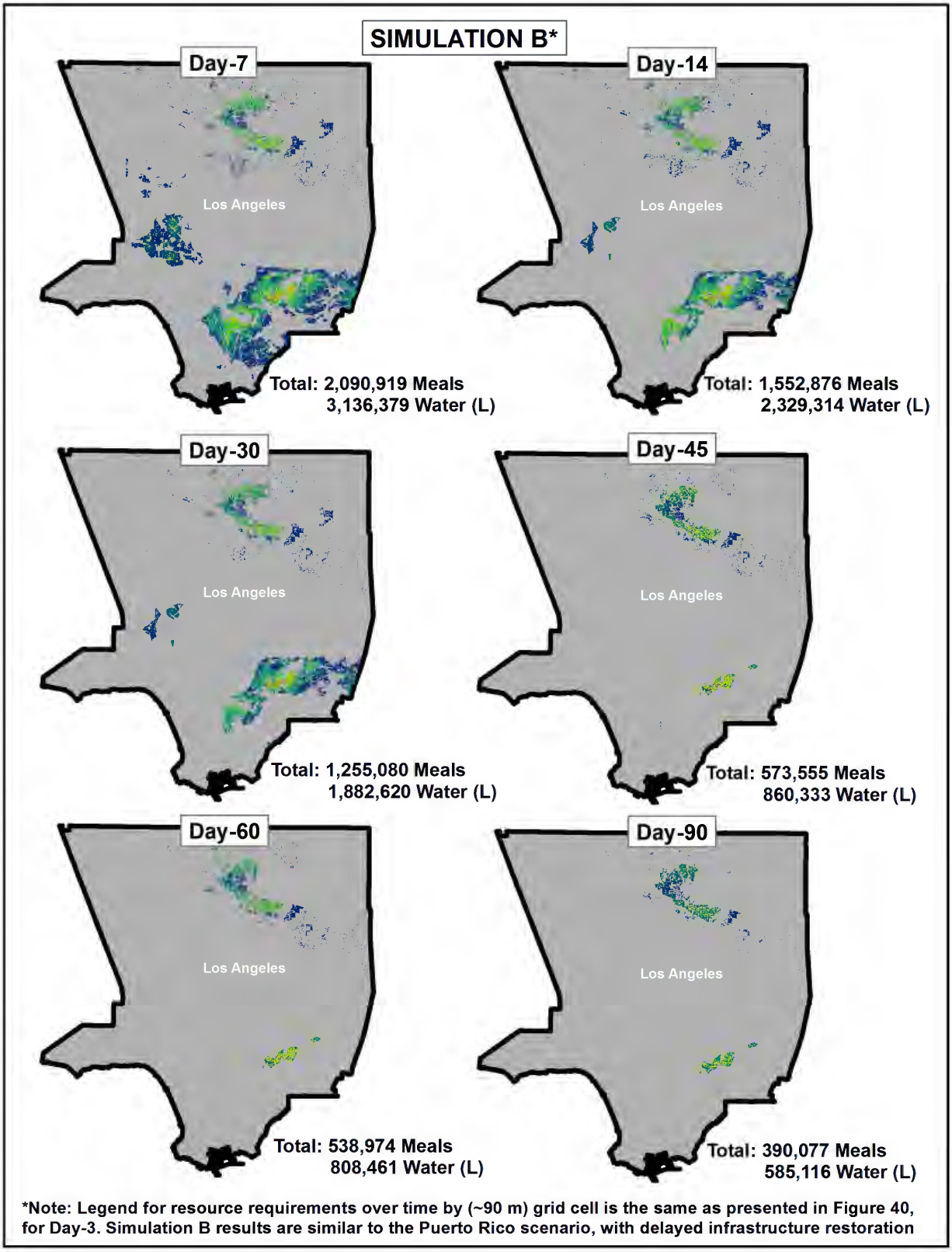

Figure 53. Resource requirements over time for Simulation B (Maximum)

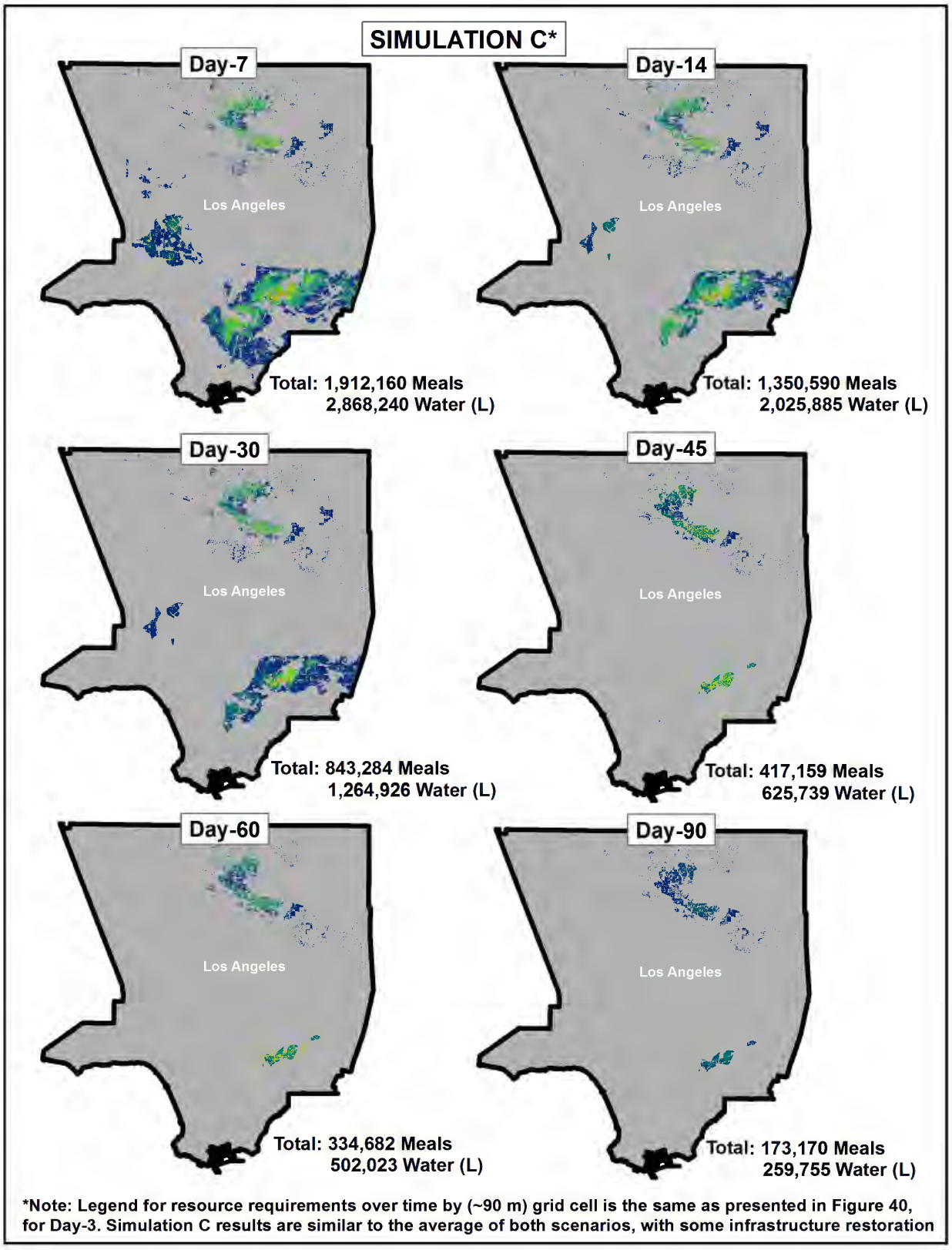

Figure 54. Resource requirements over time for Simulation C (Average)

It should be noted that there can be memory issues when processing the results of Simulation B in ArcGIS 10.6 in Windows 10 Enterprise 2016. From the formulation of Equation 18, the model results in a temporary memory allocation for calculation of all values, including those less than zero. These negative values are not in the range of valid results and in the final step are all mapped to "0" as the global minimum for the model. However, these artificial negative values become astronomical as the curves become asymptotic when values approach infinity, causing the computer to reach maximum memory limits.

To address this, the original "long integer" values were converted to "double" and the database was compressed. The small number of "null" values resulting from exceeding the "double" storage limits were then manually updated to "0" through the field calculator in ArcGIS 10.6 with no further issues.

5.2.2. *Summary Resource Requirements by Point of Distribution (POD) Sites*

In order to operationalize these results to support logistical planning in the commodity mission of the OPLAN, a summary of resource requirements by POD site was calculated, based on the methodology shown in Figure 34. These results included summary meal requirements by person, by pallet, and by truckload—which can then be used to prioritize resource distribution and support the ordering and shipping of commodities to the impacted POD sites. The final results for day-three are presented below in Figure 55, and the results for the three simulations for t = 7, 14, 30, 45, 60 and 90-days post-event are presented as a summary report in Appendix D. Summary calculations for bulk water storage and shipping requirements over time are also included the results of Appendix D, but summary information past day-three has been omitted.

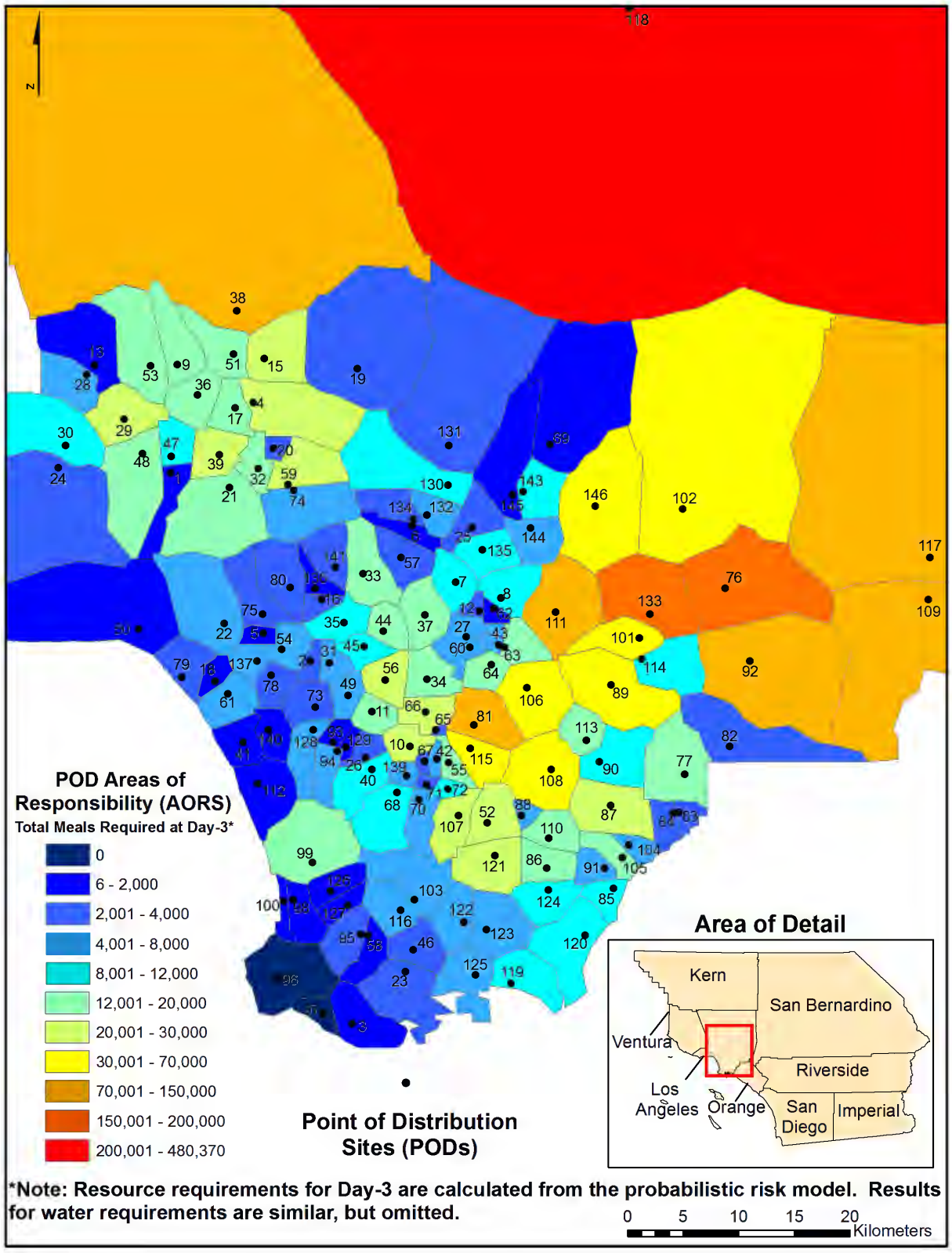

Figure 55. Summary of resource requirements by Point of Distribution (POD) sites at day-three

The results of the model and the three simulations provided each POD with a profile of their respective predicted resource requirements over time. Several characteristic POD sites and their summary resource requirements over time, taken from the data in Appendix D, are shown in Figure 56. The location of emergency logistical resource requirements at a community level is important for emergency managers, as these communities can be directly associated with a servicing POD site for ordering, shipping and distribution planning.

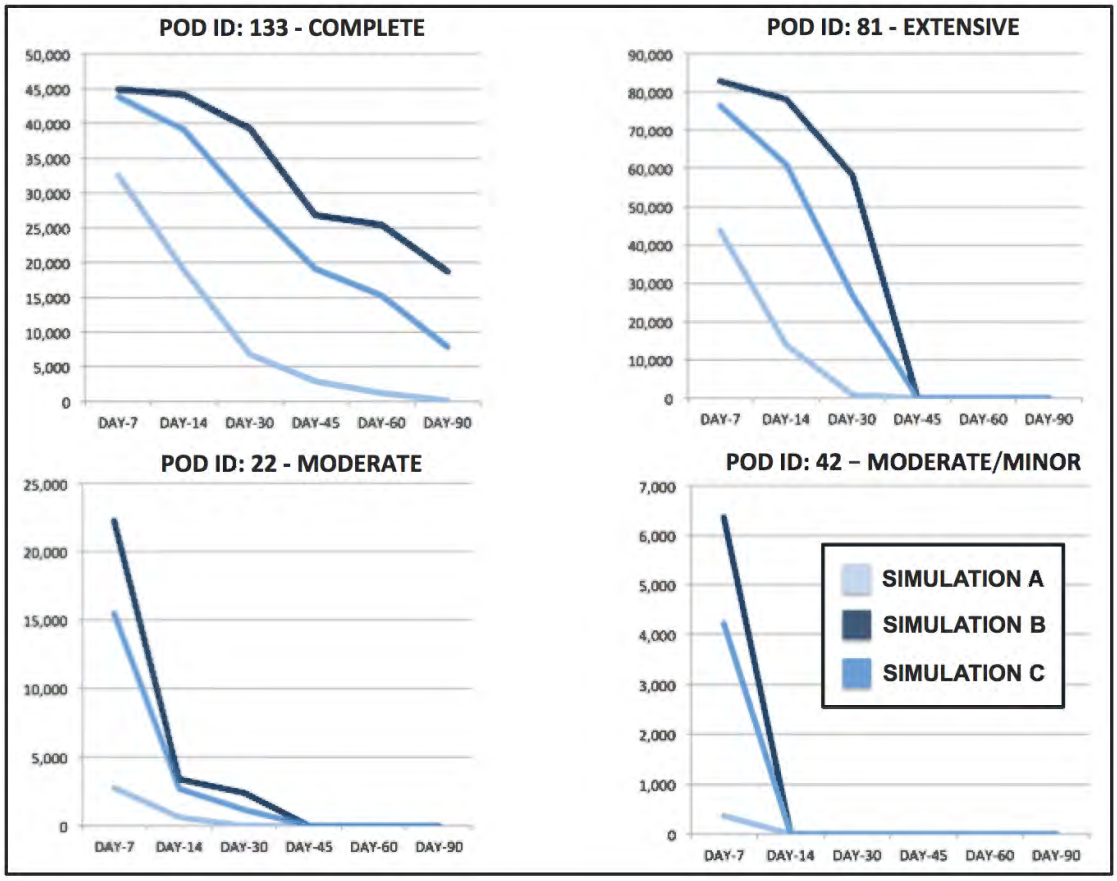

Figure 56. Characteristic POD sites and their modeled resource requirements

In conclusion, the development and application of the probabilistic risk model for emergency resource requirements in the (M) 7.8 San Andreas Earthquake Scenario and OPLAN was successful. The results can be used to enhance the OPLAN through supporting emergency management decision making and situation awareness in the commodity mission.

Chapter 6 Discussion

While Chapter 5 has provided an in-depth summary of the model results, this chapter provides a general summary of the results for application by emergency managers, along with an investigation into some of the issues and the potential for calibration and validation of the model in further research. Model-based uncertainty is summarized in an error budget analysis, which serves as the main instrument for investigation of these issues. Finally, several approaches for generalization of the model are proposed for supporting emergency logistical resource missions in global earthquake events both before and after the event occurs.

6.1. Summary of Results

In summary, the probabilistic risk model has predicted the total resource requirement at (t = 3) of 6,705,910 meals in the eight-county study region for a total "at-risk" population of 3,359,955, and 2,842,830 meals in Los Angeles County for a total "at-risk" population of 1,421,415. Similarly, requirements for 10,058,865 liters of water in the eight-county study region and 4,264,245 liters in Los Angeles County are also predicted. These estimates are in alignment with the Southern California Catastrophic Earthquake Response Operational Plan (OPLAN) assumption of supporting resource requirements for between 2.5 million and 3.5 million people (2 meals per person/day and 3 liters of water per person/day) in the eight-county study region, at three-days post-event. Therefore, the model results are a realistic estimate for total resource requirements.

Additionally, the model has provided a plausible estimate for the actual geographic locations of where these logistical resource requirements originate—which the OPLAN does not address. This is invaluable information for emergency managers, which can be used to help plan for and prioritize resource distribution in the commodity mission. In the applications of the

probabilistic risk model, three simulations of resource requirements over time up to (t = 90 days) have been provided, based on this initial data. This is a novel approach to long-term planning for the commodity mission, which has been identified as a gap in the current emergency management capabilities. A relative risk ratio has also been developed to estimate the relative risk for any random member of the general population, based on these results. This can be used in disaster preparedness and mitigation planning to address community vulnerability before an event occurs.

The resulting probabilistic risk model and its applications provide a systematic and comprehensive methodology to evaluate risks associated with the (M) 7.8 San Andreas Earthquake Scenario in estimation of "at-risk" populations for emergency logistical resource requirements. These results address several gaps in current emergency management capabilities including incorporating social vulnerability, identifying community locations for emergency logistical resource requirements and estimating resource requirements over time.

6.1.1. *Error Analysis*

No discussion of model results is complete without a discussion of model-based uncertainty and error analysis. As George Box has noted, "models, of course, are never true, but fortunately it is only necessary that they be useful" (Box 1979, 2). Because deterministic knowledge of a complex system (such as the emergency logistical resource requirements in the OPLAN) is not possible, evaluation of model-based uncertainty in the results can focus on measurement of the analysis of error in the model as a function of uncertainty associated with each parameter input to the model (O'Sullivan and Perry 2013).

To do this, an *error budget matrix,* which summarizes the estimation of error introduced in the model as a function of uncertainty in each parameter, was compiled. A formulation of the

error in the probabilistic risk model can be described as the error "delta" for each parameter, defined as the difference between the "actual" damage or value that occurs in the event and the "estimate" provided through the modeling methodology. Table 9 shows the error budget matrix for this model. Several types of errors are identified, based on definitions from O'Sullivan and Perry (2013).

Table 9. Error budget matrix from the model results

ID	Component	Parameter	Type	Error Calculation	Error
1	Hazard	Bridge Damage	Process	**ACTUAL** Bridge damage - Bridge damage **ESTIMATE** w/ assumptions	**ΔBridge**
2	Hazard	Bridge Restoration	Process	**ACTUAL** Bridge restoration timelines - Bridge restoration timeline **ESTIMATE**	**ΔBridgeRest**
3	Hazard	Gas Pipe Restoration	Process	**ACTUAL** Gas restoration timelines - Gas restoration timeline **ESTIMATE**	**ΔGasRest**
4	Hazard	Pipes	Reducible w/ Research/Issue	**ACTUAL** Pipe conveyance damage - Brittle pipe damage from O'Rourke and Ayala **ESTIMATE** w/ assumptions	**ΔPipes**
5	Hazard	Power Damage	Process	**ACTUAL** Power system damage - Power system damage **ESTIMATE** w/ assumptions	**ΔPower**
6	Hazard	Power Restoration	Process	**ACTUAL** Power system restoration timelines - Power system restoration timeline **ESTIMATE**	**ΔPowerRest**
7	Hazard	Power Restoration-3	Reducible w/ Research/Issue	**ACTUAL** Power system restoration at day three - Initial power system restoration **ESTIMATE**	**ΔPowerInit**
8	Hazard	Rail Damage	Process	**ACTUAL** Rail damage - Rail damage **ESTIMATE** w/ assumptions	**ΔRail**
9	Hazard	Rail Restoration	Process	**ACTUAL** Rail restoration timelines - Rail restoration timeline **ESTIMATE**	**ΔRailRest**
10	Hazard	Road Damage	Process	**ACTUAL** Road damage - Road damage **ESTIMATE** w/ assumptions	**ΔRoad**
11	Hazard	Road Restoration	Process	**ACTUAL** Road restoration timelines - Road restoration timeline **ESTIMATE**	**ΔRoadRest**
12	Hazard	Water Pipe Restoration	Process	**ACTUAL** Water restoration timelines - Water restoration timeline **ESTIMATE**	**ΔWaterRest**
13	Model	Numerical Precision	Measurement	**ACTUAL** Value in calculation - Rounding Error from **ESTIMATE** in calculation	**ΔRoundingErr**
14	Model	Resolution	Measurement	**ACTUAL** Model population distribution - Raster resolution aggregate **ESTIMATE**	**ΔResolution**
15	Model	Resource Multiplier	Process	**ACTUAL** Meal and water requirements - Multiplier **ESTIMATE** from OPLAN	**ΔResource**
16	Model	Resource Over Time Category	Process	**ACTUAL** Resource over time magnitude of need - Category **ESTIMATES** for calculation	**ΔCategory**
17	Model	Resource Over Time Curves	Reducible w/ Research/Issue	**ACTUAL** Resource requirements over time - Simulation curve **ESTIMATES**	**ΔSimulation**
18	Model	Resource Requirements Over Time Weights	Reducible w/ Research/Issue	**ACTUAL** Resource over time weights - Resource over time average weights **ESTIMATE**	**ΔWeights**
19	Model	Unknown Factors	Process	**ACTUAL** Hazard - Hazard **ESTIMATE**	**ΔHazard**
20	Population	AOR	Measurement	**ACTUAL** Populations serviced by POD - Huff Model **ESTIMATE**	**ΔAOR**
21	Population	Dasymetric	Measurement	**ACTUAL** Population Density - Dasymetric Mapping **ESTIMATE**	**ΔLandScan**
22	Population	Population Count	Measurement	**ACTUAL** Population - (2010, 2012, 2015, 2016 Population **ESTIMATES**)	**ΔPopulation**
23	Scenario	Ground Motion	Process	**ACTUAL** Ground motion - Modeled ground motion **ESTIMATES**	**ΔGroundMotion**
24	Vulnerability	Other Vulnerability	Process	**ACTUAL** Vulnerability - Social vulnerability **ESTIMATE**	**ΔVulnerability**
25	Vulnerability	Social Vulnerability	Process	**ACTUAL** Social Vulnerability - SoVI Model **ESTIMATE**	**ΔSoVI**
26	Vulnerability	Social Vulnerability Amplification	Reducible w/ Research/Issue	**ACTUAL** Social Vulnerability Amplification - **ESTIMATE** of Amplification from Hobor	**ΔSVAmp**

Many of these error deltas are "process" errors inherent within the science and engineering methodologies from which the components and parameters of the model are taken. These have been investigated in Chapter 3 and 4, and where appropriate assumptions have been identified and validated to support their use in the current study or their justification is cited in

the literature. However, like all models, they fall short of deterministic knowledge of a complex system and so are accounted for in the error budget matrix. Research in these areas is ongoing and can be found in the literature. In general, the best available methods for modeling these components are incorporated into the current study.

Other "measurement" errors are inherent within the computational implementation methodology behind development of the probabilistic risk model and its applications. These have been reduced as much as possible. For the purposes of the current study, these "process" and "measurement" errors are not further reducible, but instead address the inherent variability and epistemic uncertainty in the modeling of these processes (O'Sullivan and Perry 2013). From the error budget matrix, five "reducible" errors have been identified that can benefit from further research. Addressing these "reducible" errors can improve the results of the model and extend its applications. These are investigated in the next section.

6.2. Issues and Further Research

Several components of the model can be improved with further research and development. One of the major gaps in the ShakeOut scenario was the failure to perform a network system analysis to model electric power system damage and outages. Similarly, the ShakeOut scenario was not able to perform a network system analysis to model water pipe system damage and outages. Both of these lifeline infrastructure components are intricately interconnected with business restoration and food insecurity issues, as the literature has shown in Chapter 3. Therefore, more accurate estimates of damage and restoration timelines for these infrastructure indicators in the Shakeout scenario can have great potential to improve the model results.

In the current study, from Table 7, the errors for "ΔPipes" and "ΔPowerInit" can be reduced through incorporating the results of network system analyses. This will provide more robust initial parameters for the model and therefore decrease the uncertainty in the results. Additionally, if that is not possible, the simplified methodology in the current study for modeling water conveyance can be improved through incorporation of Peak Ground Deformation (PGD) data, which was not available for the current study.

It was also noted that the current study used a simplified averaging method to determine the timeline for resource requirements over time. This resulted in equal weights for each of the six infrastructure indicator restoration times, for each of the four damage categories, when used to calculate the resource requirement timeline in Table 4. Further research is needed to establish a weighting scheme that emphasizes infrastructure damage indicators with the highest correlation to resource requirements. This may be included in post-event validation of the model, as discussed below. Validation and calibration of the weightings for the infrastructure indicator restoration timelines will reduce the uncertainty associated with "ΔWeights" and improve the model results.

Finally, social vulnerability plays an important role in the model—however, there is little quantitative research on social vulnerability's effects on the amplification of resource requirements. For the current study, the ranked social vulnerability index from SoVI was fitted to a (±) 22 percent range of amplifications from community recovery rates in New Orleans for Hurricane Katrina over a 13-year period. This basic approach can serve as a first step toward more detailed studies on the subject. This will address a critical gap in the literature addressing the application of social vulnerability indices for resource planning in emergency management.

A range of amplifications based on this research agenda and published in the literature can reduce the uncertainty associated with "ΔSVAmp" and improve the model results.

Several approaches for further development of the modeling methodology to include validation of the model, generalization for global earthquake applications and extension of its applications are presented in the next section.

6.2.1. *Further Development of the Model*

While it is noted that we can never verify this model, we can validate and calibrate the model with data from actual events (O'Sullivan and Perry 2013). Model *validation* is the process of evaluating a model's predictions against independent observational data from an actual event.

In consideration of the current scenario, the model can be calibrated and validated after a large earthquake occurs, with summary logistical resource distribution information provided by emergency management authorities. Machine learning algorithms such as *Maxent* (Philips et al. 2006) can be used to determine the probability of suitable conditions for the distribution of the observed resource requirements. These results can then be correlated to the probabilistic risk model's results, and a calibration factor can be introduced into the model to align the predictions with the observed data and associated distribution. This approach will also reveal infrastructure damage indicators with the highest correlation to resource requirements, and as mentioned in the previous section, can be used to establish a suitable weighting scheme. Previous earthquake events can also be used to calibrate the model, if logistical summary information is available.

The results from the model can also be immediately integrated into an interactive Web application for presentation, through ArcGIS 10.6 Server services and the ArcGIS Portal using Esri Web AppBuilder for ArcGIS. Widgets can be customized to allow the user to identify a point, line or area and determine the average underlying risk or summary resource requirements

from each raster surface within the selected area. The user can also query the model results at the nearest cell or by address. Graphs of resource requirements over time at each POD site can also be developed using the default "graph" widget in the Esri Web AppBuilder. This web application will allow emergency managers to interactively explore the results of the model and to investigate community vulnerability at any user defined scale.

The methodology introduced in the current study can be easily generalized for any domestic earthquake event, if the modeled ground-motion data and social vulnerability index are available. Several catastrophic earthquake plans, similar to the OPLAN and ShakeOut scenario, that can immediately benefit from the results of the current study include the New Madrid Seismic Zone Catastrophic Earthquake Plan (MAE 2009), the HayWired earthquake scenario in the San Francisco Bay Area (Detweiler et al. 2018) and the Cascadia Earthquake Plan in the Pacific Northwest. Application of the model for global earthquake events and international humanitarian response is also possible with further generalization of the methodology similar to the work in Hansen and Bausch (2007) in applications of HAZUS-MH for international applications. Further research can also investigate expansion of the modeling methodology to support additional types of catastrophic disaster response events.

Finally, the error associated with "ΔSimulation" can be seen in the broader context of the development of a mathematical model for predicting resource requirements over time. The probabilities associated with the initial resource requirements (once the model has been successfully validated and calibrated) and the curves in Equations 16, 18, and 20 suggest a more general model of the process as a Stochastic Partial Differential Equation (SPDE). In this formulation, Simulation A (Minimum) and Simulation B (Maximum) can be seen as boundary conditions over time (t) for a single model, and the concavity or convexity of any curve between

this range can be seen as an unknown parametric function of time, f(t). From this function, any one of multiple potential curves can then be used to predict resource requirements over time based on the best fit to actual observations during the event.

Further research and development in this area can lead to a web-based computational implementation of this algorithm into a decision support tool for resource ordering. This tool can be used to predict future resource requirements per POD—from within the event—based on actual observations of resource requirements from the previous operational period. In its present form, the current study's applications are limited by the initial ground-motion data, as post-event damage and restoration data are not incorporated into the current modeling methodology. This further research will give emergency managers the capacity to predict the next operational period's ordering requirements, adjusting as necessary to the varying "burn-rates" of resource requirements as the event unfolds, in a further extension of the model's applications.

6.3. Conclusion

In conclusion, the probabilistic risk model and its applications provide a systematic and comprehensive methodology to evaluate risks associated with the (M) 7.8 San Andreas Earthquake ShakeOut Scenario in estimation of "at-risk" populations for emergency logistical resource requirements. These estimates are in alignment with the OPLAN assumption of supporting resource requirements for between 2.5 million and 3.5 million people (2 meals per person/day and 3 liters of water per person/day) in the eight-county study region, at three-days post-event. Therefore, the model results are a realistic estimate for total resource requirements.

These results address several gaps in current emergency management capabilities including incorporating social vulnerability, identifying community locations for emergency logistical resource requirements and estimating resource requirements over time. In so doing, this

study provides a public service and social benefit to disaster response planning by providing tools to mitigate impacts to those populations most vulnerable to disruptions in life-sustaining food and water supplies in the event of a catastrophic incident.

Further research and development with the model can lead to a decision support tool for the logistical commodity mission in all domestic earthquake response efforts in the United States. This logistical resource support tool, or LOGRESC®, as it will hereafter be known, based on the methodology and the nascent results of the current study, can then be generalized to address the gaps in current emergency management capabilities for logistical planning in global humanitarian relief efforts.

References

Applied Technology Council (ATC). 1985. *ATC-13: Earthquake Damage Evaluation Data for California.* Redwood City, CA: ATC.

Aubrecht, C., D. Özceylan, K. Steinnocher, et al. 2013. "Multi-level geospatial modeling of human exposure patterns and vulnerability indicators". *Natural Hazards* 68: 147-164.

Bach, C., A.K. Gupta, S.S. Nair, and J. Birkmann. 2013. "Critical Infrastructures and Disaster Risk Reduction". National Institute of Disaster Management and Deutsche Gesellschaft für internationale Zusammenarbeit (GIZ). New Delhi: 1-61

Bay Area Urban Area Security Initiative (UASI). 2014. "Disaster Logistics: Point of Distribution Manual". http://www.bayareauasi.org/sites/default/files/resources/Bay%20Area%20POD%20Manual_February%202014.pdf. Accessed June 2018.

Bay Area Urban Area Security Initiative (UASI) and California Governor's Office of Emergency Services (CalOES). 2014. "Regional Catastrophic Earthquake Logistics Response Plan: Annex to the San Francisco Bay Area Regional Emergency Coordination Plan". http://bayareauasi.org/sites/default/files/resources/Regional%20Logistics%20Response_February%202014.pdf. Accessed June 2018.

Bhaduri, B., E. Bright, P. Coleman, et al. 2007. "LandScan USA: a high-resolution geospatial and temporal modeling approach for population distribution and dynamics". *GeoJournal* 69: 103-117.

Bithell, J.F. 1990. "An application of density estimation to geographical epidemiology". *Statistical Medicine* 9: 691-701.

Box, G.E.P. 1979. "Some problems of statistics and everyday life". *Journal of the American Statistical Association* 74: 1-4.

Boyce, William E., Richard C. DiPrima, and Douglas B. Meade. 2017. *Elementary Differential Equations and Boundary Value Problems*, *11th Edition*. Hoboken, NJ: Wiley.

Buika, J.A. 2000. *A Public-Private Partnership to Develop the HAZUS Earthquake Risk Assessment Capabilities for the San Francisco Bay Area, California*. A paper report in the Federal Emergency Management Agency (FEMA), Mitigation Division, Washington, D.C.

Cai, Q., G. Rushton, B. Bhaduri, E. Bright, and P. Coleman. 2006. "Estimating small-area populations by age and sex using spatial interpolation and statistical inference methods". *Transactions in GIS* 10(4): 577-598.

California Governor's Office of Emergency Services (CalOES) and Federal Emergency Management Agency (FEMA). 2011. "Southern California Catastrophic Earthquake

Response Plan". http://www.caloes.ca.gov/for-businesses-organizations/plan-prepare/catastrophic-planning. Accessed June 2018.

Camacho-Vallejo, Jose-Fernando, E. Gonzalez-Rodriguez, E. Almaguer, Rosa Gonzalez-Ramirez, and G. Eicher. 2014. "A Bi-level Optimization Model for Aid Distribution after the Occurrence of a Disaster". *Journal of Cleaner Production* 105: 134-145.

Coleman-Jensen, A., Matthew P. Rabbitt, Christian A. Gregory, and A. Singh. 2017. *Household food security in the United States in 2016*. Economic Research Report No. 237, United States Department of Agriculture, Economic Research Service.

Cova, Thomas. 1999. "GIS in Emergency Management". *Geographical Information Systems* 2: 845-858.

Cribari-Neto, Francisco and Achim Zeileis. 2010. "Beta Regression in R". *Journal of Statistical Software* 34(2): 1-24.

Cutter, S.L. 1996. "Vulnerability to Environmental Hazards". *Progress in Human Geography* 20(4): 529-539.

Cutter, S.L., B.J. Boruff, and W.L. Shirley. 2003. "Social Vulnerability to Environmental Hazards". *Social Science Quarterly* 84(2): 242-261.

Cutter, S.L., C.T. Emrich, J.T. Mitchell, B.J. Boruff, M. Gall, M.C. Schmidtlein, C.G. Burton, and G. Melton. 2006. "The Long Road Home: Race, Class, and Recovery from Hurricane Katrina". *Environment* 48(2): 8-20.

Cutter, S.L. and Christina Finch. 2008. "Temporal and spatial changes in social vulnerability to natural hazards". *Proceedings of the National Academy of Sciences of the United States of America* 105(7): 2301-2306.

Dalkey, Brown, and Cochran. 1970. "Use of Self-ratings to Improve Group Estimates: Experimental Evaluation of Delphi Procedures". *Technological Forecasting* 1(3): 283-291.

Detweiler, S.T. and A.M. Wein. 2018. "The HayWired earthquake scenario—Engineering implications". *U.S. Geological Survey Scientific Investigations Report* 2017–5013.

Dodge, Y. 2003. *The Oxford Dictionary of Statistical Terms*. Oxford: Oxford University Press.

Dwyer, A., C. Zoppou, O. Nielsen, S. Day, and S. Roberts. 2004. "Quantifying Social Vulnerability: A methodology for identifying those at risk to natural hazards". *Geoscience Australia Record* 2004(14): 1-85.

Earle, Paul S., et al. 2009. "Prompt Assessment of Global Earthquakes for Response (PAGER): A system for rapidly determining the impact of earthquakes worldwide". *U.S. Geological Survey Open-File Report* 1131.

Environmental Systems Research institute (Esri). 2017. “How Original Huff Model works”. http://desktop.arcgis.com/en/arcmap/latest/tools/business-analyst-toolbox/how-original-huff-model-works.htm. Accessed June 2018.

—. 2017. “Hot Spot Analysis (Getis-Ord Gi*)”. http://desktop.arcgis.com/en/arcmap/10.5/tools/spatial-statistics-toolbox/hot-spot-analysis.htm. Accessed June 2018.

Federal Emergency Management Agency (FEMA). 2003. “HAZUS-MH MR4 Technical Manual”. https://www.fema.gov/hazus-mh-user-technical-manuals. Accessed June 2018.

—. 2006. “IS-230.C: Fundamentals in Emergency Management”. https://training.fema.gov/hiedu/ aemrc/booksdownload/fem/ and (updated as) https://emilms.fema.gov/IS230c. Accessed June 2018.

—. 2010. “Developing and Maintaining Emergency Operations Plans: Community Preparedness Guide (CPG) 101, ver. 2.0”. https://www.fema.gov/ media-library-data/20130726-1828250450014/cpg_101_comprehensive_preparedness_guide_ developing_and_maintaining_emergency_ operations_plans_2010.pdf. Accessed June 2018.

—. 2017. *FEMA Senior Leadership Briefings for Hurricane Maria: Sept. 20, 2017 to Nov. 22, 2017.* https://content.govdelivery.com/attachments/USDHSFEMA/2017. Accessed June 2018.

—. 2018. *Disaster Assistance in Puerto Rico 90 Days After Hurricane Maria*. https://www.fema.gov/news-release/2017/12/20/disaster-assistance-puerto-rico-90-days-after-hurricane-maria. Accessed June 2018.

—. 2018. *2017 Hurricane Season FEMA After-Action Report*. https://www.fema.gov/media-library/assets/documents/167249. Accessed July 2018.

Fiedrich, F., F. Gehbauer, and U. Rickers. 2000. “Optimized resource allocation for emergency response after earthquake disasters”. *Safety Science* 35: 41-57.

Field, E.H., G.P. Biasi, P. Bird, T.E. Dawson, K.R. Felzer, D.D. Jackson, K.M. Johnson, T.H. Jordan, C Madden., A.J. Michael, K.R. Milner, M.T. Page, T. Parsons, P.M. Powers, B.E. Shaw, W.R. Thatcher, R.J. Weldon II, and Y. Zeng. 2013. “Uniform California earthquake rupture forecast, version 3 (UCERF3)”. *U.S. Geological Survey Open-File Report* 2013–1165*, California Geological Survey Special Report* 228 and *Southern California Earthquake Center Publication* 1792.

Fothergill, A., E.G.M. Maestas, and J.D. Darlington. 1999. “Race, Ethnicity and Disasters in the United States: A review of the literature”. *Disasters* 23(2): 156-173.

Fothergill, A. and L. Peek. 2004. “Poverty and Disasters in the United States: A Review of Recent Sociological Findings”. *Natural Hazards* 32: 89-110.

Fotheringham, A. and D. Wong. 1991. “The modifiable areal unit problem in multivariate statistical analysis”. *Environment & Planning A* 23(7): 1025-1044

Fussell, Elizabeth. 2015. “The Long-Term Recovery of New Orleans’ Population After Hurricane Katrina”. *American Behavioral Scientist* 59: 1231-1245.

G&E Engineering Systems, Inc. (G&E). 1994. “NIBS Earthquake Loss Estimation Methods”. *Technical Manual: Electric Power Systems* 23*:*1-68.

Gillespie, David F. and Michael J. Zakour. 2013. *Community Disaster Vulnerability*. New York: Springer.

Guthrie, J., B. Lin, A. Okrent, and R. Volpe. 2013. *Americans’ food choices at home and away: how do they compare with recommendations?* United States Department of Agriculture, Economic Research Service. https://www.ers.usda.gov/amberwaves/2013/february/americans-food-choices-at-home-and-away. Accessed June 2018.

Hansen, R. and D. Bausch. 2007. “A GIS-based methodology for exporting the Hazards US (HAZUS) earthquake model for global applications”. A report in the Federal Emergency Management Agency (FEMA), Mitigation Division, Washington, D.C.

Harrald, J., S. Al-Hajj, B. Fouladi, and D. Jeong. 1992. *Estimating the demand for sheltering in future earthquakes*. Washington D.C.: The George Washington University.

Hazards and Vulnerability Research Institute (HVRI). 2018. “Social Vulnerability Index for the United States-2006-10”. University of South Carolina. http://artsandsciences.sc.edu/grog/hvri/faq. Accessed June 2018.

Hobor, G. 2015. “New Orleans’ remarkably unpredictable recovery: developing a theory of urban resilience”. *American Behavioral Scientist* 59:1214-1230.

Huang, Xing. 2016. “The Optimization Model of Earthquake Emergency Supplies Collecting with the Limited Period and Double-Level Multihub”. *Mathematical Problems in Engineering* 2016: 1-11.

Isoyama, R. and T. Katayama. 1982. “Reliability Evaluation of Water Supply Systems during Earthquakes”. Report of the Institute of Industrial Science, The University of Tokyo 30(1): 1-64

Isoyama, R., E. Ishida, K. Yune, and T. Shirozu. 1998. “Study on Seismic Damage Estimation Procedure for Water Pipes”. *Journal of Japan Water Works Association* 67(2): 2-8.

Jaynes, E. 2003. *Probability Theory: The Logic of Science*. Cambridge: Cambridge University Press.

Johnson, CAPT Michael and LTC Brent Coryell. 2016. “Logistics Forecasting and Estimates in the Brigade Combat Team”. *Army Sustainment Magazine*, *November-December*.

Jones, Lucile M., et al. 2008. “The ShakeOut Scenario: Effects of a Potential M7.8 Earthquake on the San Andreas Fault in Southern California”. *U.S. Geological Survey Open File Report 2008-1150* and *California Geological Survey Preliminary Report* 25.

Juntunen, Lorelei. 2006. “Addressing Social Vulnerability to Hazards”. *Disaster Safety Review* 4(2): 3-10.

Kircher, C.A., R.V. Whitman, and W.T. Holmes. 2006. “HAZUS Earthquake Loss Estimation Methods”. *Natural Hazards Review* 7(2): 45-59.

Lindell, Michael K. 2013. “Disaster studies”. *Current Sociology* 61(5-6): 797-825.

Lu, Chung-Cheng, Kuo-Ching Ying, and Hui-Ju Chen. 2016. “Real-time relief distribution in the aftermath of disasters—A rolling horizon approach”. *Transportation Research Part E* 93: 1-20.

Mid-America Earthquake Center (MAE). 2009. “New Madrid Seismic Zone: Catastrophic Earthquake Response Planning Project”. *MAE Center Report No*. 09-03.

Myers, R.H., D.C. Montgomery, and G.C. Vining. 2002. *Generalized Linear Models*. New York: Wiley.

Nagelkerke, N. 1991. “A note on a general definition of the coefficient of determination”. *Biometrika* 78: 691-692.

National Research Council of the National Academies (NRC). 2007. *Tools and Methods for Estimating Population at Risk from Natural Disasters and Complex Humanitarian Crises.* Washington, D.C.: The National Academies Press.

New York City Office of Emergency Management (OEM). 2013. “Hurricane Sandy After Action: Report and Recommendations”. http://www.nyc.gov/html/recovery/downloads/pdf/sandy_aar_5.2.13.pdf. Accessed June 2018.

Noriega, Gabriela R. 2011. “Social Vulnerability Analysis to Earthquake Risk in Los Angeles County, California”. PhD diss., University of California, Irvine.

Openshaw, S. 1984. *Concepts and Techniques in Modern Geography, Number 38: The Modifiable Areal Unit Problem*. Norwich, United Kingdom: Geobooks.

O'Rourke, M.J. and G. Ayala. 1993. “Pipeline Damage due to Wave Propagation”. *Journal of Geotechnical Engineering* 119(9): 1490-1498.

O’Sullivan, David, and George L.W. Perry. 2013. *Spatial Simulation: Exploring Pattern and Process*. New York: Wiley-Blackwell.

Paci-Green, Rebekah and G. Berardi. 2015. “Do global food systems have an Achilles heel? The potential for regional food systems to support resilience in regional disasters”. *Journal of Environmental Studies and Sciences* 5(4): 685-698.

Philips, Brenda D., Deborah S.K. Thomas, A. Fothergill, and L. Blinn-Pike. 2010. *Social Vulnerability to Disasters.* Boca Raton, FL: CRC Press.

Phillips, Steven J., Robert P. Anderson, and Robert E. Schapire. 2006. "Maximum entropy modeling of species geographic distributions". *Ecological Modeling* 190: 231-259.

Pitman, Jim. 2006. *Probability*. New York: Springer.

Rose, A., I.S. Wing, D. Wei, and M. Avetisyan. 2012. "Total regional economic losses from water supply disruptions to the Los Angeles county economy". *Los Angeles County Economic Development Corporation*. http://www.laedc.org/reports/ WaterSupplyDisruptionStudy_ November2012.pdf. Accessed June 2018.

Seligson, Hope. 2008. "The ShakeOut Scenario: Supplemental Study, HAZUS Enhancements and Implementation for the ShakeOut Scenario". *U.S. Geological Survey Open File Report* 2008-1150 and *California Geological Survey Preliminary Report* 25.

Sheu, J.B., 2007. "An emergency logistics distribution approach for quick response to urgent relief demand in disasters". *Transportation Research Part E 43*: 687-709.

Sousa, V., N. Almeida, M. Luísa Sousa, A. Campos Costa, and J. Saldanha Matos. 2012. "A methodology to couple vulnerability and condition of buried pipes in seismic risk assessment: Application to a subsystem of the Lisbon wastewater system". *The 15th World Conference on Earthquake Engineering.* Beijing, China.

Thomas, J.A. and K. Mora. 2014. "Community resilience, latent resources and resource scarcity after an earthquake: is society really three meals away from anarchy?". *Natural Hazards* 74: 477-490.

Tierney, K.J. 2007. "From the margins to the mainstream? Disaster research at the crossroads". *Annual Review of Sociology* 33: 503-525.

United States Army Corps of Engineers (USACE). 2008. "USACE P0ST-EVENT Commodities Ordering Model.xls". http://www.englink.usace.army.mil/igp/doc/commodities. Accessed June 2018.

Werner, S.D., S. Cho, and R.T. Eguchi. 2008. "The ShakeOut Scenario, Supplemental Study: Analysis of Risks to Southern California Highway System due to M7.8 Earthquake along Southern San Andreas Fault". *U.S. Geological Survey Open File Report* 2008-1150 and *California Geological Survey Preliminary Report* 25.

Wolffe, Richard. "Puerto Rico: US officials privately acknowledge serious food shortage". *The Guardian (U.S. Edition).* October 17, 2017.

World Health Organization (WHO). 2000. "The management of nutrition in emergencies". http:// whqlibdoc.who.int/publications/2000/9241545208.pdf. Accessed November 2016.

Yi, Wei and Linet Özdamar. 2007. “A dynamic logistics coordination model for evacuation and support in disaster response activities”. *European Journal of Operational Research* 179(3): 1177-1193.

Yu, Emily. 2015. “Analysis of National Bridge Inventory (NBI) Data for California Bridges”. Research Project, California State Polytechnic University, Pomona.

Data Citations

CA_Tract_SoVI_06_10, CA_Tract_SoVI_06_10.gdb. 2014. [File Geodatabase]. Dr. Chris Emrich, University of South Carolina, Hazards and Vulnerability Research Institute, Columbia, SC.

ds1199.zip. 2018. [downloaded file]. California Energy Commission (Electric Substations), Mr. Fui Thong. URL: https://catalog.data.gov/dataset/electric-substations-california-energy-commission-ds1199. Accessed June 2018.

LandScan “conus_night” (Layer Package). 2012. [licensed from DHS]. Geospatial Management Office (GMO)—HIFLD Support, Washington, D.C. https://gii.dhs.gov

LandScan “global” (Layer Package). 2015. [licensed data to USC]. Oak Ridge National Lab, Michael Peters, Oak Ridge, TN. http://web.ornl.gov/sci/landscan

pods_OPLAN_2011.shp. 2017. [shapefile]. California Governor’s Office of Emergency Services, Jami Childress-Byers, Sacramento, CA.

shape.zip. 2017. [downloaded file]. USGS Pasadena, Dr. Ken Hudnut, Pasadena, CA. URL: http://earthquake.usgs.gov/earthquakes/shakemap/sc/shake/ardent_sentry_2015_se/download/shape.zip.

Appendix A The Original Gravity Weighted Huff Model

Appendix A provides an overview of the "Original Gravity Weighted Huff Model", which was applied to develop the Areas of Responsibility (AORs) used to summarize logistical resource requirements resulting from the probabilistic risk model.

The Original Gravity Weighted Huff Model is based on the principle of *distance decay*, where the probability of a population choosing one site over another is a function of the distance to the site from their current location and the distance to a finite number of other sites. Attractiveness is another parameter in the Original Gravity Weighted Huff Model, where sites that are more attractive are provided an additional weighting. The Original Gravity Weighted Huff Model is defined by the following equation (Esri 2017a):

$$P_{ij} = \frac{W_i D_{ij}^{a}}{\sum_{i=1}^{n} \left(W_i D_{ij}^{a} \right)} \tag{22}$$

P_{ij} = The probability of total population in cell (j), at centroid, receiving support at POD (i)
W_i = The attractiveness weighting for each (i) POD, set to "1" in this study
D_{ij} = The distance from total population in cell (j), at centroid, to POD site (i)
a = An exponent applied to distance so that the probability of distant sites is dampened. This is set to a = 2 in this study, as it is assumed that travel throughout an affected area is more difficult after the event occurs.

In the current study, a probability of travel model was appropriate to represent the populations served by a Point of Distribution Site (POD), as this approach can represent true probability of travel of affected populations in disaster areas. The inverse distance weighting in the model can represent the impedance of travel that occurs in the scenario due to areas impacted by damage and emergency response activities (Jones et al. 2008). The number of sites considered in the model can also be controlled, which represents the limited knowledge of community PODs sites to be expected from the public.

Therefore, AORs in the current study were determined by the Original Gravity Weighted Huff Model for probability of travel to a site location and were bound by the Los Angeles County boundary. The Original Gravity Weighted Huff Model is available for download, and through Esri Business Analyst 10.6 toolbox. The Original Gravity Weighted Huff Model was adapted for the current study and implemented through Esri ArcGIS 10.6 model builder, with the following parameters:

Table 10. The Original Gravity Weighted Huff Model parameters

ID	Parameter	Value	Comment
1	Store Locations	PODS_SCCERP_2011	PODs sites replaced 'stores' in the current study
2	Store Name Field	ID	Unique ID
3	Store Attractiveness Field	NONE	This was set to 1 for all PODS with equal weights
4	Output Folder	G:\THESIS	For processing
5	Output Feature Class Name	AORS_SCCERP_2011	Not used
6	Study Area	LA_COUNTY_BOUNDARY	Limited to LA county in the current study
7	Street Network Dataset	streets	Network dataset
8	Search Radius	49.8 kilometers	Maximum nearest neighbors for 3 PODS
9	Nearest Neighbor Constraint	3	Represented limited information by public on POD locations after the event occurs
10	Distance Friction Coefficient	2	Represented impedance of travel in disaster area
11	Generate Market Area	BOTH	This was converted to polygon and replaced AORS_SCCERP_2011
12	Origin Locations	CA_Tract_06_10	Used 2010 U.S. Decennial Census Tract centroids
13	Sales Potential Field	P0010001	"Population" field from above

To determine the search radius, the “calculate distance band from neighbor count” tool was run in ArcGIS 10.6, which resulted in a maximum distance for three PODs as 49.8 kilometers. The following Python script was then implemented through ArcGIS 10.6 model builder (Figure 57):

```
# -*- coding: utf-8 -*-
# ---------------------------------------------------------------------------
# AORS.py
# Created on: 2018-04-26 15:31:03.00000
#   (generated by ArcGIS/ModelBuilder)
# Description:
# ---------------------------------------------------------------------------

# Import arcpy module
import arcpy

# Load required toolboxes
arcpy.ImportToolbox("G:/THESIS/DATA/THESIS_MASTER.gdb/MODEL")


# Local variables:
AORS_SCCERP_2011 = "G:\\THESIS\\output.gdb\\Surface_Markets"
LA_COUNTY_BOUNDARY = "G:\\THESIS\\DATA\\THESIS_MASTER.gdb\\Data\\LA_COUNTY_BOUNDARY"
PODS_SCCERP_2011 = "G:\\THESIS\\DATA\\THESIS_MASTER.gdb\\Data\\PODS_SCCERP_2011"
POP_FROM_CENTS = "G:\\THESIS\\DATA\\THESIS_MASTER.gdb\\Data\\CENSUS_2010_TRACTS"
streets = "G:\\THESIS\\DATA\\NAVTEQ\\streets"
THESIS = "G:\\THESIS"

# Process: Huff Model
arcpy.gp.toolbox = "G:/THESIS/DATA/THESIS_MASTER.gdb/MODEL";
# Warning: the toolbox G:/THESIS/DATA/THESIS_MASTER.gdb/MODEL DOES NOT have an alias.
# Please assign this toolbox an alias to avoid tool name collisions
# And replace arcpy.gp.HuffModel(...) with arcpy.HuffModel_ALIAS(...)
arcpy.gp.HuffModel(PODS_SCCERP_2011, "ID", "NONE", THESIS, "AORS_SCCERP_2011",
LA_COUNTY_BOUNDARY, CA_Tract_06_10, "P0010001", "true", streets, "2", "BOTH", "",
"true", "49.8 Kilometers", "3")
```

Figure 57. The Original Gravity Weighted Huff Model python script

The final results from the “Generate Market Areas” step were converted to polygons, and validated to ensure there is a unique POD per AOR polygon. The final results are presented in Figure 7, and were used in subsequent summary calculations in the study and in summary of the results in Appendix D.

Appendix B HAZUS-MH Power Outage Methodology Extension

Appendix B investigates the direct calculation of populations impacted by power outage in the current study, which is an extension of the HAZUS-MH loss estimation methodology. An extension of the HAZUS-MH loss estimation methodology was required to estimate populations affected by power utility outage, as the current methodology is subject to a large range of uncertainty. This is, in part, due to the modifiable areal unit problem (MAUP) in the variation of real world service area extents for the substations. Service area data are not generally available to the public.

The standard methodology—even without consideration for the MAUP effect—still cannot identify the distribution of populations sufficiently for making decisions for emergency logistical resource requirements. This is because the HAZUS-MH methodology multiplies the average probability of damage for all substations in the study area by the population of the entire region to estimate the impacted population. Populations in the most severely impacted regions are systematically underestimated and those in the least impacted regions are overestimated based on that method and variably sized service areas as an additional weighting factor are not even considered.

To extend and improve this methodology for the current study, Assumption 11 was validated, which supposes that the substations in the study area can be assumed to be more-or-less evenly distributed at the LandScan cell resolution, proportional to population density. This approach is then equivalent to directly calculating populations impacted by power outage based on the individual Landscan raster cell populations, where the probability of damage is calculated as the HAZUS-MH Technical Manual suggests.

To validate this assumption, a 198 sq. km study region was chosen in Los Angeles County to investigate the possible scenarios for populations impacted by power outage. This rectangular region extended from the city of Baldwin Park, in the north to Whittier in the south, Hacienda Heights in the east and Rosemead in the west. The study region included a total population of 425,017. This area was chosen as the ShakeOut scenario indicates a large range of ground-motion and damages in the vicinity (Jones et al. 2008).

To estimate the location of operational substations, the California Energy Commission electric substation data was investigated. While the data does not identify coordinates for the substation locations, it does identify their zip code. From this, the location of 22 operational substations were estimated as evenly distributed through each zip code that intersected the study region (Figure 58).

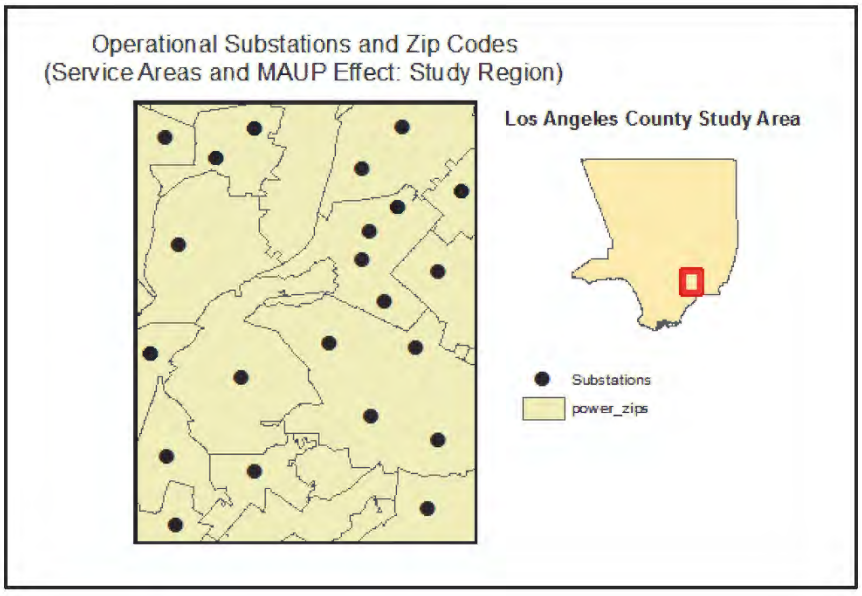

Figure 58. Study area for validation of power outage methodology extension

The probability of damage for each substation was then calculated based on the CDF damage function for the probability of complete damage to medium voltage substations with seismic components (see Figure 12). The following calculations resulted: average probability of

damage .081; maximum probability of damage, .288; and minimum probability of damage, 0. Based on the standard HAZUS-MH loss estimation methodology, the expected value for population impacted by power outage using the average was: 34,213 individuals impacted.

In consideration of the MAUP effect, three additional scenarios were investigated to extend this methodology. These three scenarios can be considered as a plausible "real-world" range of uncertainty for estimating the populations impacted by power outage. The "maximum" scenario used larger service areas for the substations in areas farther north. The "minimum" scenario estimated larger service areas in the south. The Voronoi scenario represented the average, where service areas between substations were a function of distance (Figure 59)

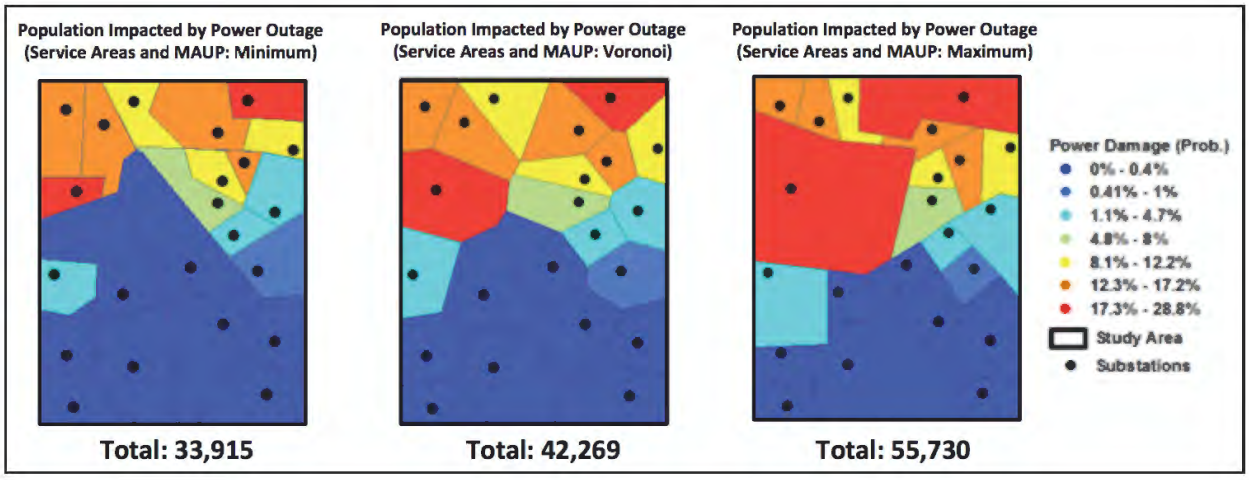

Figure 59. Substation service areas and the MAUP effect

From these results, it can be seen that the HAZUS-MH loss estimation methodology's total population impacted was most closely compared with the "minimum" scenario from the MAUP effect—which seems arbitrary and unlikely. In addition, as all impacted populations in the HAZUS-MH approach were calculated through the average "yellow" probability values, populations in the most severely impacted regions were systematically underestimated and those in the least impacted regions were overestimated. The result was that the population distribution

is arbitrary and varied significantly from the MAUP "minimum" scenario, even while the total population differed by only a small amount.

For the current study, a direct calculation approach is proposed to mitigate these issues as an extension to the HAZUS-MH loss estimation methodology. Applying the direct calculation methodology with the assumption that the substations are more-or-less evenly distributed in the study region at the LandScan cell resolution, proportional to population density, resulted in the following:

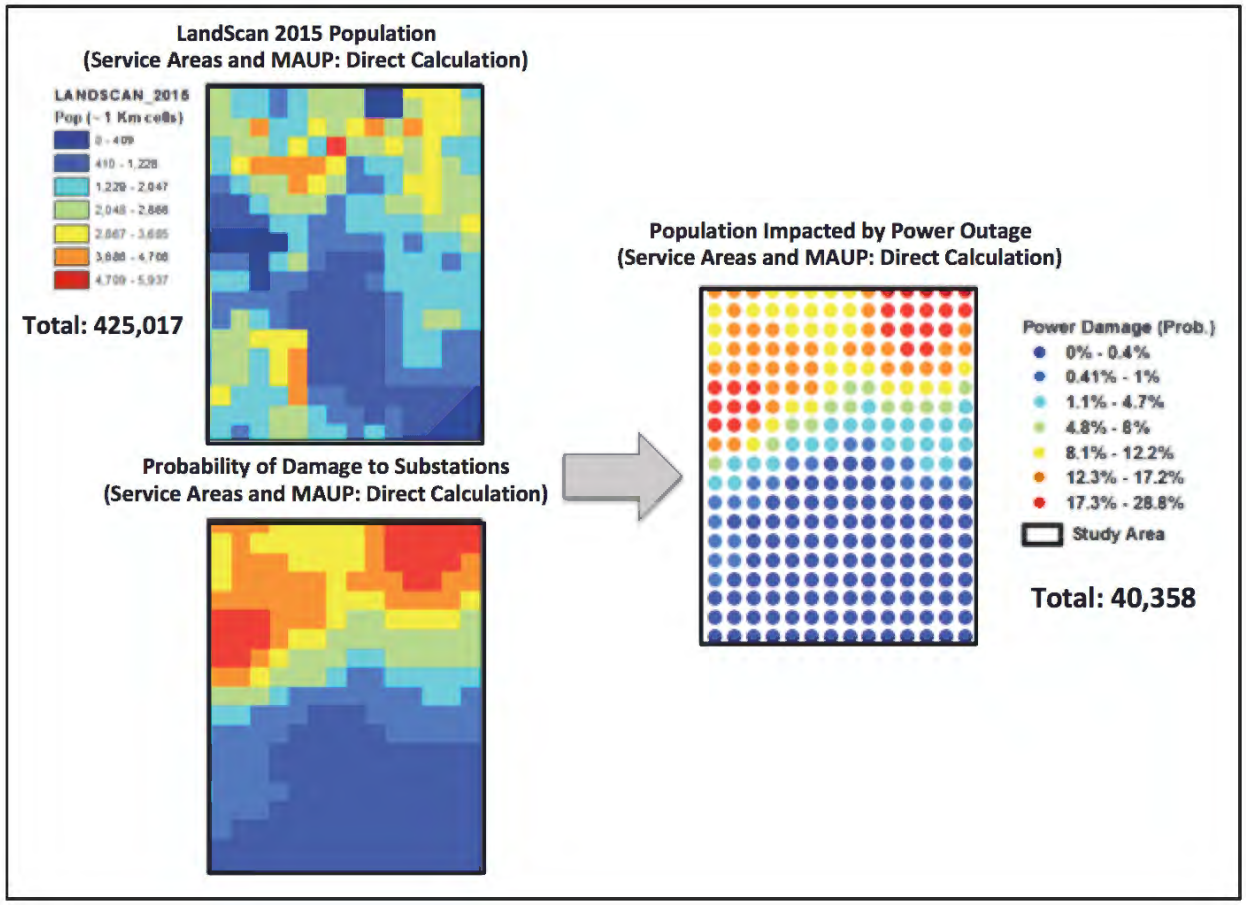

Figure 60. Direct calculation of populations subject to power outages.

This direct calculation resulted in a total population subject to power outage of: 40,358 impacted, using the CDF damage function for the probability of complete damage to medium

voltage substations with seismic components. These results were most closely compared with the Voronoi scenario, where service areas between substations were a function of distance.

The Voronoi scenario is a plausible best available estimate of "real world" substation service areas, absent actual data on the service area boundaries. In consideration of the MAUP effect, the direct calculation approach results were close to the mean of the "maximum" and the "minimum" scenarios, similar to the Voronoi scenario. Both the HAZUS-MH loss estimation results and the direct calculation approach fell within the range of uncertainty demonstrated by the MAUP scenarios.

As the affected populations were directly calculated, impacts from the variability in the service areas (and the MAUP effect) were minimized. The distribution of populations subject to power outage, which is closely tied to the impacts of nearby servicing substations, was also preserved—even without actual service area data—which is an improvement on the HAZUS-MH loss estimation methodology.

Therefore, it was validated that this assumption for a direct calculation approach of affected populations subject to power outage decreased uncertainty in comparison with the original HAZUS-MH method. Estimation of population distribution was improved and the estimation of total population subject to power outage was closer to the mean of the MAUP scenarios, and so was at least as good (and likely better) than the current standard. This approach was then used to calculate the [$POWER_{Damage}$] component of [$HAZARD_{Damage}$] in the probabilistic risk model.

Appendix C Complete Bridge Damage Validation

The result from calculation of the probability of complete bridge damage, as the component [$Bridge_{damage}$] in the current study, was shown to persist and dominate [$Hazard_{damage}$] in the five areas of "complete" bridge damage in the ShakeOut earthquake scenario (Figure 8) as identified in Werner et al. (2008). To demonstrate this, the results of the calculation of the [$Hazard_{damage}$] component of the probabilistic risk model were compared to the [$Bridge_{damage}$] component to find areas where the two datasets had equal values and the probability of complete bridge damage was greater than 50 percent.

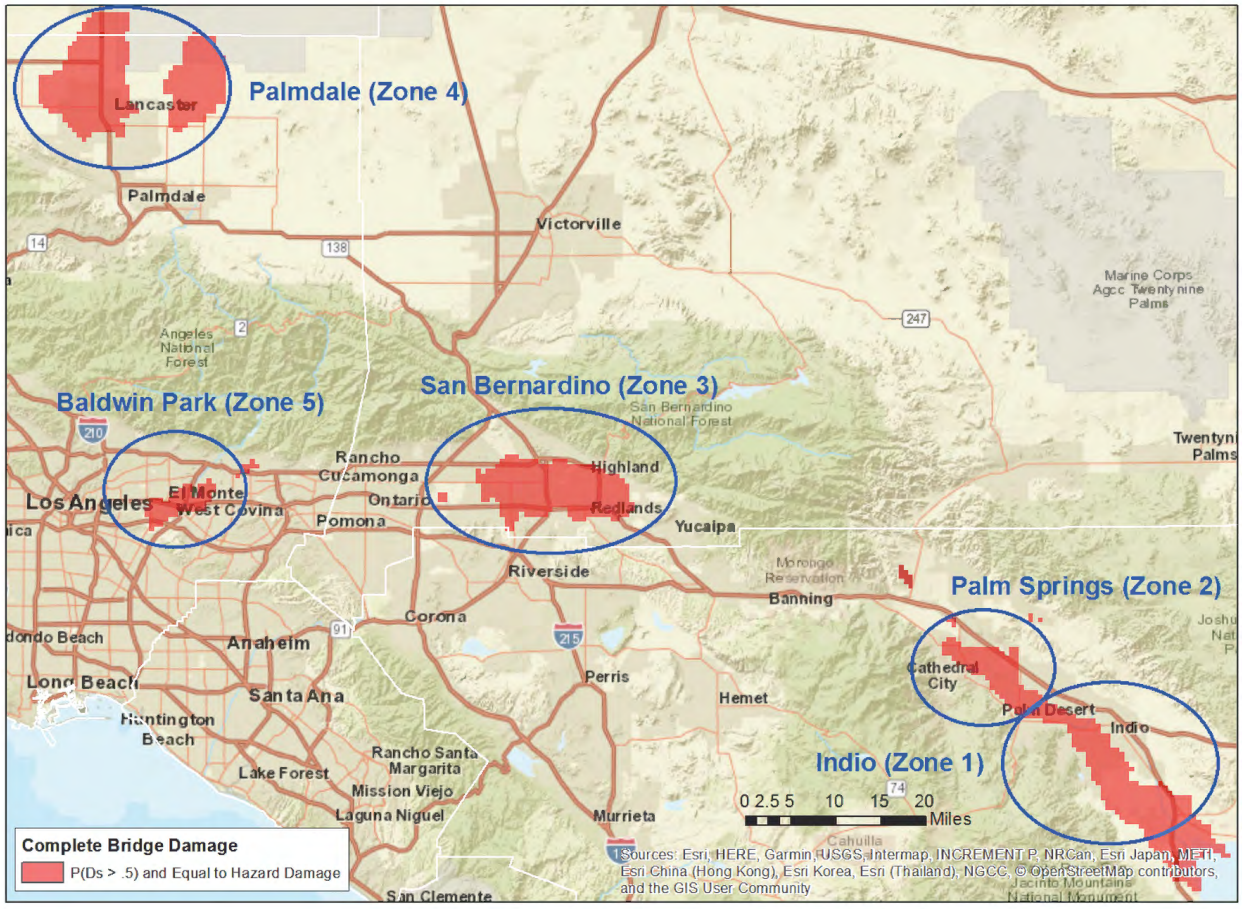

Figure 61. Validation of probability of complete bridge damage calculation

This result indicated that bridge damage dominated the hazard component calculation of the probabilistic risk model in these areas. These values were compared with Figure 14, with a near identical match in Figure 61 to the five areas of "complete" bridge damage in the ShakeOut scenario supplemental study (Werner et al. 2008).

Therefore, [$Bridge_{damage}$] as defined in the current study aligned with the findings from the ShakeOut scenario supplemental study in Werner et al. (2008) and was sufficient for calculation of the [$Hazard_{damage}$] component.

Appendix D Logistical Resource Summary Report

DAY-3 SUMMARY								
POD ID	POP (2012)	AT RISK POP	DAY-3 (MEALS)	DAY-3 (MEALS/PALLET)	DAY-3 (MEALS/TRUCK LOADS)	DAY-3 (WATER)	DAY-3 (BULK WATER/TANKERS)	DAY-3 (WATER/TRUCK LOADS)
118	371,694	240,185	480,370	834	21	720,555	21	44
76	208,014	96,784	193,568	336	8	290,352	9	18
133	167,136	88,280	176,560	307	8	264,840	8	16
117	185,071	63,282	126,564	220	5	189,846	6	12
92	243,516	47,133	94,266	164	4	141,399	4	9
81	154,654	42,898	85,796	149	4	128,694	4	8
111	182,306	42,447	84,894	147	4	127,341	4	8
109	206,499	42,441	84,882	147	4	127,323	4	8
38	323,622	39,691	79,382	138	3	119,073	3	7
102	117,610	32,842	65,684	114	3	98,526	3	6
106	97,358	27,456	54,912	95	2	82,368	2	5
146	121,241	27,134	54,268	94	2	81,402	2	5
108	119,321	25,848	51,696	90	2	77,544	2	5
89	111,576	25,142	50,284	87	2	75,426	2	5
101	42,887	23,237	46,474	81	2	69,711	2	4
115	97,117	22,488	44,976	78	2	67,464	2	4
52	87,753	14,762	29,524	51	1	44,286	1	3
87	100,600	14,702	29,404	51	1	44,106	1	3
107	76,121	14,527	29,054	50	1	43,581	1	3
39	88,059	14,027	28,054	49	1	42,081	1	3
29	83,282	13,593	27,186	47	1	40,779	1	3
10	85,995	12,467	24,934	43	1	37,401	1	2
66	79,651	12,301	24,602	43	1	36,903	1	2
4	104,008	11,793	23,586	41	1	35,379	1	2
56	109,685	10,662	21,324	37	1	31,986	1	2
121	93,239	10,291	20,582	36	1	30,873	1	2
59	92,704	10,231	20,462	36	1	30,693	1	2
15	67,726	10,192	20,384	35	1	30,576	1	2
55	43,685	9,943	19,886	35	1	29,829	1	2
113	39,978	9,736	19,472	34	1	29,208	1	2
51	46,378	9,642	19,284	33	1	28,926	1	2
17	87,144	8,978	17,956	31	1	26,934	1	2
34	80,903	8,834	17,668	31	1	26,502	1	2
53	44,914	8,494	16,988	29	1	25,482	1	2
64	41,517	8,458	16,916	29	1	25,374	1	2
63	43,055	8,392	16,784	29	1	25,176	1	2
36	62,037	8,295	16,590	29	1	24,885	1	2
11	64,304	8,182	16,364	28	1	24,546	1	2
9	43,674	7,996	15,992	28	1	23,988	1	1
86	58,808	7,989	15,978	28	1	23,967	1	1
44	168,695	7,948	15,896	28	1	23,844	1	1
110	61,454	7,878	15,756	27	1	23,634	1	1
32	49,450	7,210	14,420	25	1	21,630	1	1
37	141,373	7,049	14,098	24	1	21,147	1	1
48	82,237	7,038	14,076	24	1	21,114	1	1
99	178,123	6,756	13,512	23	1	20,268	1	1
105	36,071	6,618	13,236	23	1	19,854	1	1
33	152,436	6,617	13,234	23	1	19,851	1	1
77	85,954	6,076	12,152	21	1	18,228	1	1
21	67,298	6,066	12,132	21	1	18,198	1	1
114	24,089	5,601	11,202	19	0	16,803	0	1
30	88,857	5,347	10,694	19	0	16,041	0	1
120	62,806	5,130	10,260	18	0	15,390	0	1
130	84,226	4,778	9,556	17	0	14,334	0	1
143	69,868	4,750	9,500	16	0	14,250	0	1
68	77,869	4,733	9,466	16	0	14,199	0	1
119	131,238	4,728	9,456	16	0	14,184	0	1
72	19,120	4,725	9,450	16	0	14,175	0	1
7	50,595	4,690	9,380	16	0	14,070	0	1
85	39,060	4,412	8,824	15	0	13,236	0	1
47	28,551	4,374	8,748	15	0	13,122	0	1
135	69,174	4,313	8,626	15	0	12,939	0	1
124	38,713	4,294	8,588	15	0	12,882	0	1
90	56,615	4,264	8,528	15	0	12,792	0	1
8	61,453	4,201	8,402	15	0	12,603	0	1
35	85,267	4,193	8,386	15	0	12,579	0	1
40	79,747	4,138	8,276	14	0	12,414	0	1

DAY-3 SUMMARY								
POD ID	POP (2012)	AT RISK POP	DAY-3 (MEALS)	DAY-3 (MEALS/PALLET)	DAY-3 (MEALS/TRUCK LOADS)	DAY-3 (WATER)	DAY-3 (BULK WATER/TANKERS)	DAY-3 (WATER/TRUCK LOADS)
45	71,541	4,040	8,080	14	0	12,120	0	1
74	74,990	4,000	8,000	14	0	12,000	0	1
42	22,390	3,988	7,976	14	0	11,964	0	1
123	77,585	3,682	7,364	13	0	11,046	0	1
91	22,486	3,519	7,038	12	0	10,557	0	1
61	76,475	3,518	7,036	12	0	10,554	0	1
116	70,961	3,428	6,856	12	0	10,284	0	1
132	80,198	3,339	6,678	12	0	10,017	0	1
103	39,191	3,331	6,662	12	0	9,993	0	1
88	21,363	3,276	6,552	11	0	9,828	0	1
43	30,535	3,157	6,314	11	0	9,471	0	1
139	30,069	3,118	6,236	11	0	9,354	0	1
70	36,974	3,068	6,136	11	0	9,204	0	1
94	77,552	2,868	5,736	10	0	8,604	0	1
60	29,759	2,818	5,636	10	0	8,454	0	1
27	43,681	2,750	5,500	10	0	8,250	0	1
31	47,290	2,723	5,446	9	0	8,169	0	1
54	52,595	2,718	5,436	9	0	8,154	0	1
49	43,875	2,539	5,078	9	0	7,617	0	0
122	32,035	2,481	4,962	9	0	7,443	0	0
144	39,100	2,413	4,826	8	0	7,239	0	0
22	95,321	2,389	4,778	8	0	7,167	0	0
104	12,678	2,388	4,776	8	0	7,164	0	0
125	47,400	2,339	4,678	8	0	7,017	0	0
28	27,704	2,314	4,628	8	0	6,942	0	0
128	62,653	2,240	4,480	8	0	6,720	0	0
137	45,078	2,212	4,424	8	0	6,636	0	0
79	69,230	1,991	3,982	7	0	5,973	0	0
46	43,190	1,977	3,954	7	0	5,931	0	0
26	33,596	1,927	3,854	7	0	5,781	0	0
82	28,491	1,859	3,718	6	0	5,577	0	0
67	11,697	1,807	3,614	6	0	5,421	0	0
57	46,573	1,804	3,608	6	0	5,412	0	0
78	36,377	1,792	3,584	6	0	5,376	0	0
20	18,048	1,657	3,314	6	0	4,971	0	0
80	40,996	1,625	3,250	6	0	4,875	0	0
84	20,163	1,585	3,170	6	0	4,755	0	0
71	10,694	1,459	2,918	5	0	4,377	0	0
23	39,996	1,422	2,844	5	0	4,266	0	0
83	13,741	1,421	2,842	5	0	4,263	0	0
73	32,643	1,367	2,734	5	0	4,101	0	0
24	31,635	1,278	2,556	4	0	3,834	0	0
141	38,812	1,271	2,542	4	0	3,813	0	0
19	34,623	1,257	2,514	4	0	3,771	0	0
25	28,104	1,254	2,508	4	0	3,762	0	0
2	22,107	1,250	2,500	4	0	3,750	0	0
16	27,661	1,205	2,410	4	0	3,615	0	0
75	30,906	1,195	2,390	4	0	3,585	0	0
131	34,322	1,189	2,378	4	0	3,567	0	0
134	26,364	1,174	2,348	4	0	3,522	0	0
12	16,246	1,158	2,316	4	0	3,474	0	0
95	33,361	1,119	2,238	4	0	3,357	0	0
65	5,901	1,030	2,060	4	0	3,090	0	0
41	25,494	995	1,990	3	0	2,985	0	0
136	30,084	935	1,870	3	0	2,805	0	0
112	33,249	903	1,806	3	0	2,709	0	0
145	15,178	879	1,758	3	0	2,637	0	0
140	20,050	827	1,654	3	0	2,481	0	0
127	23,834	819	1,638	3	0	2,457	0	0
58	25,846	798	1,596	3	0	2,394	0	0
126	20,736	715	1,430	2	0	2,145	0	0
6	17,056	705	1,410	2	0	2,115	0	0
18	18,761	693	1,386	2	0	2,079	0	0
62	8,469	657	1,314	2	0	1,971	0	0
98	22,959	639	1,278	2	0	1,917	0	0
93	12,838	583	1,166	2	0	1,749	0	0
69	10,658	564	1,128	2	0	1,692	0	0

DAY-3 SUMMARY								
POD ID	POP (2012)	AT RISK POP	DAY-3 (MEALS)	DAY-3 (MEALS/PALLET)	DAY-3 (MEALS/TRUCK LOADS)	DAY-3 (WATER)	DAY-3 (BULK WATER/TANKERS)	DAY-3 (WATER/TRUCK LOADS)
13	6,093	521	1,042	2	0	1,563	0	0
5	10,152	450	900	2	0	1,350	0	0
129	9,125	449	898	2	0	1,347	0	0
1	5,256	330	660	1	0	990	0	0
3	15,246	296	592	1	0	888	0	0
100	9,338	223	446	1	0	669	0	0
50	78	3	6	0	0	9	0	0
TOTALS	8,992,637	1,421,415	2,842,830	4,931	110	4,264,245	125	263

	SIMULATION A (MEALS)																	
	DAY-7			DAY-14			DAY-30			DAY-45			DAY-60			DAY-90		
POD ID	MEALS	PALLETTS	TRUCK LOADS	MEALS	PALLETTS	TRUCK LOADS	MEALS	PALLETTS	TRUCK LOADS	MEALS	PALLETTS	TRUCK LOADS	MEALS	PALLETTS	TRUCK LOADS	MEALS	PALLETTS	TRUCK LOADS
118	370,344	643	16	238,626	414	10	94,108	163	4	41,208	72	2	17,228	30	1	1,071	2	0
76	125,790	218	5	66,865	116	3	21,061	37	1	9,046	16	0	3,960	7	0	346	1	0
133	115,873	201	5	62,276	108	3	20,121	35	1	8,577	15	0	3,762	7	0	519	1	0
117	68,077	118	3	26,353	46	1	3,660	6	0	1,512	3	0	654	1	0	34	0	0
81	43,785	76	2	13,847	24	1	826	1	0	0	0	0	0	0	0	0	0	0
111	32,833	57	1	10,397	18	0	206	0	0	0	0	0	0	0	0	0	0	0
101	32,514	56	1	18,886	33	1	6,750	12	0	2,903	5	0	1,252	2	0	116	0	0
102	29,892	52	1	9,528	17	0	91	0	0	0	0	0	0	0	0	0	0	0
109	29,479	51	1	9,422	16	0	87	0	0	0	0	0	0	0	0	0	0	0
92	28,791	50	1	9,170	16	0	65	0	0	0	0	0	0	0	0	0	0	0
106	28,590	50	1	9,132	16	0	390	1	0	0	0	0	0	0	0	0	0	0
146	20,136	35	1	6,423	11	0	126	0	0	0	0	0	0	0	0	0	0	0
89	19,338	34	1	6,182	11	0	183	0	0	4	0	0	1	0	0	0	0	0
115	19,228	33	1	6,018	10	0	134	0	0	0	0	0	0	0	0	0	0	0
108	17,341	30	1	5,451	9	0	110	0	0	0	0	0	0	0	0	0	0	0
38	11,972	21	1	3,685	6	0	58	0	0	3	0	0	0	0	0	0	0	0
107	8,667	15	0	2,626	5	0	92	0	0	0	0	0	0	0	0	0	0	0
113	7,835	14	0	2,486	4	0	34	0	0	0	0	0	0	0	0	0	0	0
55	7,203	13	0	2,260	4	0	105	0	0	0	0	0	0	0	0	0	0	0
29	6,144	11	0	1,967	3	0	27	0	0	0	0	0	0	0	0	0	0	0
51	5,786	10	0	1,796	3	0	31	0	0	0	0	0	0	0	0	0	0	0
53	5,742	10	0	1,850	3	0	63	0	0	0	0	0	0	0	0	0	0	0
64	5,250	9	0	1,580	3	0	67	0	0	0	0	0	0	0	0	0	0	0
63	4,893	8	0	1,468	3	0	31	0	0	0	0	0	0	0	0	0	0	0
114	4,316	7	0	1,383	2	0	13	0	0	0	0	0	0	0	0	0	0	0
9	3,999	7	0	1,299	2	0	15	0	0	0	0	0	0	0	0	0	0	0
72	3,734	6	0	1,194	2	0	71	0	0	0	0	0	0	0	0	0	0	0
15	3,671	6	0	1,008	2	0	11	0	0	0	0	0	0	0	0	0	0	0
39	2,780	5	0	610	1	0	11	0	0	0	0	0	0	0	0	0	0	0
66	1,654	3	0	207	0	0	12	0	0	0	0	0	0	0	0	0	0	0
47	1,424	2	0	436	1	0	0	0	0	0	0	0	0	0	0	0	0	0
52	1,411	2	0	47	0	0	0	0	0	0	0	0	0	0	0	0	0	0
105	1,331	2	0	301	1	0	0	0	0	0	0	0	0	0	0	0	0	0
36	1,249	2	0	331	1	0	8	0	0	0	0	0	0	0	0	0	0	0
10	1,182	2	0	0	0	0	0	0	0	0	0	0	0	0	0	0	0	0
32	1,118	2	0	257	0	0	8	0	0	0	0	0	0	0	0	0	0	0
104	985	2	0	299	1	0	0	0	0	0	0	0	0	0	0	0	0	0
87	845	1	0	0	0	0	0	0	0	0	0	0	0	0	0	0	0	0
34	775	1	0	0	0	0	0	0	0	0	0	0	0	0	0	0	0	0
11	642	1	0	0	0	0	0	0	0	0	0	0	0	0	0	0	0	0
48	624	1	0	180	0	0	0	0	0	0	0	0	0	0	0	0	0	0
121	619	1	0	0	0	0	0	0	0	0	0	0	0	0	0	0	0	0
56	591	1	0	0	0	0	0	0	0	0	0	0	0	0	0	0	0	0
17	423	1	0	0	0	0	0	0	0	0	0	0	0	0	0	0	0	0
4	392	1	0	0	0	0	0	0	0	0	0	0	0	0	0	0	0	0
86	355	1	0	0	0	0	0	0	0	0	0	0	0	0	0	0	0	0
42	355	1	0	0	0	0	0	0	0	0	0	0	0	0	0	0	0	0
110	334	1	0	0	0	0	0	0	0	0	0	0	0	0	0	0	0	0
59	326	1	0	0	0	0	0	0	0	0	0	0	0	0	0	0	0	0
43	254	0	0	0	0	0	0	0	0	0	0	0	0	0	0	0	0	0
139	249	0	0	0	0	0	0	0	0	0	0	0	0	0	0	0	0	0
7	247	0	0	0	0	0	0	0	0	0	0	0	0	0	0	0	0	0
88	242	0	0	0	0	0	0	0	0	0	0	0	0	0	0	0	0	0
60	218	0	0	0	0	0	0	0	0	0	0	0	0	0	0	0	0	0
103	207	0	0	43	0	0	0	0	0	0	0	0	0	0	0	0	0	0
67	198	0	0	0	0	0	0	0	0	0	0	0	0	0	0	0	0	0
91	121	0	0	0	0	0	0	0	0	0	0	0	0	0	0	0	0	0
71	118	0	0	0	0	0	0	0	0	0	0	0	0	0	0	0	0	0
21	92	0	0	0	0	0	0	0	0	0	0	0	0	0	0	0	0	0
28	81	0	0	0	0	0	0	0	0	0	0	0	0	0	0	0	0	0
65	81	0	0	0	0	0	0	0	0	0	0	0	0	0	0	0	0	0
85	69	0	0	0	0	0	0	0	0	0	0	0	0	0	0	0	0	0
70	62	0	0	0	0	0	0	0	0	0	0	0	0	0	0	0	0	0
20	49	0	0	0	0	0	0	0	0	0	0	0	0	0	0	0	0	0
12	47	0	0	0	0	0	0	0	0	0	0	0	0	0	0	0	0	0

	SIMULATION A (MEALS)																	
	DAY-7			DAY-14			DAY-30			DAY-45			DAY-60			DAY-90		
POD ID	MEALS	PALLETTS	TRUCK LOADS	MEALS	PALLETTS	TRUCK LOADS	MEALS	PALLETTS	TRUCK LOADS	MEALS	PALLETTS	TRUCK LOADS	MEALS	PALLETTS	TRUCK LOADS	MEALS	PALLETTS	TRUCK LOADS
8	45	0	0	0	0	0	0	0	0	0	0	0	0	0	0	0	0	0
130	40	0	0	0	0	0	0	0	0	0	0	0	0	0	0	0	0	0
90	35	0	0	0	0	0	0	0	0	0	0	0	0	0	0	0	0	0
27	29	0	0	0	0	0	0	0	0	0	0	0	0	0	0	0	0	0
30	27	0	0	0	0	0	0	0	0	0	0	0	0	0	0	0	0	0
124	27	0	0	0	0	0	0	0	0	0	0	0	0	0	0	0	0	0
143	25	0	0	0	0	0	0	0	0	0	0	0	0	0	0	0	0	0
62	18	0	0	0	0	0	0	0	0	0	0	0	0	0	0	0	0	0
77	16	0	0	0	0	0	0	0	0	0	0	0	0	0	0	0	0	0
135	15	0	0	0	0	0	0	0	0	0	0	0	0	0	0	0	0	0
37	14	0	0	0	0	0	0	0	0	0	0	0	0	0	0	0	0	0
122	9	0	0	0	0	0	0	0	0	0	0	0	0	0	0	0	0	0
125	9	0	0	0	0	0	0	0	0	0	0	0	0	0	0	0	0	0
119	7	0	0	0	0	0	0	0	0	0	0	0	0	0	0	0	0	0
40	4	0	0	0	0	0	0	0	0	0	0	0	0	0	0	0	0	0
120	3	0	0	0	0	0	0	0	0	0	0	0	0	0	0	0	0	0
83	3	0	0	0	0	0	0	0	0	0	0	0	0	0	0	0	0	0
144	1	0	0	0	0	0	0	0	0	0	0	0	0	0	0	0	0	0
TOTALS	1,083,300	1,881	47	525,889	913	23	148,575	258	6	63,253	110	3	26,857	47	1	2,086	4	0

*Note: All PODS with 0 resource requirements at Day-7 and later are not shown.

	SIMULATION B (MEALS)																	
	DAY-7			DAY-14			DAY-30			DAY-45			DAY-60			DAY-90		
POD ID	MEALS	PALLETTS	TRUCK LOADS	MEALS	PALLETTS	TRUCK LOADS	MEALS	PALLETTS	TRUCK LOADS	MEALS	PALLETTS	TRUCK LOADS	MEALS	PALLETTS	TRUCK LOADS	MEALS	PALLETTS	TRUCK LOADS
118	450,298	782	20	446,573	775	19	414,443	720	18	367,515	638	16	344,525	598	15	245,465	426	11
76	186,401	324	8	180,882	314	8	152,400	265	7	84,450	147	4	79,744	138	3	59,104	103	3
133	171,321	297	7	166,605	289	7	142,382	247	6	80,856	140	4	76,594	133	3	57,375	100	2
117	116,127	202	5	107,722	187	5	76,673	133	3	13,523	23	1	12,710	22	1	9,404	16	0
81	82,910	144	4	78,081	136	3	58,229	101	3	0	0	0	0	0	0	0	0	0
111	75,261	131	3	56,168	98	2	40,033	70	2	0	0	0	0	0	0	0	0	0
92	74,215	129	3	47,878	83	2	32,597	57	1	0	0	0	0	0	0	0	0	0
109	65,504	114	3	48,769	85	2	32,811	57	1	0	0	0	0	0	0	0	0	0
102	58,020	101	3	50,972	88	2	34,821	60	2	0	0	0	0	0	0	0	0	0
106	52,734	92	2	49,995	87	2	36,779	64	2	0	0	0	0	0	0	0	0	0
101	45,003	78	2	44,182	77	2	39,323	68	2	26,861	47	1	25,333	44	1	18,702	32	1
108	44,507	77	2	28,972	50	1	20,130	35	1	0	0	0	0	0	0	0	0	0
89	42,856	74	2	32,958	57	1	23,697	41	1	26	0	0	25	0	0	15	0	0
146	42,084	73	2	34,788	60	2	24,063	42	1	0	0	0	0	0	0	0	0	0
115	41,770	73	2	33,058	57	1	24,139	42	1	0	0	0	0	0	0	0	0	0
38	37,753	66	2	20,021	35	1	13,709	24	1	45	0	0	43	0	0	12	0	0
107	24,312	42	1	14,290	25	1	10,546	18	0	0	0	0	0	0	0	0	0	0
52	22,526	39	1	254	0	0	173	0	0	0	0	0	0	0	0	0	0	0
39	22,233	39	1	3,347	6	0	2,348	4	0	0	0	0	0	0	0	0	0	0
87	19,961	35	1	0	0	0	0	0	0	0	0	0	0	0	0	0	0	0
66	19,750	34	1	1,155	2	0	859	1	0	0	0	0	0	0	0	0	0	0
10	19,163	33	1	0	0	0	0	0	0	0	0	0	0	0	0	0	0	0
55	18,160	32	1	12,078	21	1	8,991	16	0	273	0	0	0	0	0	0	0	0
29	17,956	31	1	10,122	18	0	6,910	12	0	0	0	0	0	0	0	0	0	0
113	17,384	30	1	13,330	23	1	9,409	16	0	0	0	0	0	0	0	0	0	0
51	16,151	28	1	9,589	17	0	6,769	12	0	0	0	0	0	0	0	0	0	0
15	15,060	26	1	5,472	10	0	3,896	7	0	0	0	0	0	0	0	0	0	0
64	15,037	26	1	8,661	15	0	6,390	11	0	0	0	0	0	0	0	0	0	0
63	14,275	25	1	7,905	14	0	5,710	10	0	0	0	0	0	0	0	0	0	0
4	13,718	24	1	0	0	0	0	0	0	0	0	0	0	0	0	0	0	0
34	13,468	23	1	0	0	0	0	0	0	0	0	0	0	0	0	0	0	0
53	13,224	23	1	9,632	17	0	6,813	12	0	0	0	0	0	0	0	0	0	0
121	12,141	21	1	0	0	0	0	0	0	0	0	0	0	0	0	0	0	0
9	11,695	20	1	6,334	11	0	4,092	7	0	0	0	0	0	0	0	0	0	0
86	11,094	19	0	0	0	0	0	0	0	0	0	0	0	0	0	0	0	0
17	10,815	19	0	0	0	0	0	0	0	0	0	0	0	0	0	0	0	0
11	10,797	19	0	0	0	0	0	0	0	0	0	0	0	0	0	0	0	0
36	10,787	19	0	1,626	3	0	1,074	2	0	0	0	0	0	0	0	0	0	0
110	10,731	19	0	0	0	0	0	0	0	0	0	0	0	0	0	0	0	0
56	10,528	18	0	0	0	0	0	0	0	0	0	0	0	0	0	0	0	0
32	10,431	18	0	1,395	2	0	984	2	0	0	0	0	0	0	0	0	0	0
105	9,932	17	0	1,640	3	0	1,034	2	0	0	0	0	0	0	0	0	0	0
114	9,401	16	0	7,250	13	0	4,848	8	0	0	0	0	0	0	0	0	0	0
59	9,108	16	0	0	0	0	0	0	0	0	0	0	0	0	0	0	0	0
72	8,606	15	0	6,270	11	0	4,854	8	0	6	0	0	0	0	0	0	0	0
47	6,474	11	0	2,168	4	0	1,401	2	0	0	0	0	0	0	0	0	0	0
42	6,361	11	0	0	0	0	0	0	0	0	0	0	0	0	0	0	0	0
7	5,280	9	0	0	0	0	0	0	0	0	0	0	0	0	0	0	0	0
88	5,042	9	0	0	0	0	0	0	0	0	0	0	0	0	0	0	0	0
91	4,838	8	0	0	0	0	0	0	0	0	0	0	0	0	0	0	0	0
48	4,405	8	0	875	2	0	549	1	0	0	0	0	0	0	0	0	0	0
43	4,153	7	0	0	0	0	0	0	0	0	0	0	0	0	0	0	0	0
139	3,804	7	0	0	0	0	0	0	0	0	0	0	0	0	0	0	0	0
104	3,607	6	0	1,634	3	0	1,043	2	0	0	0	0	0	0	0	0	0	0
21	3,595	6	0	0	0	0	0	0	0	0	0	0	0	0	0	0	0	0
60	3,539	6	0	0	0	0	0	0	0	0	0	0	0	0	0	0	0	0
124	3,473	6	0	0	0	0	0	0	0	0	0	0	0	0	0	0	0	0
67	2,778	5	0	0	0	0	0	0	0	0	0	0	0	0	0	0	0	0
77	2,688	5	0	0	0	0	0	0	0	0	0	0	0	0	0	0	0	0

	SIMULATION B (MEALS)																	
	DAY-7			DAY-14			DAY-30			DAY-45			DAY-60			DAY-90		
POD ID	MEALS	PALLETTS	TRUCK LOADS	MEALS	PALLETTS	TRUCK LOADS	MEALS	PALLETTS	TRUCK LOADS	MEALS	PALLETTS	TRUCK LOADS	MEALS	PALLETTS	TRUCK LOADS	MEALS	PALLETTS	TRUCK LOADS
85	2,606	5	0	0	0	0	0	0	0	0	0	0	0	0	0	0	0	0
71	2,173	4	0	0	0	0	0	0	0	0	0	0	0	0	0	0	0	0
28	2,089	4	0	0	0	0	0	0	0	0	0	0	0	0	0	0	0	0
90	1,836	3	0	0	0	0	0	0	0	0	0	0	0	0	0	0	0	0
103	1,818	3	0	224	0	0	157	0	0	0	0	0	0	0	0	0	0	0
8	1,755	3	0	0	0	0	0	0	0	0	0	0	0	0	0	0	0	0
65	1,614	3	0	0	0	0	0	0	0	0	0	0	0	0	0	0	0	0
70	1,486	3	0	0	0	0	0	0	0	0	0	0	0	0	0	0	0	0
130	1,480	3	0	0	0	0	0	0	0	0	0	0	0	0	0	0	0	0
20	1,109	2	0	0	0	0	0	0	0	0	0	0	0	0	0	0	0	0
120	1,062	2	0	1	0	0	1	0	0	0	0	0	0	0	0	0	0	0
84	935	2	0	0	0	0	0	0	0	0	0	0	0	0	0	0	0	0
83	789	1	0	0	0	0	0	0	0	0	0	0	0	0	0	0	0	0
12	696	1	0	0	0	0	0	0	0	0	0	0	0	0	0	0	0	0
143	643	1	0	0	0	0	0	0	0	0	0	0	0	0	0	0	0	0
27	570	1	0	0	0	0	0	0	0	0	0	0	0	0	0	0	0	0
30	536	1	0	0	0	0	0	0	0	0	0	0	0	0	0	0	0	0
135	507	1	0	0	0	0	0	0	0	0	0	0	0	0	0	0	0	0
62	486	1	0	0	0	0	0	0	0	0	0	0	0	0	0	0	0	0
119	322	1	0	0	0	0	0	0	0	0	0	0	0	0	0	0	0	0
37	241	0	0	0	0	0	0	0	0	0	0	0	0	0	0	0	0	0
122	207	0	0	0	0	0	0	0	0	0	0	0	0	0	0	0	0	0
125	178	0	0	0	0	0	0	0	0	0	0	0	0	0	0	0	0	0
74	167	0	0	0	0	0	0	0	0	0	0	0	0	0	0	0	0	0
40	131	0	0	0	0	0	0	0	0	0	0	0	0	0	0	0	0	0
13	108	0	0	0	0	0	0	0	0	0	0	0	0	0	0	0	0	0
144	58	0	0	0	0	0	0	0	0	0	0	0	0	0	0	0	0	0
19	38	0	0	0	0	0	0	0	0	0	0	0	0	0	0	0	0	0
145	20	0	0	0	0	0	0	0	0	0	0	0	0	0	0	0	0	0
23	12	0	0	0	0	0	0	0	0	0	0	0	0	0	0	0	0	0
82	2	0	0	0	0	0	0	0	0	0	0	0	0	0	0	0	0	0
TOTALS	2,090,919	3,630	91	1,552,876	2,696	67	1,255,080	2,179	54	573,555	996	25	538,974	936	23	390,077	677	17

*Note: All PODS with 0 resource requirements at Day-7 and later are not shown.

	SIMULATION C (MEALS)																	
	DAY-7			DAY-14			DAY-30			DAY-45			DAY-60			DAY-90		
POD ID	MEALS	PALLETTS	TRUCK LOADS	MEALS	PALLETTS	TRUCK LOADS	MEALS	PALLETTS	TRUCK LOADS	MEALS	PALLETTS	TRUCK LOADS	MEALS	PALLETTS	TRUCK LOADS	MEALS	PALLETTS	TRUCK LOADS
118	462,393	803	20	424,456	737	18	348,771	606	15	272,494	473	12	218,552	379	9	113,891	198	5
76	180,369	313	8	156,878	272	7	103,776	180	5	59,309	103	3	47,681	83	2	24,285	42	1
133	164,745	286	7	143,574	249	6	95,814	166	4	56,395	98	2	45,321	79	2	23,019	40	1
117	114,663	199	5	92,967	161	4	46,815	81	2	9,737	17	0	7,779	14	0	4,071	7	0
81	76,596	133	3	60,922	106	3	26,996	47	1	0	0	0	0	0	0	0	0	0
111	67,410	117	3	45,420	79	2	20,256	35	1	0	0	0	0	0	0	0	0	0
92	66,685	116	3	39,945	69	2	17,647	31	1	0	0	0	0	0	0	0	0	0
109	61,030	106	3	41,205	72	2	18,554	32	1	0	0	0	0	0	0	0	0	0
102	55,309	96	2	42,170	73	2	18,516	32	1	0	0	0	0	0	0	0	0	0
106	49,427	86	2	39,810	69	2	17,937	31	1	0	0	0	0	0	0	0	0	0
101	43,852	76	2	39,060	68	2	28,372	49	1	19,071	33	1	15,293	27	1	7,863	14	0
146	39,593	69	2	28,343	49	1	12,338	21	1	0	0	0	0	0	0	0	0	0
108	38,954	68	2	23,881	41	1	10,537	18	0	0	0	0	0	0	0	0	0	0
89	38,924	68	2	26,742	46	1	12,186	21	1	22	0	0	17	0	0	10	0	0
115	36,995	64	2	26,240	46	1	11,693	20	1	0	0	0	0	0	0	0	0	0
38	33,068	57	1	16,393	28	1	7,302	13	0	45	0	0	39	0	0	31	0	0
107	20,352	35	1	11,384	20	0	5,160	9	0	0	0	0	0	0	0	0	0	0
113	15,758	27	1	10,883	19	0	4,939	9	0	0	0	0	0	0	0	0	0	0
29	15,594	27	1	8,456	15	0	3,692	6	0	0	0	0	0	0	0	0	0	0
39	15,497	27	1	2,704	5	0	1,175	2	0	0	0	0	0	0	0	0	0	0
55	15,355	27	1	9,603	17	0	4,384	8	0	86	0	0	0	0	0	0	0	0
52	14,999	26	1	207	0	0	93	0	0	0	0	0	0	0	0	0	0	0
51	13,975	24	1	7,838	14	0	3,525	6	0	0	0	0	0	0	0	0	0	0
87	13,603	24	1	0	0	0	0	0	0	0	0	0	0	0	0	0	0	0
66	13,004	23	1	915	2	0	418	1	0	0	0	0	0	0	0	0	0	0
10	12,766	22	1	0	0	0	0	0	0	0	0	0	0	0	0	0	0	0
64	12,295	21	1	6,854	12	0	3,078	5	0	0	0	0	0	0	0	0	0	0
53	12,086	21	1	8,020	14	0	3,498	6	0	0	0	0	0	0	0	0	0	0
63	11,971	21	1	6,430	11	0	2,921	5	0	0	0	0	0	0	0	0	0	0
15	11,730	20	1	4,433	8	0	1,977	3	0	0	0	0	0	0	0	0	0	0
9	10,735	19	0	5,644	10	0	2,437	4	0	0	0	0	0	0	0	0	0	0
4	9,965	17	0	0	0	0	0	0	0	0	0	0	0	0	0	0	0	0
114	8,857	15	0	6,086	11	0	2,641	5	0	0	0	0	0	0	0	0	0	0
34	8,771	15	0	0	0	0	0	0	0	0	0	0	0	0	0	0	0	0
121	8,355	15	0	0	0	0	0	0	0	0	0	0	0	0	0	0	0	0
36	8,190	14	0	1,417	2	0	626	1	0	0	0	0	0	0	0	0	0	0
86	7,990	14	0	0	0	0	0	0	0	0	0	0	0	0	0	0	0	0
110	7,677	13	0	0	0	0	0	0	0	0	0	0	0	0	0	0	0	0
32	7,601	13	0	1,124	2	0	486	1	0	0	0	0	0	0	0	0	0	0
72	7,536	13	0	4,981	9	0	2,359	4	0	0	0	0	0	0	0	0	0	0
105	7,399	13	0	1,392	2	0	585	1	0	0	0	0	0	0	0	0	0	0
11	7,398	13	0	0	0	0	0	0	0	0	0	0	0	0	0	0	0	0
17	7,166	12	0	0	0	0	0	0	0	0	0	0	0	0	0	0	0	0
56	6,934	12	0	0	0	0	0	0	0	0	0	0	0	0	0	0	0	0
59	6,320	11	0	0	0	0	0	0	0	0	0	0	0	0	0	0	0	0
47	5,316	9	0	1,891	3	0	795	1	0	0	0	0	0	0	0	0	0	0
42	4,225	7	0	0	0	0	0	0	0	0	0	0	0	0	0	0	0	0
7	3,726	6	0	0	0	0	0	0	0	0	0	0	0	0	0	0	0	0
91	3,519	6	0	0	0	0	0	0	0	0	0	0	0	0	0	0	0	0
48	3,368	6	0	763	1	0	328	1	0	0	0	0	0	0	0	0	0	0
88	3,299	6	0	0	0	0	0	0	0	0	0	0	0	0	0	0	0	0
104	3,122	5	0	1,372	2	0	572	1	0	0	0	0	0	0	0	0	0	0
43	2,804	5	0	0	0	0	0	0	0	0	0	0	0	0	0	0	0	0
124	2,662	5	0	0	0	0	0	0	0	0	0	0	0	0	0	0	0	0
139	2,632	5	0	0	0	0	0	0	0	0	0	0	0	0	0	0	0	0
21	2,624	5	0	0	0	0	0	0	0	0	0	0	0	0	0	0	0	0
60	2,363	4	0	0	0	0	0	0	0	0	0	0	0	0	0	0	0	0
77	2,155	4	0	0	0	0	0	0	0	0	0	0	0	0	0	0	0	0
67	1,918	3	0	0	0	0	0	0	0	0	0	0	0	0	0	0	0	0
85	1,886	3	0	0	0	0	0	0	0	0	0	0	0	0	0	0	0	0
71	1,519	3	0	0	0	0	0	0	0	0	0	0	0	0	0	0	0	0
28	1,385	2	0	0	0	0	0	0	0	0	0	0	0	0	0	0	0	0
90	1,360	2	0	0	0	0	0	0	0	0	0	0	0	0	0	0	0	0
103	1,330	2	0	185	0	0	84	0	0	0	0	0	0	0	0	0	0	0
8	1,300	2	0	0	0	0	0	0	0	0	0	0	0	0	0	0	0	0
70	1,105	2	0	0	0	0	0	0	0	0	0	0	0	0	0	0	0	0
130	1,072	2	0	0	0	0	0	0	0	0	0	0	0	0	0	0	0	0
65	1,034	2	0	0	0	0	0	0	0	0	0	0	0	0	0	0	0	0

	SIMULATION C (MEALS)																	
	DAY-7			DAY-14			DAY-30			DAY-45			DAY-60			DAY-90		
POD ID	MEALS	PALLETTS	TRUCK LOADS	MEALS	PALLETTS	TRUCK LOADS	MEALS	PALLETTS	TRUCK LOADS	MEALS	PALLETTS	TRUCK LOADS	MEALS	PALLETTS	TRUCK LOADS	MEALS	PALLETTS	TRUCK LOADS
120	878	2	0	2	0	0	1	0	0	0	0	0	0	0	0	0	0	0
20	761	1	0	0	0	0	0	0	0	0	0	0	0	0	0	0	0	0
84	757	1	0	0	0	0	0	0	0	0	0	0	0	0	0	0	0	0
83	632	1	0	0	0	0	0	0	0	0	0	0	0	0	0	0	0	0
143	486	1	0	0	0	0	0	0	0	0	0	0	0	0	0	0	0	0
12	474	1	0	0	0	0	0	0	0	0	0	0	0	0	0	0	0	0
27	384	1	0	0	0	0	0	0	0	0	0	0	0	0	0	0	0	0
135	353	1	0	0	0	0	0	0	0	0	0	0	0	0	0	0	0	0
62	348	1	0	0	0	0	0	0	0	0	0	0	0	0	0	0	0	0
30	347	1	0	0	0	0	0	0	0	0	0	0	0	0	0	0	0	0
119	238	0	0	0	0	0	0	0	0	0	0	0	0	0	0	0	0	0
37	159	0	0	0	0	0	0	0	0	0	0	0	0	0	0	0	0	0
122	150	0	0	0	0	0	0	0	0	0	0	0	0	0	0	0	0	0
74	142	0	0	0	0	0	0	0	0	0	0	0	0	0	0	0	0	0
125	119	0	0	0	0	0	0	0	0	0	0	0	0	0	0	0	0	0
13	100	0	0	0	0	0	0	0	0	0	0	0	0	0	0	0	0	0
40	96	0	0	0	0	0	0	0	0	0	0	0	0	0	0	0	0	0
144	49	0	0	0	0	0	0	0	0	0	0	0	0	0	0	0	0	0
19	38	0	0	0	0	0	0	0	0	0	0	0	0	0	0	0	0	0
145	19	0	0	0	0	0	0	0	0	0	0	0	0	0	0	0	0	0
23	12	0	0	0	0	0	0	0	0	0	0	0	0	0	0	0	0	0
82	2	0	0	0	0	0	0	0	0	0	0	0	0	0	0	0	0	0
TOTALS	1,912,160	3,320	83	1,350,590	2,345	59	843,284	1,464	37	417,159	724	18	334,682	581	15	173,170	301	8

*Note: All PODS with 0 resource requirements at Day-7 and later are not shown.